ISOLATION OF HUMAN SALIVARY EXOSOME ON THE MORPHOLOGY AND GENE EXPRESSION OF HUMAN PERIODONTAL LIGAMENT FIBROBLAST CELL LINE

TUAN SITI MASTAZLIHA BTE LONG TUAN KECHIK

UNIVERSITI SAINS MALAYSIA

2018

ISOLATION OF HUMAN SALIVARY EXOSOME ON THE MORPHOLOGY AND GENE EXPRESSION OF HUMAN PERIODONTAL LIGAMENT FIBROBLAST CELL LINE

By

TUAN SITI MASTAZLIHA BTE LONG TUAN KECHIK

Thesis submitted in fulfillment of the requirements

for the degree of

Master of Science

January 2018

ACKNOWLEDGEMENT

TABLE OF CONTENTS

APPENDICES

LIST OF TABLES

LIST OF FIGURES

Page

LIST OF SYMBOLS/ABBREVIATONS

α	Alpha
β	Beta
<	Less than
>	More than
°C	Degree Celsius
μg	Microgram
μl	Microliter
μM	Micromolar
$2^{-(\Delta\Delta C_T)}$	Relative quantity of gene expression
A	Adenine
aFGF	Acidic Fibroblast Growth Factor
AFM	Atomic Force Microscopy
APS	Ammonium Persulfate
BCA	Bicinchoninic Acid
Bdnf	Brain-Derived Neurotrophic Factor
bFGF	Basic Fibroblast Growth Factor
BMP	Bone Morphogenetic Protein
BMP-2	Bone Morphogenetic Protein-2
BSA	Bovine Serum Albumin
C	Constant region

C	Cytosine
cDNA	Complementary Deoxyribonucleic Acid
COL1	Collagen Type I
COL3	Collagen Type III
C_T	Threshold Cycle
DCX	Doublecortin
DIC	Differential Interference Contrast
DNA	Deoxyribonucleic Acid
ECL	Enhanced Chemiluminescene
ECM	Extracellular Matrix
EGF	Epidermal Growth Factor
F	Forward
FESEM	Field Emission Scanning Electron Microscopy
FGF	Fibroblast Growth Factor
FTLA	Finite Track-Length Adjusted
G	Guanine
g	Gram
GAPDH	Glyceraldehyde-3-Phosphate Dehydrogenase
gDNA	Genomic Deoxyribonucleic Acid
H	Heavy polypeptide chain
HIV	Human Immunodeficiency Virus

HLF	Human Ligament Fibroblast
HMDS	Hexamethyldisilazane
HPdLF	Human Periodontal Ligament Fibroblast
HPdLLT	Human Periodontal Ligament-like Tissue
HPRT	Hypoxanthine-Guanine Phosphoribosyl Transferase
Hsp	Heat Shock Protein
HUPO	Human Plasma Proteome Project
HV	High Voltage
ICH-GCP	International Conference on Harmonization - Guidelines for Good Clinical Practice
Ier3	Immediate Early Response 3
Ig	Immunoglobulin
JEPeM	Human Research Ethics Committee, Universiti Sains Malaysia
keV	Kilo Electronvolt
kV	Kilo Volt
L	Light polypeptide chain
LAMP-3	Lysosome-Associated Membrane Protein-3
M	Molar
M	Mass
MEM	Minimum Essential Medium
mg	Milligram

miRNA   Micro Ribonucleic Acid

ml   Mililiter

MOH   Ministry of Health Malaysia

mRNA   Messenger Ribonucleic Acid

MSC   Mesenchymal Stem Cell

MVB   Multivesicular Body

nM   Nanomolar

NOSHA   National Oral Health Survey of Adults

NTA   Nanoparticle Tracking Analysis

OD   Optical Density

p   P Value

PBS   Phosphate Buffer Saline

PBST   Phosphate Buffer Saline with Tween-20

PDL   Periodontal Ligament

PLLA   Porous Poly-L-Lactide

PRP   Proline-rich Protein

qPCR   Real-time Polymerase Chain Reaction

R   Reverse

REM   Reflection Electron Microscope

RNA   Ribonucleic Acid

RPM   Revolutions per Minute

rRNA	Ribosomal Ribonucleic Acid
RT	Room Temperature
RT-qPCR	Quantitative Reverse Transcription Polymerase Chain Reaction
RUNX2	Runt-related Transcription Factor 2
SDS	Sodium Dodecyl Sulfate
SDS-PAGE	Sodium Dodecyl Sulfate-Polyacrylamide Gel Electrophoresis
SEM	Scanning Electron Microscope
STEM	Scanning Transmission Electron Microscope
TEM	Transmission Electron Microscope
TEMED	Tetramethylethylenediamine
TGF	Transforming Growth Factor
TGF-β1	Transforming Growth Factor-Beta 1
U	Uracil
V	Variable region
V	Volume
Vgf	VGF Nerve Growth Factor Inducible
WD	Working Distance
WHO	World Health Organization
x	Times
xg	Times Earth's Gravitational Force

PENGASINGAN EKSOSOM AIR LIUR MANUSIA TERHADAP MORFOLOGI DAN EKSPRESI GEN SEL SELANJAR PERIODONTAL LIGAMEN FIBROBLAS MANUSIA

ABSTRAK

Peningkatan insiden penyakit periodontal telah mendorong kepada kemajuan terapi periodontal termasuklah regenerasi tisu periodontal. Pembangunan eksosom yang diperolehi dari air liur manusia telah menjadi salah satu kajian penting untuk menaiktaraf bidang kejuruteraan tisu berasaskan sel. Berikutan kemantapan fungsi yang telah ditunjukkan oleh eksosom, kami telah mengasing dan mengkaji kesan eksosom daripada air liur manusia terhadap pengekspresian gen faktor pertumbuhan asas fibroblas (bFGF) dan kolagen jenis 1 (COL1) bagi sel selanjar periodontal ligamen fibroblas (HPdLF) manusia. Sampel air liur tanpa ransangan yang dikumpul daripada subjek lelaki sihat telah digunakan. Eksosom diasingkan melalui ultraemparan sementara pengesahan dan penentuan keadaan penyimpanan eksosom dalam kehadiran dan ketidakhadiran perencat protease telah dijalankan melalui mikroskop elektron imbasan (SEM), pemendapan Western dan Analisis Penjejakan Nanopartikel (NTA). Perubahan morfologi dan bilangan sel HPdLF yang dirawat dengan eksosom telah diperhatikan dibawah mikroskop inversi dan dikira dibawah penggunaan pewarnaan tripan biru. Tahap ekspresi gen bFGF dan COL1 dalam kehadiran dan ketidakhadiran eksosom daripada air liur manusia bagi sel HPdLF ditentukan melalui kaedah kuantitatif transkripsi berbalik reaksi rantai polimerase (RT-qPCR). Kajian ini telah membuktikan eksosom daripada air liur adalah stabil pada beberapa suhu yang diuji dengan dan tanpa perencat protease. Analisis SEM menunjukkan eksosom adalah bulat, berbentuk vesikel dengan julat saiz di antara 10

nm hingga 100 nm. Keputusan pemendapan Western mengesahkan eksosom yang diasing mengekspresikan penanda eksosom CD63. NTA telah menganggarkan kepekatan dan saiz eksosom secara individual. Tiada perbezaan ketara dalam kedua-dua morfologi dan bilangan sel HPdLF yang dirawat dan tidak dirawat dengan eksosom, namun, eksosom telah meningkatkan kawalatur bagi ekspresi gen bFGF. Kajian ini merumuskan bahawa eksosom daripada air liur manusia adalah biomaterial yang stabil dan mampu meningkatkan kawalatur gen bFGF yang diekspresikan oleh sel HPdLF. Oleh itu, ia berkemungkinan mempunyai potensi untuk menjadi biomaterial alternatif bagi kejuruteraan tisu bagi regenerasi periodontal.

ISOLATION OF HUMAN SALIVARY EXOSOME ON THE MORPHOLOGY AND GENE EXPRESSION OF HUMAN PERIODONTAL LIGAMENT FIBROBLAST CELL LINE

ABSTRACT

The increasing incidence of periodontal diseases has led to the advancement in periodontal therapy including periodontal tissue regeneration. The development of human salivary-derived exosomes has become one of the promising researches to improve cell-based tissue engineering. Due to established functions showed by exosomes, human salivary exosomes were isolated and its effect on the morphology and gene expression of basic fibroblast growth factor (bFGF) and collagen type 1 (COL1) in human periodontal ligament fibroblast (HPdLF) cell line was studied. Unstimulated saliva samples collected from healthy male subjects were used. Exosomes were isolated by ultracentrifugation while the confirmation and establishment of its storage condition were carried out by Scanning Electron Microscopy (SEM), Western blot assay and Nanoparticle Tracking Analysis (NTA) in the presence and absence of protease inhibitor. Morphology and number of HPdLF cells treated with exosomes were viewed under inverted microscope and calculated by using trypan blue respectively. Determination of the gene expression level of bFGF and COL1 in the presence and absence of human salivary exosomes in HPdLF cells was performed using quantitative reverse transcriptase polymerase chain reaction (RT-qPCR). This study showed that salivary exosomes were stable at several temperatures tested with and without protease inhibitor. SEM analysis demonstrated the round shape of exosomes, ranged between 10 nm to 100 nm in diameter. Western blot result confirmed that isolated exosomes expressed exosomal marker CD63. NTA estimated

the concentration and individual size of exosomes. There was no significant difference in the morphology and number of HPdLF cells for both exosome treated and untreated samples, however, exosomes upregulated bFGF gene expression. This study concluded that human salivary exosomes are stable biomaterial and able to upregulate bFGF gene that was expressed by HPdLF cells. Thus, they might have potential to be used as alternative biomaterial in tissue engineering for periodontal regeneration.

CHAPTER I

BACKGROUND OF THE STUDY

1.1   INTRODUCTION

In dentistry, oral diseases and dental improvements have always been one of the main focuses of research. Oral health is essential to general health and quality of life. Good oral health is characterized by a good oral state of being, of an individual and should be free from mouth and facial pain, oral and throat cancer, oral infection and sores, periodontal (gum) disease, tooth decay, tooth loss, and other diseases and disorders that limit an individual's capacity in biting, chewing, smiling, speaking, and psychosocial wellbeing (WHO 2012). Severe periodontal or gum disease, which may result in tooth loss, is found in 15-20% of middle-aged (35-44 years) adults. The statistics in 2012 reported that, 60-90% of school children and nearly 100% of adults have dental cavities worldwide. Globally, about 30% of people aged 65-74 have no natural teeth (WHO, 2012).

The Ministry of Health Malaysia (MOH) also reported on the alarming statistics of oral health among Malaysians. The National Oral Health Survey of Adults (NOSHA) highlighted that 94% of dentate adults have some form of periodontal disease and this has remained unchanged for the past 20 years (MOH, 2013). The percentages of those with moderate periodontal disease increased from 23% in 1990, to 26.3% in 2000 and 47% (unweighted data) in 2010, and in the severe category, from

6% in 1990 to 17.8% in 2010 (MOH, 2013). These statistical figures should raise concern on the awareness of proper oral health care in our population. Therefore, the efforts made by professionals and researchers in the dentistry field coincide with the current high demand for the search for dental problem solutions. Subsequently, these new researches are opening new doors for new substances to be developed on and one of the substances that seem to give a bright hope for a better future in oral health is the human saliva.

With the current increase of periodontal disease cases, the efforts in developing the tissue regeneration to overcome these health problems also increase with time and technology. Even though the conventional periodontal therapies were already well-established, they still have their limitations. Periodontal therapies for periodontal diseases that are commonly performed by dentist are scaling and root planing. These are just a few of the basic treatments done to remove the bacterial pathogens and the surrounding teeth's tissues that are infected. These procedures can stop the disease from worsening; however, they normally do not restore the damaged tissue back to its original form. Hence, tissue engineering in periodontal regeneration has been introduced with the primary goal: to reform the lost tissue and restore to its original form. This also includes the bone structures with well-oriented periodontal ligament anchoring to the dental cementum (Iwata *et al.*, 2014).

Recently, the combination of emerging biotechnologies and salivary diagnostics extended the range of saliva-based diagnostics. From the oral cavity to the whole physiologic system, most compounds found in the blood are also present in saliva. Accordingly, saliva can reflect the physiologic state of the body, including emotional, endocrinal, nutritional and metabolic variations and acts as a source for the monitoring of oral and also systemic health (Spielman and Wong, 2011). Human saliva

contains not only hormones and regular digestive enzymes but also other important proteins (Mese and Matsuo, 2007, Gröschl, 2009). A review paper published in 2012 has discussed the progresses in the analysis of human salivary proteome and their diagnostic possibilities for various diseases. It summarized that there is a significant potential of saliva in basic and clinical research (Kawas *et al.*, 2012). Therefore, more research is needed to discover the potential of biomarkers for early disease detection. With the approaching modern technology, oral fluid diagnostics may become a powerful tool for oral and systemic diagnosis in the future.

Moving forward, since there is already a good amount of research in the topic of salivary proteins and biomarkers, the next step in related research in this field should be explored by including the exosomes section. Exosomes is derived from endocytic membrane vesicles and assumed to contribute in the cell to cell communication. Besides its basic function as transporter for protein and ribonucleic acid (RNA), its content includes messenger RNA (mRNA), microRNA (miRNA); and deoxyribonucleic acid (DNA) (Palanisamy *et al.*, 2010, Thakur *et al.*, 2014). Palanisamy *et al.* (2010) isolated exosomes from human saliva and characterized their structural and transcriptome contents. By demonstrating mRNA presented in salivary exosomes, their findings support the hypothesis that exosomes shuttle RNA between cells and could be a possible resource for disease diagnostics. Even though exosomes have been identified in human saliva, their biochemical and biophysical characteristics are still largely unknown (Palanisamy *et al.*, 2010).

Due to the encouraging biological function of exosomes in salivary fluid and the increasing numbers of the periodontal cases, we would like to find out the possible potential effects of exosomes on periodontal cells. This is done in order to find an innovative approach in resolving oral health problems, in particular, periodontal

diseases. We hypothesize that the salivary exosomes play an important role in influencing and manipulating the growth of the periodontal cells. As reported by previous studies on the salivary components and functions, the exosomes derived from human saliva and its contents can be one of the new factors and material in enhancing the development of periodontal cell advancement.

1.2   PROBLEM STATEMENT

The current periodontal therapeutic procedures are limited to a certain extent only and needs improvements. Therefore, the ultimate goal of periodontal therapy is the regeneration of the damaged periodontal tissue. Even though exosomes can be transported between different cells and influence the physiological pathway in the recipient cells, the proof of the effect of human salivary exosomes on the proliferation of human periodontal ligament fibroblast cells still has not been scientifically established.

1.3   RESEARCH JUSTIFICATION

In researching for the review of related literature, there is a gap of knowledge with the relation or influence of exosomes on periodontal ligament fibroblast. As human saliva-derived exosome is known as a type of biological component which can be extracted easily and economically with less cost needed, this knowledge can be the basis for the development of cell-based therapy for clinical use.

1.4   OBJECTIVES

1.4.1   General Objective

To study the effect of human salivary derived exosomes on the gene expression of Human Periodontal Ligament Fibroblast (HPdLF) cells.

1.4.2   Specific Objectives

1.   To isolate, confirm and establish the storage condition of the human salivary exosomes.

2.   To compare the morphology and the proliferation of HPdLF cells in the presence and absence of human salivary exosomes.

3.   To compare the gene expression level of basic fibroblast growth factor (bFGF) and collagen type 1 (COL1) in the presence and absence of human salivary exosomes in HPdLF cells.

1.5   HYPOTHESIS

Human salivary exosomes upregulate gene expressions of HPdLF cells.

CHAPTER II

LITERATURE REVIEW

2.1   HUMAN SALIVA

Saliva is a clear, biological fluid, secreted inside the mouth by the salivary glands under the control of the sympathetic and parasympathetic autonomic nervous systems. The salivary glands include the parotid, submandibular, sublingual and other minor glands beneath the oral mucosa. The combination of gingival crevice fluid with oral bacteria and debris form this complex mixture of saliva (Humphrey and Williamson, 2001). Different glands secrete different types of saliva. Saliva secreted by parotid gland is watery in consistency while those secreted by submandibular, sublingual glands and minor mucous glands are more viscous due to the high content of glycoproteins (Edgar *et al.*, 2013).

Human saliva contains almost 99% water and the other 1% consists of electrolytes, mucus, glycoproteins, enzymes, and antibacterial compounds. It also contains many growth factors such as epidermal growth factor (EGF) and transforming growth factor (TGF) (Zelles *et al.*, 1995, Humphrey and Williamson, 2001). However, there are differences in the source of secretions and organic content level for unstimulated and stimulated saliva as shown in Table 2.1 and Table 2.2 (Edgar *et al.*, 2013).

Table 2.1: The composition of saliva.

Compositions	Unstimulated Saliva	Stimulated Saliva
Water (%)	99.55	99.53
Solids (Organic and inorganic materials) (%)	0.45	0.47
Flow Rate (ml/min)	0.32 ± 0.23	2.08 ± 0.84
pH	7.04 ± 0.28	7.61 ± 0.17
Total Organic (mmol/L)	**1630.00 ± 720.00**	**1350.00 ± 290.00**
• Protein	830.00 ± 480.00	460.00 ± 200.00
• MUC5B	440.00 ± 520.00	320.00 ± 330.00
• MUC7	317.00 ± 290.00	453.00 ± 390.00
• Amylase	8.40 ± 10.30	5.50 ± 4.70
• Lactoferrin	4.93 ± 0.61	0.00
• Statherin	51.20 ± 49.00	60.90 ± 53.00
• Albumin	79.40 ± 33.30	32.40 ± 27.10
• Glucose	0.20 ± 0.24	0.22 ± 0.17
• Lactate	3.57 ± 1.26	2.65 ± 0.92
• Urea	6.86	2.57 ± 1.64

[Extracted from Edgar *et al.* (2013)]

Table 2.2: The secretion of saliva.

Unstimulated Saliva	Stimulated Saliva
Rich in mucins	Rich in minerals
Viscous	Watery and thin
Secretion percentages based on glands:	Secretion percentages based on glands:
- Submandibular: 60% - Parotid: 25% - Sublingual: 7-8% - Minor gland: 7-8%	- Parotid: 60% - Submandibular: 30% - Sublingual and minor glands: 10%
Functions:	Functions:
- Coating of the teeth - Salivary pellicle - Lubrication of oral mucosa	- Clearance - Buffer system - Remineralization

[Extracted from Edgar *et al.* (2013)]

Saliva has multiple functions, but its main function is the protection against hard-tissue loss and soft-tissue damage. The protection against hard tissue loss is mainly on the tooth substance which can be damaged by abrasion, attrition, erosion and dental caries. Meanwhile the protection against soft tissue damage is by providing the lubricating effect on the oral tissue which may be caused by candidiasis and abrasive mucosal lesions. Moreover, the saliva's protective effect is by their ability to acquire enamel pellicle formation and as lubricating agent. The mucous glycoproteins in saliva, such as MUC5B, MUC7 and proline-rich glycoproteins give a resistant effect to physical damage as they help prevent oral mucosa from dehydration (Dawes, 2008).

In 1995, Schenkels *et al*. published a research article on biochemical composition of human saliva in relation to other mucosal fluids by describing several salivary components and their distributions. Some of the components mentioned are histatins and proline-rich proteins (PRPs). Histatins are polypeptides that possess exceptional anti-fungal and anti-bacterial activities meanwhile PRPs is a closely related unstructured protein group that consists of acidic PRPs and basic PRPs. Among the proteins studied, mucins are the most abundant and are found in saliva alongside with the other acidic PRPs members, α-amylase, cystatins, statherin, lysozyme, and many more. The presence of these proteins in saliva provides important clues for further knowledge and research on the physiology of the proteins, especially in oral cavity (Schenkels *et al.*, 1995).

Another point that should be taken into consideration is that saliva gives many advantages as a diagnostic medium and can also be used in a wide variation of types of testing. Saliva is a better biological sample for multiple noninvasive collections as it does not involve either venipuncture or other methods of introduction of instruments into the body in order to be obtained. This type of sample also is also safer as it does

not involve the different hazards commonly associated with blood collection and other biological fluid samples. A notable example of this is the absence of the usage of sharp object which can cause cross contamination among patients and may bring danger to both patients and health care personnel (Hofman, 2001).

Saliva gives more accurate reflection of the active free hormone concentration in the body, especially for steroid hormones that is involved with specific binding globulins in the blood (Read, 1989). Saliva also contains low concentration of antigens. Therefore, human immunodeficiency virus (HIV) and hepatitis infections are much less of a danger from saliva than from blood (Major *et al.*, 1991). Meanwhile, the collection of saliva sample is inexpensive and convenient compared to other sample collection methods such as diurnal and monthly variations of several steroid hormones that needs multiple samples collected to give meaningful substantial results (Read, 1989).

Aframian *et al.* (2006) had established the normal range of oral mucosal pH and correlates the measurements of salivary flow rate in healthy individuals according to age and gender. Such study is useful in creating possibilities for oral related diseases and disorders like oral malodor, mouth breathing, dysgeusia, acidic diet consumption and gastrointestinal disorders affecting the mouth. They manage to present a reliable, easy and relatively quick method to manipulate the system that may serve as a future diagnostic tool in number of applications (Aframian *et al.*, 2006).

Another study has reported the establishment of human saliva as diagnostic tool and therapeutic material. In conjunction with their study, technologies built for the discovery of salivary biomarkers are also increasing. Researchers reported the finding of salivary proteome which can provide an insight into complex cellular

regulatory networks. A complete catalog of saliva proteome knowledge base had been generated, including the stratification according to their parotid, submandibular/sublingual origins. The international Human Plasma Proteome Project (HUPO), which is a collaboration of many laboratories using MS technology compiled a core dataset of 3020 distinct proteins in 2005 (Spielman and Wong, 2011).

With the many findings to prove the true wonders of human saliva, approach should be taken to investigate the effect of human saliva as a factor for cell growth especially for oral cells.

2.2   HUMAN SALIVARY EXOSOMES

There are three classes of extracellular vesicles (EVs) which are (1) ectosomes or shedding microvesicles (SMVs); (2) apoptotic bodies; and (3) exosomes. These extracellular vesicles were classified based on the mode of biogenesis (formation of membrane vesicles) (Kalra *et al.*, 2016, Merchant *et al.*, 2017). All three EV subtypes are lipid bilayer membranes, however differentiated by their sizes and buoyant densities (Mathivanan *et al.*, 2010), other than by protein markers. Ectosomes (SMVs) are large vesicles ranging from 100-1000 nm in diameter (Muralidharan-Chari *et al.*, 2009), ubiquitously assembled at and released from the plasma membrane through outward protrusion or budding (Stein and Luzio, 1991). Ectosomes molecular compositions are still largely unknown, however recent studies suggested that ectosomes are enriched in cell type dependent proteins (CK18, MMPs, glycoproteins and others) and mainly studied in cancer studies (Kalra *et al.*, 2016). Apoptotic bodies are heterogenous vesicles that are released from cells undergoing apoptotic cell clearance and with diameter ranging around 50-5000 nm (Taylor *et al.*, 2008,

Mathivanan *et al.*, 2010). As these vesicles are involved with apoptosis (cell death), they have external features that can trigger phagocytosis; the final step in cell dismantling and recycling of biomolecule building blocks (Kalra *et al.*, 2016).

Exosomes are small vesicles, with a diameter ranging between 30-120 nm. They are secreted by all types of cultured cells and found in abundance in body fluids including blood, urine, ascites, amniotic fluid and cultured medium of cell cultures (Keller *et al.*, 2006). The exosome is a multi-protein complex capable of degrading various types of RNA molecules (Reviews, 2016). There is a growing interest with the clinical applications of exosomes due to their potential use in various areas like in prognosis, therapy, biomarkers and many more functions (Yang *et al.*, 2016).

Exosomes are small, right-side out structures and formed intracellularly by inward budding of endosome membrane. This result in vesicles-containing endosomes called multivesicular bodies (MVBs). When MVBs fuse with the cell membrane, they release their internal vesicles into the extracellular environment. Once released into extracellular space, these microvesicles are termed exosomes (Gallo *et al.*, 2012). Exosomes contain cell and cell-state specific cargos of protein, mRNA and microRNA (miRNA). They could be transferred into recipient cells to modulate protein synthesis. It is also suggested that exosomes play a significant role in the intercellular communication by transferring both proteomic and genomic materials between cells (Simpson *et al.*, 2009). Due to the functions and biogenesis of the exosomes, it is relevant to focus on exosomes compared to other EVs to study on the proliferation of cells.

In 2009, Gonzalez-Begne and his research team catalogued 491 proteins in the exosomes fraction of human parotid saliva using Multi-Dimensional Protein Identification (MudPIT) mass spectrometry. Seventy two of the proteins detected were previously identified as urinary exosomes proteins as well as proteins that are commonly associated with other tissues and cell type's exosomes (Gonzalez-Begne *et al.*, 2009). From the total of 491 proteins detected from human parotid salivary exosomes fraction, 43% were cytosolic origin proteins that involved in processes such as phosphatidylinositol signaling system, calcium signaling pathway, inositol metabolism, protein export, and signal transduction; 26% were integral plasma membrane proteins that involved in extracellular matrix-receptor interaction, epithelial cell signaling, T-cell and B-cell receptor signaling, cytokine receptor interaction, and antigen processing; and 13% were associated/peripheral plasma membrane proteins (Gonzalez-Begne *et al.*, 2009, Ishikawa *et al.*, 2014).

Meanwhile, proteomic analysis that was done on human whole saliva by Ogawa *et al.* (2011) revealed that exosomes contained Alix, Tsg101, CD63 and Hsp70. It also includes all exosomal markers, immunoglobulin A and polymeric immunoglobulin receptor for both types of exosomes found in the whole saliva (exosome I and exosome II). However, CD26 in whole saliva was present on the exosome II only and metabolically active in cleaving chemokines (CXLCL11 and CXCL12). Both types of exosomes were different in size and protein composition where exosome I was larger than exosome II with an electron-dense structure. Exosome II round shape matched those observed in exosomes from other sources (Ogawa *et al.*, 2011).

Exosomes also represent as a promising candidate for a natural drug delivery as it could be modulated to deliver drugs to target cells and into cells via membrane fusion or endocytosis. Unlike liposome, exosome are generally well tolerated by our bodies and do not have inherent toxicity (Lai *et al.*, 2012). Based on research findings on cell lines and primary cell cultures condition medium derived exosomes and exosomes that are derived from other body fluids (serum/plasma, urine and saliva), the results suggest that extracellular mRNAs, miRNAs and proteins may be contained and protected in membrane-bound structure. Studies have shown that exosomes are selectively taken up by cells distal from their release. They can reprogram the recipient cells due to their active molecular cargo (Pant *et al.*, 2012).

A study done in 2010, had successfully given a result of the structural-mechanical characterization of nanoparticles for exosomes in human saliva. The substructure of single human salivary exosomes was observed by correlating the data with Field Emission Scanning Electron Microscopy (FESEM) and Atomic Force Microscopy (AFM) images. They reported the form of tri-lobed structures of single isolated sub-100 nm human salivary exosomes and demonstrated their reversible elastic nanomechanical properties by quantitative single receptor level detection of the specific markers, CD63 receptors (Sharma *et al.*, 2010).

Palanisamy *et al.* (2010) found that the isolated exosomes from saliva appeared as electron-dense membranous structures and abundant CD63 immunoreactivity on the surface from Electron Microscopy (EM) result. The same trace peak of CD63 enrichment was also shown from Fluorescence-activated cell sorting (FACS) analysis. Furthermore, mRNAs were proven to be present in salivary exosomes as 509 core mRNA transcripts were revealed from their microarray assessment. The RNA present

in exosomes was proven to be functional as modulation of gene expression as observed in keratinocytes incubated with the exosomes (Palanisamy *et al.*, 2010).

A more thorough study in terms of the quantitative, nanoscale morphological, biochemical and surface biomolecular properties of human salivary exosomes should be given priority to further explore the benefits of in developing the newly advanced model of human salivary exosomes identification.

2.3   PERIODONTITIS AND PERIODONTAL REGENERATION

Periodontium components consist of the gingiva, cementum, the periodontal ligament (PDL), and the alveolar bone (Figure 2.3 and Figure 2.4). Gingivae surround the teeth and tightly bound it to the underlying bones which act as an effective barrier to protect deeper tissue (Bath-Balogh and Fehrenbach, 2011). The gingiva is divided anatomically into marginal, attached and interdental areas as shown as in Figure 2.4. Cementum is an acellular, bone-like hard tissue that covers the tooth root and attaches the teeth to the alveolar bone by anchoring the PDL (Edwards and Kanjirath, 2010, Bath-Balogh and Fehrenbach, 2011). The alveolar bone is thickened ridge of bone that contains the tooth sockets to hold the teeth and divides it into the maxillae (ridge on the inferior surface) and the mandible (ridge on the superior surface) (Bath-Balogh and Fehrenbach, 2011).
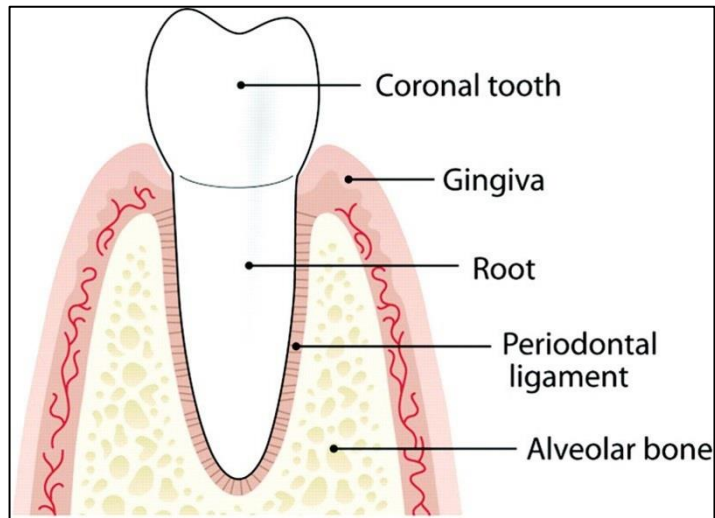
Figure 2.3: Diagram of the components of a normal periodontium with healthy tissues. [Extracted from Edwards and Kanjirath (2010)]
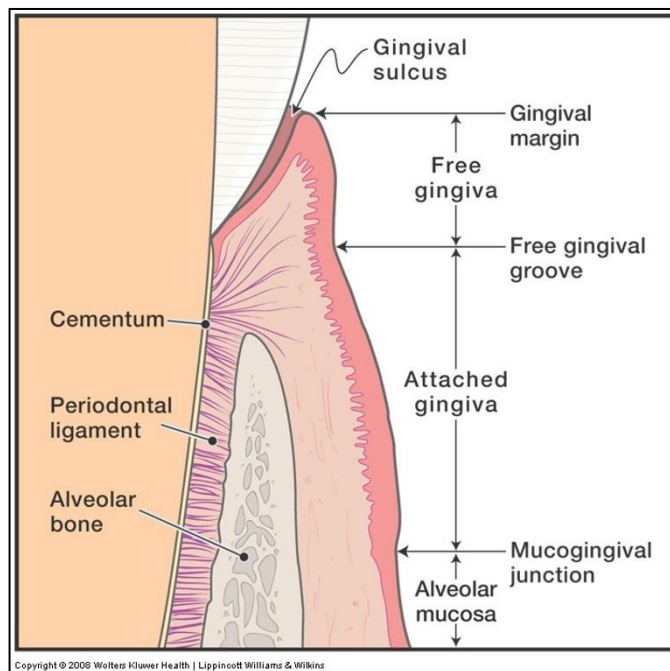
Figure 2.4: Diagram of the gingival tissue in cross section, showing more detailed components of a periodontium. [Extracted from Nield-Gehrig and Willmann (2007)]

The PDL is a group of specialized vascular connective tissue that attaches the tooth to the alveolar bone and connects it to the jaws (McCulloch *et al.*, 2000). The PDL consists of cells (fibroblasts, epithelial cells, undifferentiated mesenchymal cells, and bone and cementum cells) and extracellular compartment of fibers bundles (Type 1, 3 and 5 collagen fibers) that embedded in intercellular substance (Nanci and Bosshardt, 2006). As shown in Figure 2.5, the PDL collagen fibers are categorized according to their orientation and location. The PDL collagen fiber groups are alveolar crest fibers (run from the cervical part of the root to the alveolar bone crest); horizontal fibers (attach to the cementum apical to the alveolar crest fibers and run perpendicularly from the root of the tooth to the alveolar bone); oblique fibers (run in oblique direction to insert into bone coronally); apical fibers (surrounding the apex of the root to the bone); and interradicular fibers (found between roots of multirooted teeth) (Nanci, 2013) (Figure 2.5).

In general, periodontal diseases are defined as the inflammation of the periodontal structures (alveolar bone, PDL, cementum and gingiva) that support the teeth. The most common periodontal inflammations are the plaque-induced inflammatory conditions which are the gingivitis and periodontitis (Popova *et al.*, 2013, Al-Jehani, 2014). Periodontitis is one of the most common disease which affecting high number of patients worldwide. It is characterized by the progressive loss of the alveolar bones around the teeth and the destruction of connective tissue, which without treatment, can lead to the loosening and subsequent loss of teeth. This disease is caused by the chronic inflammation due to the infection of periodontal bacteria that adhere to and grow on the tooth's surface, triggering the immune response against the microorganism (Al-Jehani, 2014, Mathew *et al.*, 2014).
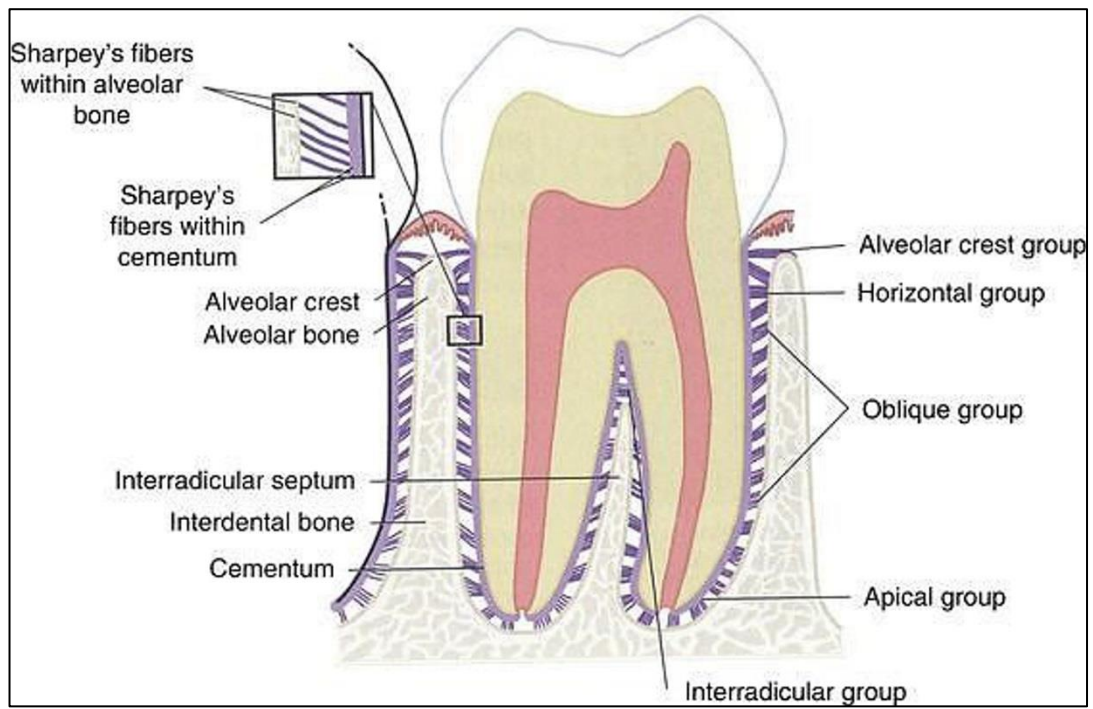
Figure 2.5: Diagram of the types of periodontal ligaments based on their directions and locations. [Extracted from Bath-Balogh and Fehrenbach (2011)]

Periodontitis occur initially in the form of gingivitis, which is the inflammation of the soft tissue above the bone level and the formation of periodontal pocket between the surface of the tooth and the soft tissue. The bacteria then will accumulate in the periodontal pocket and stimulate the production of inflammatory cell mediators (including interleukins, tumor necrosis factor, prostaglandin E2 and matrix metalloproteinases). It then reduces the production of new collagen fibers and pathologically creating deepened sulcus and tissue destruction (Edwards and Kanjirath, 2010, Mathew *et al.*, 2014).

The common treatments of periodontal diseases are scaling and root planing where the sub-gingival calculus (tartar) and biofilm deposits are removed by mechanically scraping it from tooth surfaces. Other than this, it can also be treated with locally administration of antibiotics, Periostat®, to decrease alveolar bone loss and improve the damage caused by periodontal disease. Even though treatment with drug action benefits with minimal side-effects, it does not kill the microorganism that caused the disease. It just able to inhibit the body's host response to destroy the tissue (Mathew *et al.*, 2014). However, as the diseases develop into chronic stages, more various approaches have been introduced, including the regenerative periodontal therapy.

The regenerative periodontal therapy comprises techniques which are designed to restore those destructed parts of the tooth-supporting structures (Ramseier *et al.*, 2000). Based on American Academy of Periodontology (2001) glossary, the term 'regeneration' is defined as the reconstruction of lost and injured tissues in such a way that both the original structures and their function are completely restored. Periodontal regeneration is defined histologically as regeneration of the tooth's supporting tissues, including alveolar bone, periodontal ligament, and cementum over a previously

diseased root surface (American Academy of Periodontology, 2001) (Wang *et al.*, 2005). The aim of the procedure is to restore the lost periodontal tissues by creating new attachment and formation of periodontal ligament with its fibers into newly formed cementum and alveolar bone (Ramseier *et al.*, 2000). This new attachment is the union of connective tissue with a root surface that has been deprived of its original attachment apparatus by epithelial adhesion (Wang *et al.*, 2005).

The conventional established method of periodontal regeneration techniques over the years are mostly focused on trying to improve the biological compatibility of the root surface to new connective tissue attachment. The early techniques introduced includes the interdental denudation/infrabony technique (Prichard, 1957), the use of free gingival grafts to cover the surgical site (Ellegaard *et al.*, 1974) and coronally advanced flap (Fuentes *et al.*, 1993). Then, the guided tissue regeneration (GTR) procedures were developed. GTR-based techniques were used to create epithelial exclusion via repopulation of controlled cells and tissues of the periodontal wound, space maintenance and clot stabilization (Nyman *et al.*, 1982, Caton *et al.*, 1987, Nyman *et al.*, 1987, Wang *et al.*, 2005).

Furthermore, there are also bone replacement grafts such as autografts, allografts, xenografts and alloplasts for the correction of periodontal osseous defects. This is done by increasing the bone level, reducing crestal bone loss, increasing clinical attachment level and reducing probing pocket depths (Reynolds *et al.*, 2003, Wang *et al.*, 2005). Researches also used growth factors and bone morphogenetic proteins (BMPs) for periodontal regeneration. Growth factor plays a major role in regenerative response and differential factor on regenerating periodontal tissues such as transforming growth factor-β (TGF-β), platelet derived growth factor (PDGF), insulin-like growth factor (IGF) and FGF (Wang *et al.*, 2005).

Technologies in periodontal regeneration are evolving as fast as any other medical fields. The emergence of tissue engineering in reconstructing and mimicking natural processes by the usage of synthetic polymer scaffolds as well as development in cell culture methods to produce replacement cells to take over the damaged cells are now the promising future in this field (Bartold, 2015).

2.4   HUMAN PERIODONTAL LIGAMENT FIBROBLAST (HPdLF)

Several researches have used HPdLF cell in their investigation, including tissue engineering and other types of research. This is due to the well adaptation of this cell, especially for *in-vitro* studies. PDL fibroblast has been suggested or identified as multipotent cells with rapid turnover, high modeling capacity and has a remarkable capacity of renewal and repair (Nomura *et al.*, 2012, Alves *et al.*, 2014). PDL was reported to be able to express bone associated molecules and proteins such as alkaline phosphatase (ALP), osteopontin (OPN) and osteocalcin (OCN) (Ivanovski *et al.*, 2001, Lallier, 2005). PDL has progenitor cells that may differentiate into osteoblasts, important for the physiological maintenance of alveolar bone and for tissue repair. PDL, alongside cementoblasts and bone cells are the common precursors residing in periodontal ligament that can lead cell differentiation (Nanci and Bosshardt, 2006).

Periodontal ligament fibroblast (PDLF) is responsible in maintaining the tissue integrity, produce osteoblast-related extracellular matrix proteins and show higher alkaline phosphatase activity compared to gingival fibroblast. It also involved in immune and inflammatory events in periodontal diseases (Han and Amar, 2002, Murakami *et al.*, 2003, Takashiba *et al.*, 2003).

The current trend of HPdLF usage in tissue regeneration plays a major contribution to the tissue engineering clinical field. A group of researchers from Philipps-University of Marburg, Germany published a successful report on a study of periodontal ligament regeneration by periodontal progenitor preseeding on natural tooth root surfaces. Based on their findings, they concluded that periodontal progenitor cell type as well as mineral surface topography and molecular environment play a crucial role in the regeneration of true periodontal anchorage. This in turn would facilitate the use of non-periodontal progenitors and stem cells for periodontal regeneration in the future (Dangaria *et al.*, 2011).

In 2014, a research was done to evaluate the effects of HPdLF behavior when cultured on 2D and 3D collagen gel. The study suggested that the 3D cultures could support HPdLF proliferation and enhance the differentiation and mineralized matrix formation which in turn can lead to a huge potential in periodontal regenerative therapy. The results showed an increase in cell proliferation and gene expression of ALP and COL1, hence indicating the potential of HPdLF to exhibit phenotypic characteristics demonstrated by ALP activity, calcified nodule formation and gene expression of osteogenic markers (Alves *et al.*, 2014).

Based on other studies, PDL cell involvement in periodontal wound healing has become the base of periodontal regeneration concepts used in promoting repopulation of the wound area adjacent to the root surface. Nowadays, researchers are using natural biological mediators which can regulate key cellular events in tissue and regeneration including cell proliferation, chemotaxis, differentiation and matrix synthesis (Nyman *et al.*, 1987, Oates *et al.*, 2001, Manoranjan *et al.*, 2012). Hence, there are many *in vitro* studies focusing on the effect of mediators in the proliferation of HPdLF such as the effect of platelet derived growth factor isoform AB (PDGF-AB)

(Manoranjan *et al.*, 2012), platelet derived growth factor isoform BB (PDGF-BB) (Mumford *et al.*, 2001), TGF-β1 and IL-I (Oates *et al.*, 1993) and others.

Implantation was one of the treatments for periodontal defect and over the years, mesenchymal stem cells have been well established for periodontal regeneration for regenerative dentistry. Currently, researchers are focusing in finding the contribution of implanted PDL cells for periodontal tissue regeneration (Yu *et al.*, 2013).

Referring to previous researches conducted, there is a big potential seen in this type of cell line and can be used in further studies. Additional research and study is not only recommended because of its importance but also for the prospective relevant ideas that can be used in the advancement of oral biology. HPdLF cells can be one of the important and reliable sources which can be manipulated to be used in bioengineering and periodontal regeneration.

2.5   GENE OF INTEREST

HPdLF cells have the ability to differentiate and proliferate into osteoblast-like and cementoblast-like cells, which are important in periodontal regeneration (Yun *et al.*, 2006). In tissue engineering, there are three main elements that are being used to enhance regeneration of bone and periodontal regeneration. They are stem or progenitor cells, conductive scaffolds or extracellular matrix and signaling molecules (Dabra *et al.*, 2012).

Signaling molecules (cytokines) are proteins that affect the growth and function of cells, locally or systematically. The two types of signaling molecules are growth factors and morphogens, which can alter the cell phenotype. The cytokines' pleotropic effect includes mitogenic effects, chemotactic effects and angiogenic effects (Pandit *et al.*, 2011). As one of the growth factor involved in wound healing, bFGF gives pleotropic effects on the cell (Ganapathy *et al.*, 2012) while COL1 is involved in the ECM formation. (Lee *et al.*, 2005). Both elements are important in periodontal regeneration. Hence, in order to study the effects of the human salivary exosomes on the proliferation of HPdLF cells, the bFGF and COL1 gene expression levels were measured in this research.

2.5.1   Fibroblast Growth Factor

FGF are membranes of heparin binding growth factor family with 22 identified members. They are characterized as structurally related signaling molecules (Ornitz and Itoh, 2001). However, the most characterized forms of FGF are basic FGF (bFGF) and acidic FGF (aFGF). They both are single chain proteins that are proteolytically derived from different precursor molecule to generate biologically active proteins of 15,000 molecular weight (Raja *et al.*, 2009).

FGFs are believed to act as competence growth factors that possess the ability to bind to heparin and heparan sulfate. bFGF was revealed to be associated with the extracellular matrix (ECM) and basement membranes by its attachment to heparan sulfate. Three proteins of the FGF family, which are the aFGF, bFGF and keratinocyte growth factor are thought to be important regulators of wound healing as they can stimulate proliferation of many cell types that are involved in the process. This includes vascular endothelial cells, fibroblasts, keratinocytes, chondrocytes and

myoblasts, for both *in vitro* and *in vivo* (Raja *et al.*, 2009). Other than that, bFGF also can induce cell migration, neovascularization and formation of granulation tissue in animal models (Bennett and Schultz, 1993).

To clarify the regulatory mechanisms of periodontal generation, previous study reported the effects of bFGF on proliferation of HPDL cells by examining the ALP activity, formation of calcified nodule and ECM synthesis. They found that bFGF enhanced the proliferative responses of PDL cells in a dose-dependent manner, but inhibited the induction of ALP activity of PDL cells and formed mineralized nodule on PDL cells. As a result, they concluded that bFGF may play an important role in wound healing for periodontal regenerations by inducing growth of immature PDL cells to suppress cytodifferentiation of PDL cells into mineralized tissue forming cells (Takayama *et al.*, 1997).

Takayama *et al.,* (2001) investigated the characterization of the biological effects of bFGF in non-human primates by topically applying gelatinous carrier containing human recombinant bFGF to the inflamed furcation class II defects in male primates. The results obtained indicate that a topical application of bFGF can enhance considerable periodontal regeneration.

Another study reported the effects of bFGF on the regeneration of cementum and periodontal ligament in experimentally induced partial defects in a beagle dog model by applying bFGF in a collagen gel to the defected sites. The results suggested that bFGF in a collagen gel is a suitable therapy for damaged PDL and could lead to readily achievable methods of treatment for periodontal disease (Sato *et al.*, 2004).

2.5.2 Collagen

Collagen expression highly correlates with the ECM production level. The higher the production of collagen; the higher the level of ECM produced. Collagens are the most abundant proteins in ECM and also accounts for 90% of bone morphogenetic protein content (Kern *et al.*, 2001). COL1 is the major type of collagen in PDL (Docheva *et al.*, 2011).

A research study to evaluate the degree of ECM production had been done by comparing the amounts of collagen on aligned and randomly oriented structures by assessing the effects of fiber alignment and direction of mechanical stimuli on the ECM generation of human ligament fibroblast (HLF). They found that it has significantly more collagen (about 15%) produced when cells were mechanically strained, causing the changes in morphology of the cells and therefore affects the ECM production level as well (Lee *et al*., 2005) . An *in vitro* human periodontal ligament-like tissue (HPdLLT) formation with porous poly-L-lactide (PLLA) matrix has been established by three-dimensional culturing of HPdLF with hydrophilically modified ammonia solution. From the cell proliferation analysis, it showed the progressive growth and maturation of ECM by the secretion of COL1 and collagen type III (COL3) (Liao *et al.*, 2013). Since HPdLF is the predominant cell type in PDL and ECM is majorly composed by collagen, it is relevant to use collagen expression level to determine the up-regulation or down-regulation of ECM on the HPdLF when being treated with exosomes derived from human saliva.

CHAPTER III

HUMAN SALIVA-DERIVED EXOSOME: ISOLATION, CONFIRMATION AND ESTABLISHMENT OF THE STORAGE CONDITION

3.1   INTRODUCTION

Exosome research is an expanding field and the development of the isolation methods have rapidly progressing as well. The advance in isolation techniques were summarized in details by a number of review papers published (Lässer *et al.*, 2012, Greening *et al.*, 2015, Zeringer *et al.*, 2015, Li *et al.*, 2017). The established isolation techniques are ultracentrifugation-based techniques (Théry *et al.*, 2006), size-based techniques (Cheruvanky *et al.*, 2007, Lai *et al.*, 2010, Wang *et al.*, 2010), exosome precipitation (Zeringer *et al.*, 2015, Li *et al.*, 2017), immunoaffinity capture-based techniques (Théry *et al.*, 2006, Wang *et al.*, 2010, Zarovni *et al.*, 2015), and microfluidic techniques (Wang *et al.*, 2013, He *et al.*, 2014, Lee *et al.*, 2015).

The increasing efficiency in the technological progress of exosome isolation techniques has widened the choice of techniques to suit the researches. Every technique has its own advantages and disadvantages. For our research, we chose the ultracentrifugation method as it is cost effective and with low contamination risks along with large sample capacity that can yield substantial amounts of exosomes. This technique requires minor technical expertise and considered as moderately time-wise

technique as it consumes little or no sample pretreatments at all (Zeringer *et al.*, 2015). In estimation, about 56% of all exosome isolation techniques employed by users were accounted in exosome research (Zarovni *et al.*, 2015). These ultracentrifugation-based techniques have become the ideal option of isolation method for exosome isolations among researchers.

Exosomes confirmation can be based on their properties which includes the protein marker (Palanisamy *et al.*, 2010, Sharma *et al.*, 2010, Ogawa *et al.*, 2011), their size range, density, morphology, composition and zeta potential (Van Der Pol *et al.*, 2010). This chapter aims to confirm the presence of the isolated exosomes from human saliva based on some properties by Scanning Electron Microscopy (SEM), Western blot and Nanoparticle Tracking Analysis (NTA). Successively, the influence of storage condition on exosomes recovery will be determined.

Investigation on exosome's recovery yield and stability by various storage conditions was previously been done using exosomes originated from certain human cells type (Lee *et al.*, 2016) and human urinary exosomes (Zhou *et al.*, 2006). Their results indicated that different storage temperature and period did influence the exosome's recovery yield and morphology, including the protein and RNA contents from the exosomes (Lee *et al.*, 2016). Their studies also highlighted the importance of protease inhibitor as preservation to maintain the quality and stability of the exosomes (Zhou *et al.*, 2006). Therefore, this research specifically aims on human salivary exosomes and to investigate the effect of different storage conditions and preservations on them.

Until now, exosomes are implied primarily in antigen presentation. Several proteins involved in cell adhesion and co-stimulation that includes ICAM-1, CD86, CD63, and CD82, MHC class I and MHC class II and are commonly expressed in exosomes. There are no exosomes specific markers; consequently, proteins that are enriched in exosomes, from all different cellular origins, are commonly used for exosomes detection. These proteins are tetraspanin (CD9, CD63, and CD81, etc.), cytoskeleton associated protein (ezrin, actin, etc.) and multivesicular biogenesis (TSG101 and Alix). CD63 is a cell surface protein that is included in tetraspanin family which mediates signal transduction events that is important in the regulation of cell development, activation, growth and motility (Figure 3.1). As reported by *Ogawa et al*., (2011), both types of exosomes (exosome I and exosome II) had TSG101 and CD63 exosomal markers. The other studies also reported on exosomal marker CD63 (Michael *et al.*, 2010, Gallo *et al.*, 2012, Lässer *et al.*, 2012, Lee *et al.*, 2016).

Proteins can be detected immunologically following electrophoresis, a technique known as Western blotting. This method relies on the fact that most epitopes (sites recognized by antibodies, generally comprising several amino acids) are still recognizable following denaturing of the protein with SDS and binding to the surface of a membrane. Antibodies are populations of protein molecules (immunoglobulins) that are synthesized by an animal in response to a foreign macromolecule, called an antigen or immunogen (Hoffman *et al.*, 2016). The terms antibody and immunoglobulin (Ig) are used interchangeably, however, immunoglobulins are defined as a family of globular proteins that comprise antibody molecules and molecules having patterns of molecular structure in common with antibodies (Woof and Burton, 2004). The chemical structure of antibodies is related to its function: binding versatility, binding specificity, and biological activity (Liddell, 2013). All

antibodies are constructed from paired heavy (H) and light (L) polypeptide chains, each are composed of constant (C) and variable (V) regions. There are five classes of antibodies based on the structure of their heavy-chain C domain, or isotypes: immunoglobulin G (IgG), IgA, IgM, IgD and IgE (Figure 3.2). IgG, the major antibody in serum is made up of four polypeptide chains, comprising two identical light chains and two identical heavy chains, forming a flexible Y-shaped structure. Each of the four chains has a variable region at its amino terminus, which contribute to the antigen-binding site, and a constant region, which determines the isotype (Figure 3.2) (Maverakis *et al.*, 2015).

Briefly, antibodies bind antigens through weak chemical interactions, and bonding is essentially non-covalent. Electrostatic interactions, hydrogen bonds, van der Waals forces, and hydrophobic interactions are all known to be involved depending on the interaction sites. Antigen and antibody interact through a high affinity binding much like lock and key and exist in a dynamic equilibrium. The overall strength of the binding of an antibody to an antigen is termed as avidity for that antigen. Since antibodies are bivalent or polyvalent, this is the sum of the strengths of individual antibody-antigen interactions. The strength of an individual interaction between a single binding site on an antibody and its target epitope is termed the affinity of that interaction. Avidity and affinity can be judged by the dissociation constant for the interactions they describe. The lower the dissociation constant, the higher the avidity or affinity, and the stronger the interaction (van Oss *et al.*, 1986, Braden *et al.*, 1995). The principles of specificity and cross-reactivity of the antigen-antibody interaction are useful in clinical laboratory for diagnostic purposes. One of the critical features of any successful Western blot is the highly specific interaction between an antibody and an antigen. The antigen, usually a protein or peptide, is the target of the antibody.

Therefore, a technique known as Western blotting commonly carried out where proteins can be detected immunologically following electrophoresis. The choice of a primary antibody for a western blot will depend on the antigen to be detected and what antibodies are available to that antigen. In general, the primary antibody that recognizes the target protein in a western blot is not directly detectable. Therefore, tagged secondary antibodies are used as the means of ultimately detecting the target antigen (indirect detection) (Schwartz and Bochkariov, 2017).

The mixture of proteins separated based on molecular weight on the gel through gel electrophoresis will be transferred onto a membrane where each protein will produce specific bands for detection. The membrane is then incubated with labels antibodies specific to the protein of interest. Primary antibodies are applied first, which then recognized by a secondary antibody which conjugated with color, radioactivity or an enzyme (example, horseradish peroxidase (HRP)) for detection. The unbound antibody is washed off by detergent-containing buffers, leaving only bound antibody to the protein of interest later then detected by developing the film. The detection signal produced under imaging systems (example, luminescence, color reaction and autoradiography) corresponding to the position of the target protein, where only one band should be visible (Mahmood and Yang, 2012).
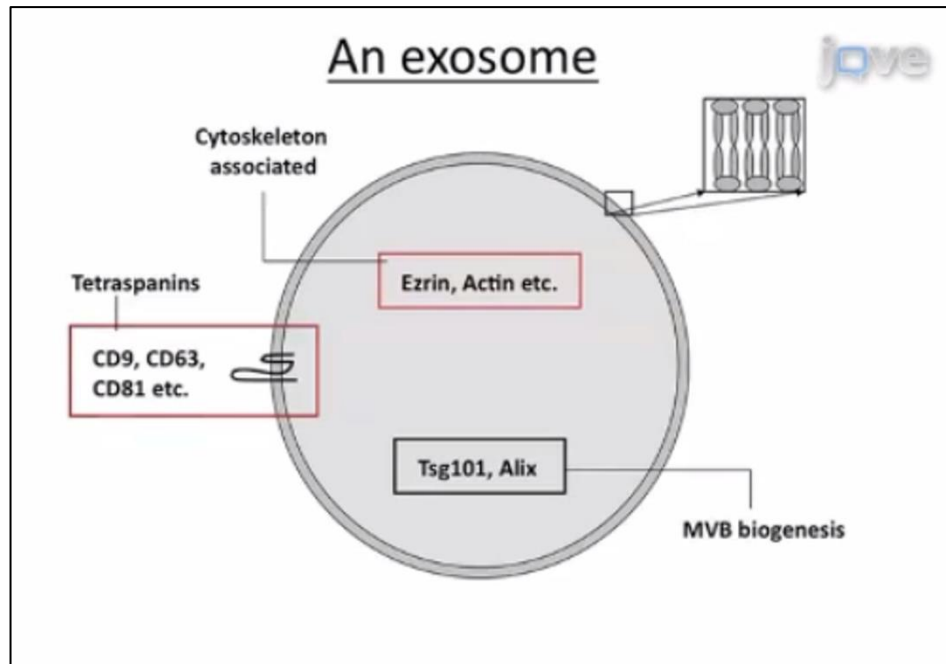
Figure 3.1: The proteins involved in an exosome. [Extracted from Lässer *et al.* (2012)]
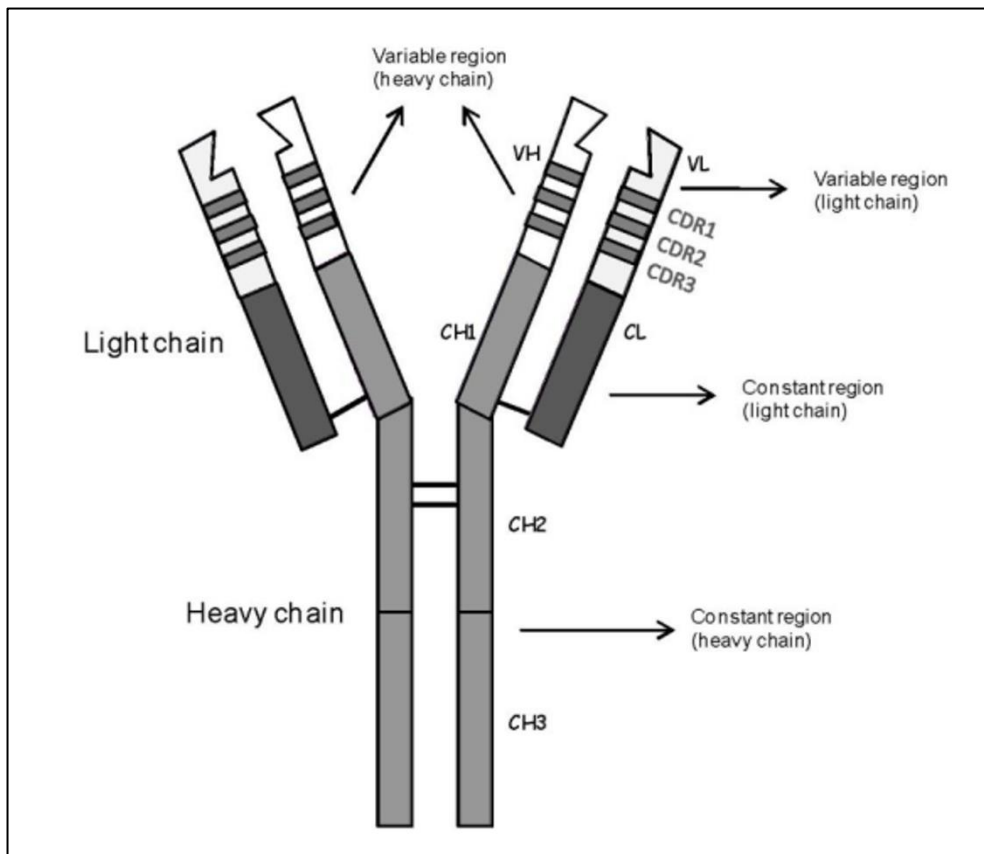
Figure 3.2: The schematic representation of the structure of a monomeric immunoglobulin, showing both heavy and light chain variable regions. VH: heavy chain variable region; VL: light chain variable region; CH: heavy chain constant region; CL: light chain constant region; CDR: complementarity-determining region. [Extracted from Bendandi (2010)]

SEM is one of the electron microscope types alongside with Transmission Electron Microscope (TEM) (Williams and Carter, 1996), Reflection Electron Microscope (REM) (Yagi, 1987) and Scanning Transmission Electron Microscope (STEM) (Crewe, 1974). SEM gives details of specimens in terms of surface topography, their crystalline structure, chemical composition and electrical behavior under various conditions (Vernon-Parry, 2000). Due to the advantages given by SEM, it has also been used to study specifically for characterization of exosomes. Exosomes derived from three different types of human cells (HEK293T, ECFC and MSC) were characterized by both SEM and NTA (Sokolova *et al.*, 2011). The exosomes from plasma obtained from ovarian cancer patients, benign tumor patients and normal control were detected using SEM to determine their sizes (Szajnik *et al.*, 2013). In 2015, a research was done to examine the morphology of exosomes by comparing the images between SEM and TEM as the alternative method and from SEM, they were able to distinguish exosomes from other contaminating extracellular vesicles based on the size distribution (Wu *et al.*, 2015).

Previously, there had been a lack of suitable techniques for quantifying the isolated exosomes. Instead of determining its protein concentration by using protein assay only, recently, the Nanoparticle Tracking Analysis (NTA) technique has been derived and is listed as new reliable alternative method for exosomes quantification too. NTA is a newly developed method for the direct and real-time visualization and analysis of nanoparticles in liquids. This method was used to calculate the yield of exosome isolated by finding out the number of particles in a certain volume of samples.

NTA can calculate the number of particles directly regardless of the concentration level. NTA samples are prepared in an appropriate liquid (water-based solution) with a concentration level of 10^{7}-10^{9} parts/ml and are placed in the sample

chamber with a volume of 0.3 ml. The laser then illuminates the samples in the chamber with the dispersed light being captured by a high sensitivity camera, via the microscope. Particles are individually tracked and visualized on the screen of the control computer. The smallest particles appear as fast-moving dots of light while larger particles diffuse more slowly. The tracking of particles is recorded as 30 seconds video and stored at a rate of 30 frames per second. It is then displayed via the NTA software to show the "individual track" of each particle. The final output is then selected by the user from a simple particle distribution curve to a complex three dimensional display enabling different materials of very similar particle size to be easily differentiated (Malloy, 2011).

Since exosome's recovery yield and its stability is important for further application in research, the collection, storage and confirmation of human salivary exosomes need to be established. Studies on exosomes originated from other sources, reported on the advantageous condition of exosomes. The best storage is at below –70°C for preservation of fresh exosomes derived from human cells (Lee *et al.*, 2016)and at -80°C for urinary exosomes with preservation of protease inhibitor (Zhou *et al.*, 2006). Like exosomes originated from other sources, plasma exosomes were reported to lose majorly their exosomal proteins (including RNA and miRNA) and having a low exosome's recovery yield from storage at 4°C and below (Zhou *et al.*, 2006, Ge *et al.*, 2014, Lee *et al.*, 2016). Even though Michael *et al.* (2010) had successfully isolated exosomal miRNAs from the salivary gland, yet, the studies on the stability of exosomes derived directly from human saliva or any salivary glands sources have not yet been established. Therefore, this research aims to fulfill the gaps so the human salivary exosomes discovery can be further continued.

3.2   METHODOLOGY

3.2.1   Saliva Collection

Human saliva samples were collected in accordance to the recommendations in the International Conference on Harmonization - Guidelines for Good Clinical Practice (ICH-GCP) and the Declaration of Helsinki (European Medicines Agency, 2002). The protocol was approved by the Human Research Ethics Committee, Universiti Sains Malaysia (JEPeM) (FWA Reg. No: 00007781; IRB Reg. No: 00004494) (Appendix 1).

Saliva samples were collected from five healthy male subjects following ethical approval. Male subjects were chosen as they reported to secrete higher volume of saliva (Heintze *et al.*, 1983, Lagerlof and Dawes, 1984, Ekström *et al.*, 2012) and more exosomes yield (Díaz-Martín *et al.*, 2013) compared to female. Written informed consent forms and questionnaires (Appendix 2) data sheets were obtained from all participants. All the subjects were free of malignancy, periodontitis, immunodeficiency, autoimmune disorders, hepatitis, or HIV infection. The subjects' ages were ranged between 25 to 35 years old.

During collection, subjects were asked to refrain from eating, drinking, or using oral hygiene products for at least one hour prior to collection and were asked to rinse their mouth with water. After that, about 5 ml of unstimulated saliva was collected from each subject by using paper cup and transferred into centrifuge tubes.

3.2.2 Exosomes Isolation

The protocol for human salivary exosomes isolation was based on Shahidan (2011) on miRNA analysis on saliva. The saliva sample collected was centrifuged at 6,000xg for 20 minutes to remove debris. The supernatant was then removed and allocated in six different tubes. Samples were divided into two groups; a) with the presence of protease inhibitor (ratio 1:1) and b) absence of protease inhibitor.

To establish the methods for the storage and preservation of human salivary exosomes, a pair of samples consist from both groups (1 tube of sample with protease inhibitor and 1 tube of sample without protease inhibitor) were subjected to three different protocols: a) stored at 4ºC for 1 hour; b) stored at -20ºC for 1 week; and c) stored at -80ºC for 1 month. After the storage period, all samples underwent the exosomes collection process (Zhou *et al.*, 2006). All samples were properly labelled as shown in Appendix 3.

Samples were proceeded with ultracentrifugation at 110,000xg for 2 hours at 4ºC. Following ultracentrifugation, supernatant was removed and the pellet containing the exosomes was kept. The pellet was dissolved in 1 ml of Phosphate Buffer Saline (PBS) (Appendix 5) for each tube and being keep in -20°C until further use (Shahidan, 2011). The flow of the isolation process is shown in Appendix 4.

3.2.3 Scanning Electron Microscopy

Morphology of exosomes was inspected under SEM. The -20ºC isolated exosomes sample with protein inhibitor was randomly chosen for viewing under. Method of slide preparation was based on the method of Yamada *et al.,* (2012) with a slight modification to suit the sample type. One hundred microliter of isolated exosomes was

diluted in 100 µl of Phosphate Buffer Saline (PBS) (Bio-Rad, United States) (ratio 1:1) and re-suspended in the tube. Five microliters of the sample was dropped on a round glass slide and slowly spread. The slide was then let to dry in an air dryer incubator for 24 hours (Yamada *et al.*, 2012). The slide was then coated with gold-coating and was viewed under a High Voltage (HV) of 5.00 kV and a Working Distance (WD) of 9.5 mm. The slide was viewed under 30,000x, 50,000x, 60,000x and 120,000x magnifications respectively. The image obtained was measured to find out the range in sizes of exosomes.

3.2.4   Bradford Protein Assay

Protein concentration of the human salivary exosomes was determined using Coomassie Plus Bradford Assay Kit (Thermo Scientific, United States). Unknown protein concentrations of samples were estimated by referring them to the absorbance obtained from standard protein dilutions series. A standard curve was plotted using the average blank-corrected 595 nm measurement for each Bovine Serum Albumin (BSA) standard against its concentration as suggested by manufacturer in Appendix 7. About 5 µl for each standard or samples was pipetted into the microplate wells and then 250 µl of the Coomassie Reagent was added to each well.

The samples in the well plate are let to mix with plate shaker for 30 seconds and incubated for 10 minutes at room temperature (RT). The absorbance was measured at 600 nm with Sunrise^{TM} ELISA Microplate Reader (Tecan, Switzerland). The average 600 nm measurement for the Blank replicates was subtracted from all other individual standard and samples replicates. A curve-fitting algorithm was plotted for the standard curve and the protein concentrations of samples were determined and tabulated.

3.2.5 SDS-PAGE and Western blot

The presence of exosomes in all samples was confirmed with SDS-PAGE and Western blotting. All reagents used were from Bio-Rad (United States). For this research, anti-CD63 used was CD63 Monoclonal Antibody (MEM-259) (catalog number MA1-19281) (ThermoFisher Scientific, United States). For housekeeping gene, the used antibody was β-actin Monoclonal Antibody (AC-15) (catalog number MA1-91399) (ThermoFisher Scientific, United States). Both antibodies were conjugated with Goat anti-Mouse IgG (H+L) Secondary Antibody, HRP (catalog number 31430) (ThermoFisher Scientific, United States). The datasheets for these antibodies are included in Appendix 5.

The 12% resolving gel was prepared (Appendix 5) and let to solidify for 15 minutes. Gel was then stacked with stacking gel (Appendix 5) and let to properly solidify. Working sample buffer was prepared by adding 10 µl of 2-mercapthoethanol with 90 µl of sample buffer (Appendix 5) and 1 µl of blue dye. All samples were prepared by adding 6 µl of sample with 6 µl of working sample buffer, then boiled for 3 minutes and spun at 12,000xg for 3 minutes.

Electrophoresis components were assembled and the chamber was filled with Running Buffer as prepared in Appendix 5. Five microliter of sample was loaded to the wells alongside with pre-stained molecular weight markers. SDS-PAGE was run at 30 mA (200 Volts) per gel for 40 minutes. Gels were then soaked in Coomassie Blue solution and incubated on shaker for 30-40 minutes. The excess dye solution was removed and de-stained with de-staining solution (Appendix 5). The gels were left on shaker overnight to completely remove the background. Gels were then rinsed with double distilled water before viewing.

SDS-PAGE gels prepared were then transferred onto nitrocellulose membrane. Equilibrate absorbent pads, nitrocellulose membrane and gel were briefly soaked in transfer buffer and kept on shaker for 10-15 minutes before arranged on Trans-Blot® SD Semi-Dry Transfer Cell. Instrument was run at 12 V for 30 minutes. After transfer step, nitrocellulose membrane was blocked with 5% non-fat dry milk in Phosphate Buffer Saline with Tween-20 (PBST) (Bio-Rad, United States) (Appendix 5) for 1 hour at room temperature. Membranes were then incubated with anti-CD63 and anti-β-actin (housekeeping gene) (1: 1,000 in PBS) (Appendix 5) for 2 hours at room temperature, each and consecutively, under gentle agitation on a shaker. Membranes were washed with PBST before conjugated with Goat anti-Mouse IgG (H+L) secondary antibody, horseradish peroxidase (HRP) conjugate for 2 hours at room temperature. The antibody-antigen reactions were visualized by using Enhanced Chemiluminescene (ECL) Plus western blotting detection (Pierce, United States) and viewed under Alpha Innotech Fluorchem FC2. PageRuler Pre-Stained Protein Ladder (ThermoFisher Scientific, United States) was used to check the molecular weight of the targeted protein. Quantification of protein bands densitometry was carried out using ImageJ 1.50i software by Wayne Rasband (National Institutes of Health, USA). ImageJ is an open source image processing program for multidimensional image data with a focus on scientific imaging. The bands intensity values were resulted in peak area unit of pixel.

3.2.6 Nanoparticle Tracking Analysis

The number of human saliva-derived exosome particles per volume, the mean size of exosomes and the concentration of the exosomes yield was calculated. This was done using NanoSIGHT NS300 (Malvern, United Kingdom) with the NTA Version: NTA 3.0. Exosome samples were diluted to 100x in PBS for viewing under the camera. About 0.3 ml of samples was injected into the sample chamber and directly viewed. The images of the exosomes were captured in 10 seconds movie form and the particles tracked were calculated and graphed. The results obtained were in "finite track-length adjusted" (FTLA) size per concentration graph and average FTLA size per concentration graph with standard error of the mean. The 10 seconds movie form of exosomes were presented in image capture form for the 1st second, 3rd second, 5th second and 8th second to show the real live visualization done by the NTA.

3.3   RESULTS

3.3.1   Confirmation of Exosomes

This research confirmed the exosomes isolated based on the exosomes morphology, size range, and the presence of the protein markers. Exosomes morphology was analyzed by SEM. SEM image viewed under 30,000x magnifications (Figure 3.3) showed the exosomes presented in clumps. When the magnifications were increased to 50,000x magnifications (Figure 3.4), the fine shape of exosomes which were round, in vesicle form could be observed. Meanwhile, a single exosome could be observed under 120,000x magnifications (Figure 3.5).

Exosomes size range was analyzed by SEM and NTA. From SEM analysis, Figure 3.4 showed measurement of five exosomes with 55.37 nm, 53.18 nm, 67.02nm, 67,09 nm and 43.71 nm of diameter. Figure 3.5 shows the singular exosome detected with size of 87.72 nm. The few randomly chosen exosomes measured sizes were within the exosome size range as reported by previous researches. This result was supported by another exosomes size range analysis, the NTA. The size distribution profile data (Figure 3.8) were shown over-plotted in Graph A, meanwhile the mean and the standard error of the mean were shown in Graph B, with the size of the exosomes peaks annotated. The average FTLA sizes per concentration result from detection graphs (Figure 3.8) were merged and represented in tabulated form (Table 3.9). The modal particle sizes were described as in few keys. The SD is the measure of the width (spread) of the size distribution profile. The D10, D50 and D90 values indicated percent under size, as shown the Table 3.9, 50% of the exosomes 189.4 nm or smaller, giving another indication of the spread of particles sizes within the sample. The mean size of exosomes was 203.0 nm with 11.00 nm of standard error.

The exosomes protein markers were detected from SDS-PAGE and Western blot analysis. SDS-PAGE gel (Figure 3.6) showed protein separation bands for all samples and the Western blot result (Figure 3.7) showed the detection of CD63 (70 kDa) in all samples. The β-actin, the internal control protein marker was also detected. Band intensity or thickness are indicative of the proteins relative abundance, therefore, from the results analyzed by ImageJ software, 4°C sample without protease inhibitor (6204.326 pixel) showed strongest bands intensity compared to other samples (Appendix 6). However, for this research, the purpose of Western blot was to check on the presence of human salivary exosome protein markers only, while actual quantification of protein concentrations was based on Bradford protein assay results.

Human salivary exosomes concentration was also measured by Bradford protein assay and NTA. The concentration was measured to determine the exosomes treatment concentration for cell culture procedure (Chapter V). Protein assay chart (Figure 3.11) showed the values for all samples concentrations in µg/ml. Different from protein assay, NTA analysis measured exosomes concentration by visualization and detection of exosome particles per volume. The -20°C sample with protease inhibitor was chosen for measurement. The concentration calculated from NTA was 7.99×10^8 particles/ml and about 40.5 particles were captured per frame (Table 3.9). The images of the exosomes were also captured from the 10 seconds real-time movie of exosomes visualization (Figure 3.10). These results were concurrent with the findings that had been reported on the morphology and visualization from other researches (Ogawa *et al.*, 2011, Wu *et al.*, 2015).

Therefore, from the morphology, size range and protein marker analysis results we can now confirm that exosomes were successfully isolated from human saliva samples.
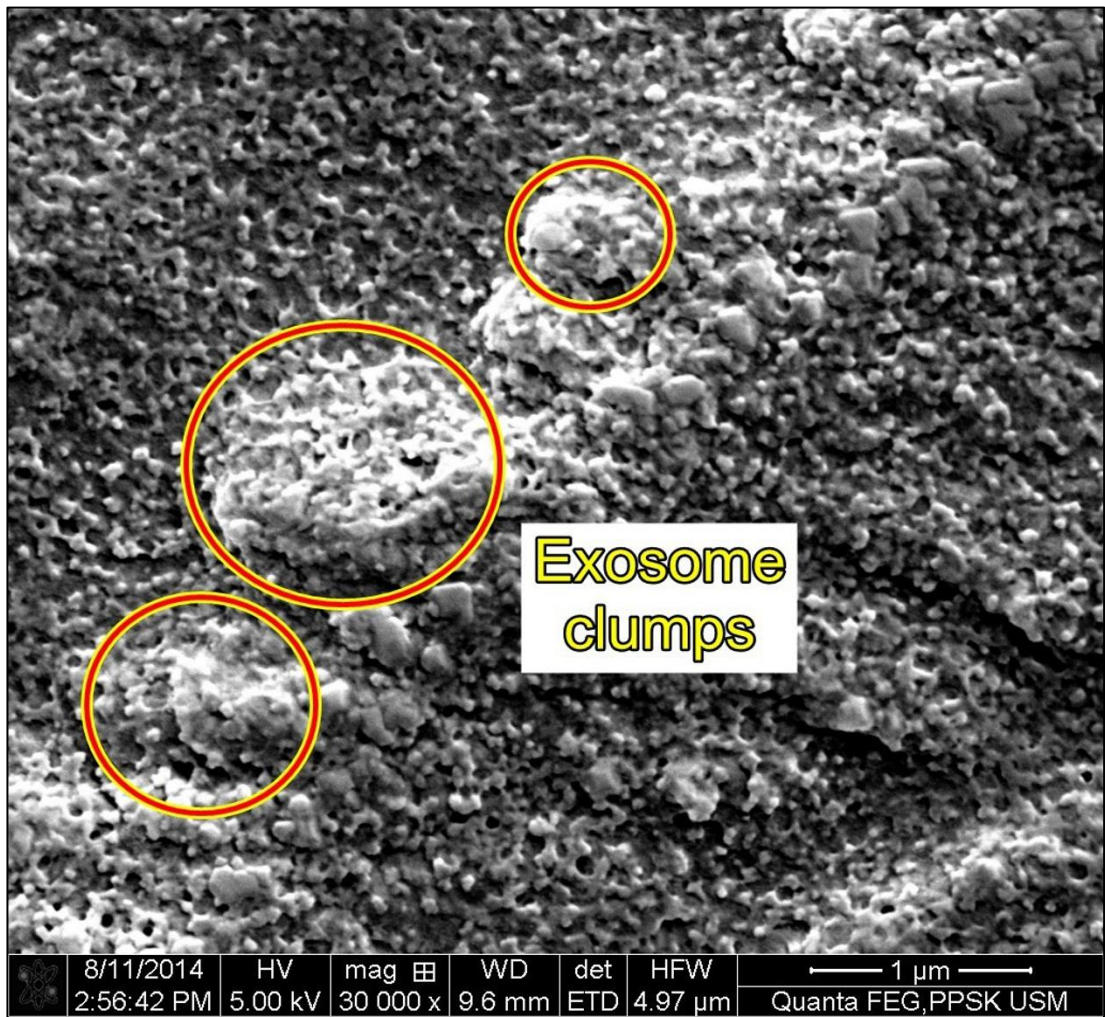
Figure 3.3: The image of human salivary exosomes under 30,000x magnifications of SEM. The exosomes appeared to be in clumps.
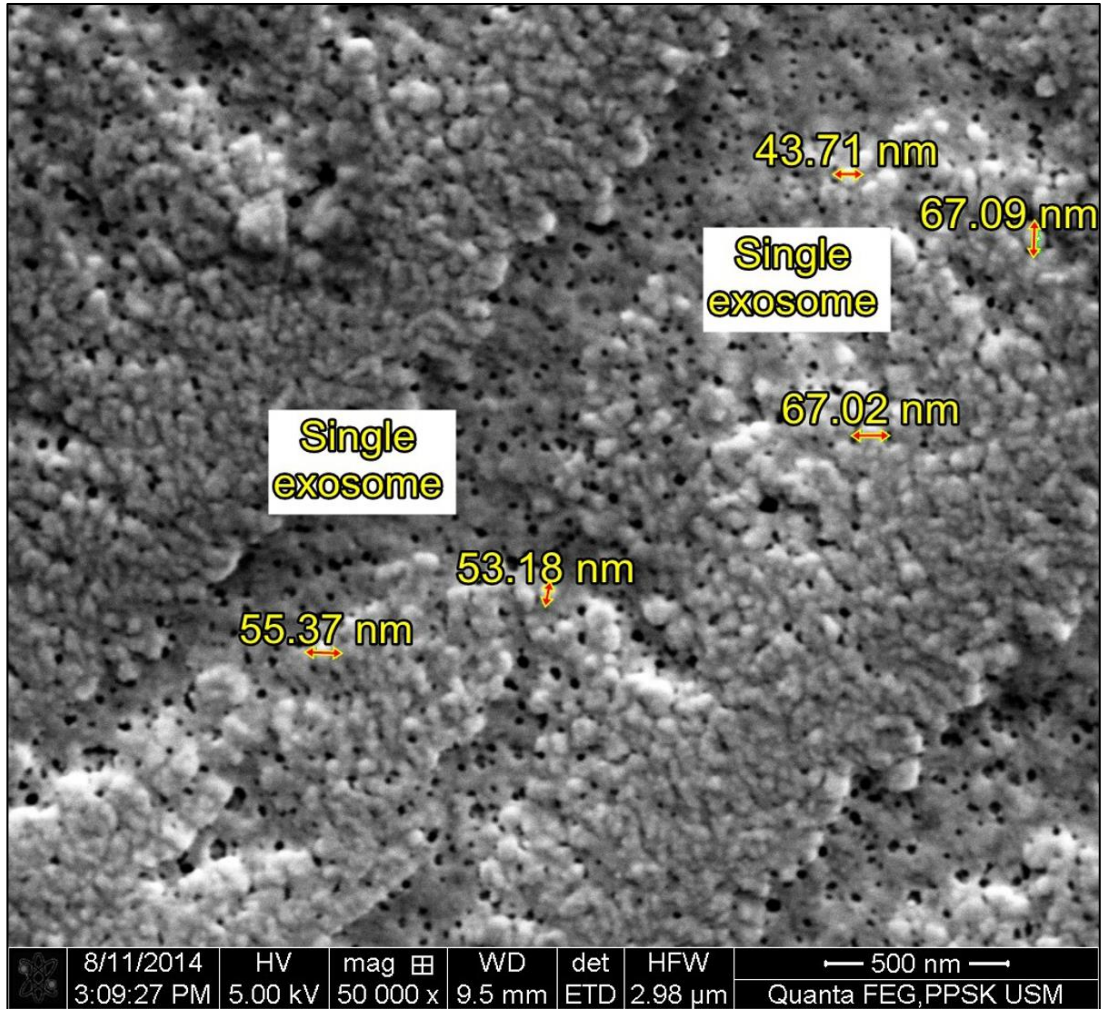
Figure 3.4: The image of human salivary exosomes under 50,000x magnifications of SEM. Few randomly chosen exosome vesicles were measured and their sizes are stated as labeled.
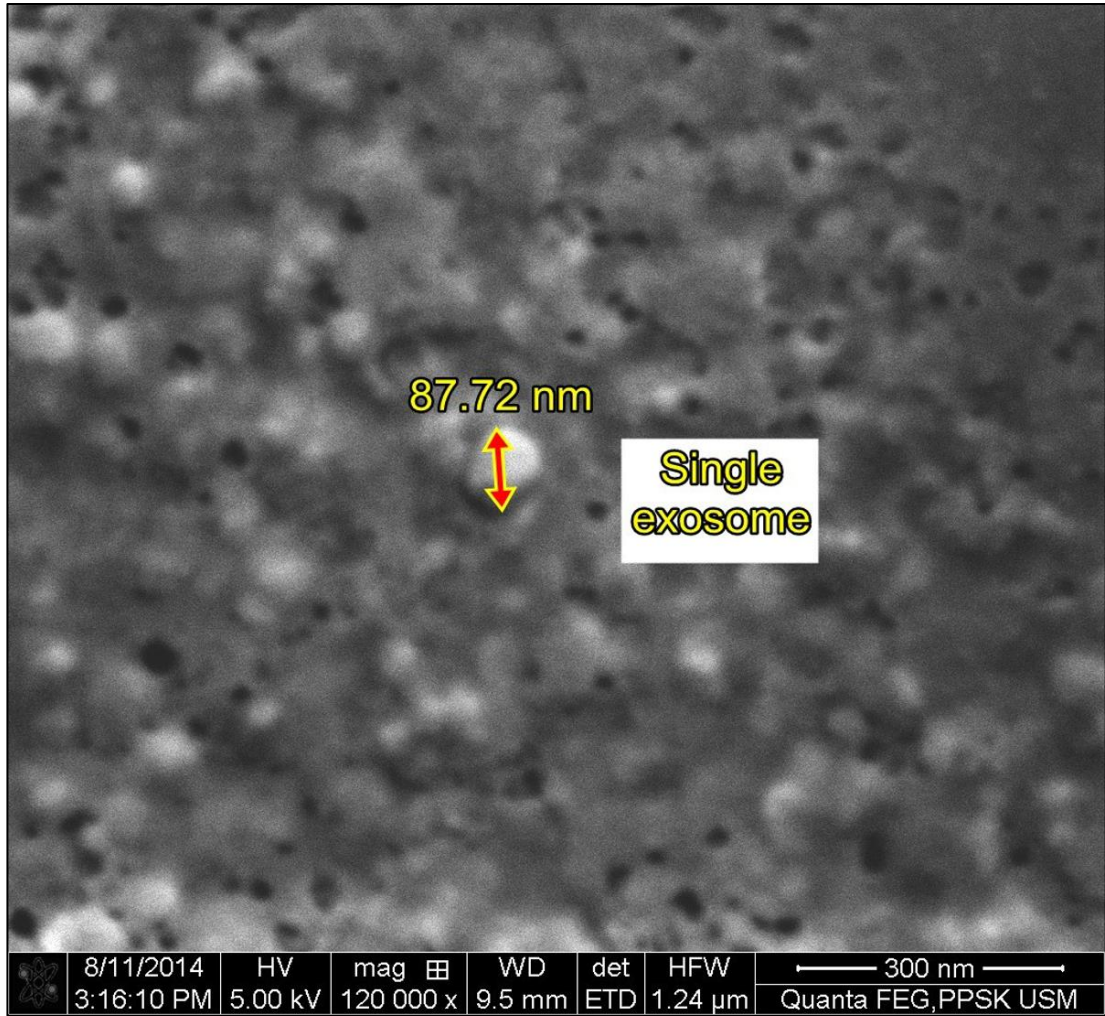
Figure 3.5: The image of human salivary exosomes under 120,000x magnifications of SEM. A single vesicle of exosome was captured and the size was measured and stated as labeled.
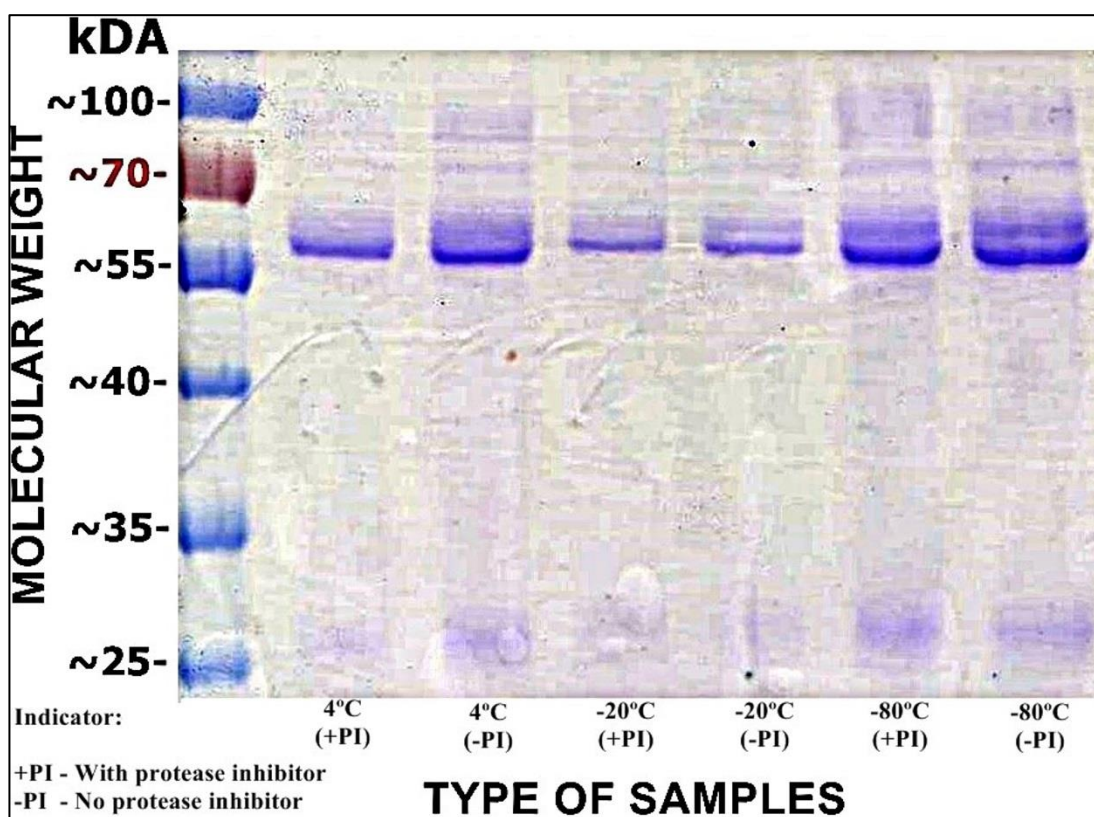
Figure 3.6: The image of the SDS-PAGE for all types of samples. The result shows the protein separation bands appeared almost the same intensity for all samples regardless with or without protease inhibitor for all conditions with the strongest band detected at 55-70 kDa of molecular weight.
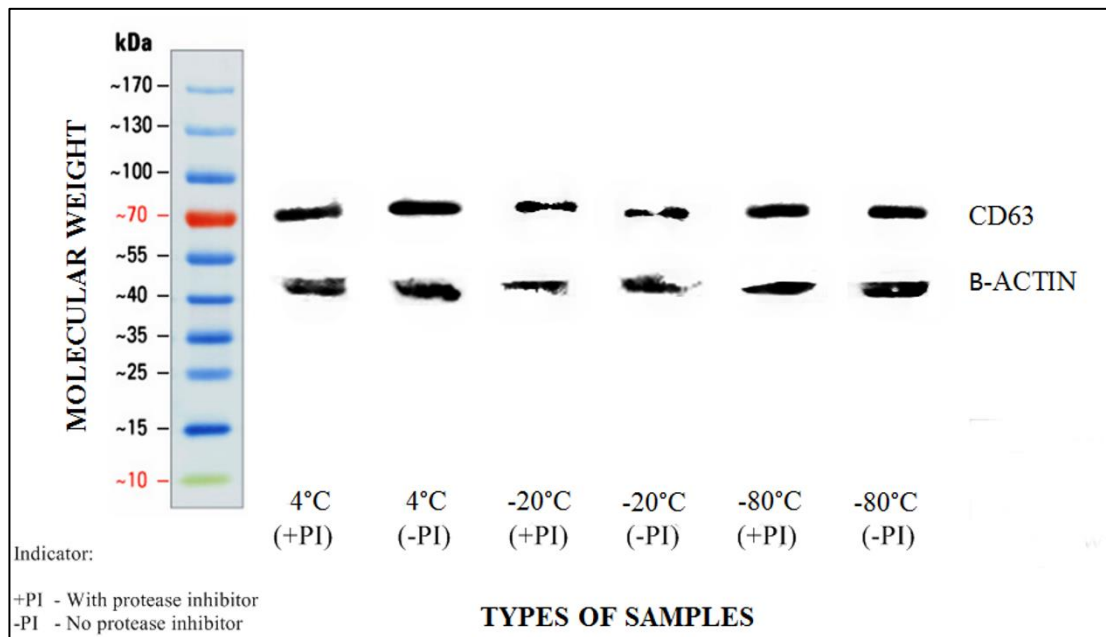
Figure 3.7: CD63 expression by western blot. All samples showed expression of CD63 at 70 kDa and the β-actin antibody was used as internal control.
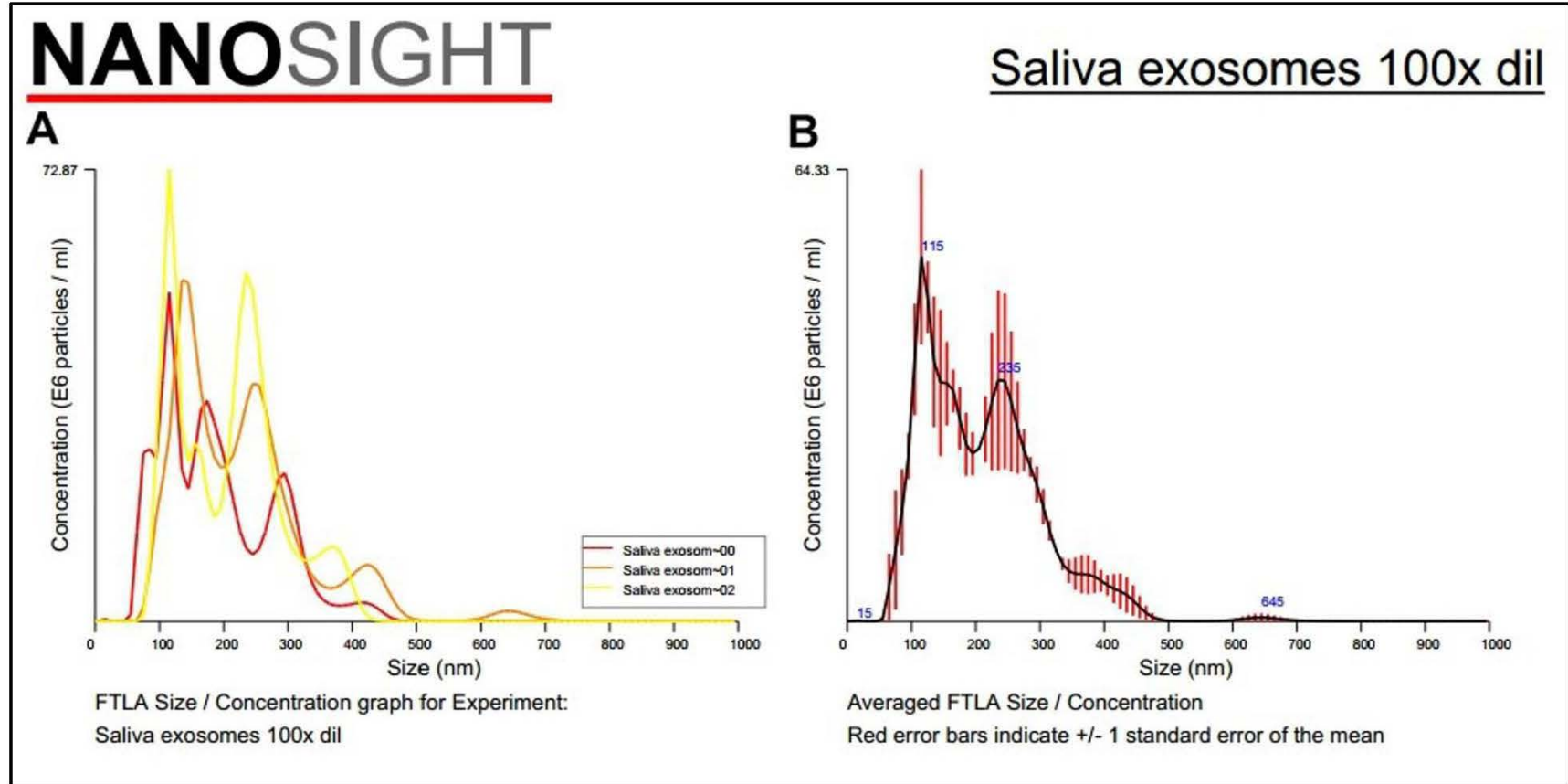
Figure 3.8: Nanoparticle Tracking Analysis (NTA) on the human salivary exosomes under 100x dilutions. Graph A shows the FTLA size per concentration graph, taken as triplicates and Graph B showed the averaged FTLA size per concentration with standard error of the mean.

Table 3.9: The result list obtained from NTA result.

Nanoparticle Tracking Analysis	
Statistics	**Merged Data Results (nm)**
Mean	204.20
Mode	117.20
SD	92.90
D10	96.80
D50	187.50
D90	317.60
Statistics	**Mean ± Standard Error (nm)**
Mean	203.00 ± 11.00
Mode	123.50 ± 8.10
SD	90.80 ± 7.00
D10	96.60 ± 9.20
D50	189.40 ± 13.30
D90	325.20 ± 18.70
Concentration	$7.99^8 \pm 5.29^7$ particles/ml
	40.50 ± 2.70 particles/frame
	50.20 ± 1.90 centers/frame
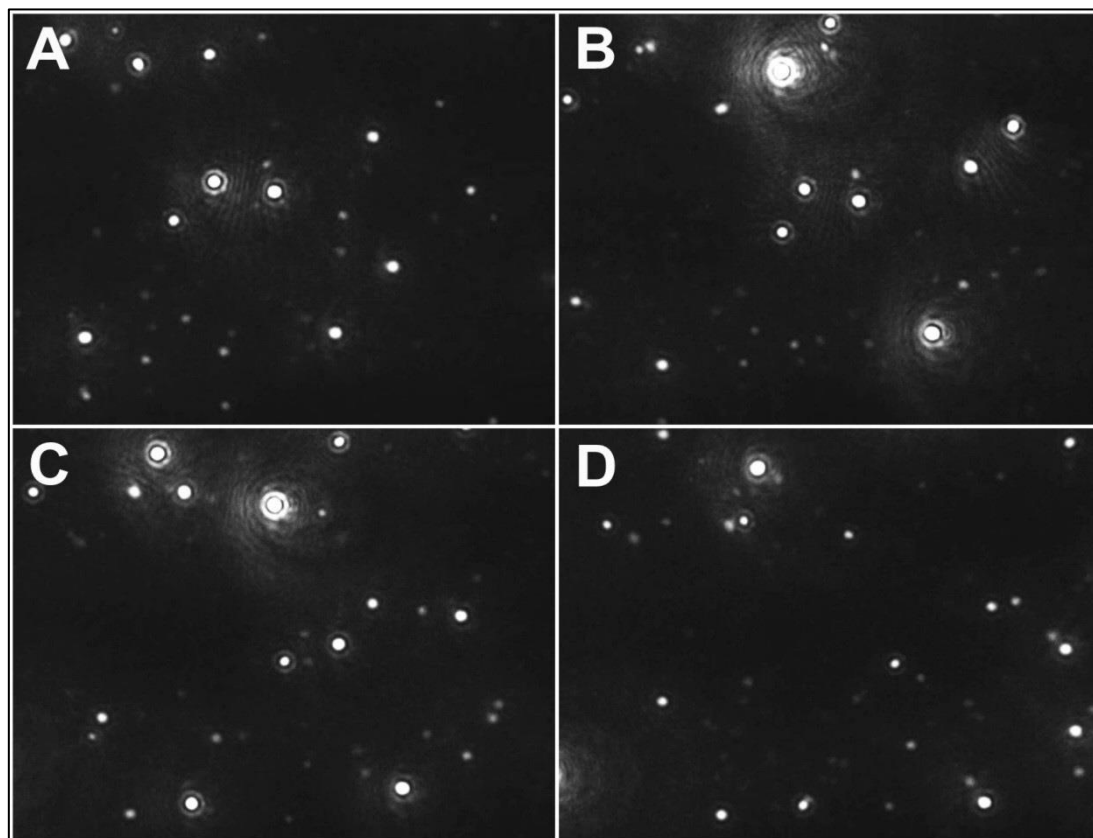
Figure 3.10: The images of 10 seconds real-time movie of exosomes captured from NTA. A) Image was captured at the 1st second. B) Image was captured at the 3rd second. C) Image was captured at the 5th second. D) Image was captured at the 8th second. Exosomes appeared to be shiny and in vesicle form.

The Protein Concentration Against The Different Temperature Storage And Presence Of Protease Inhibitors
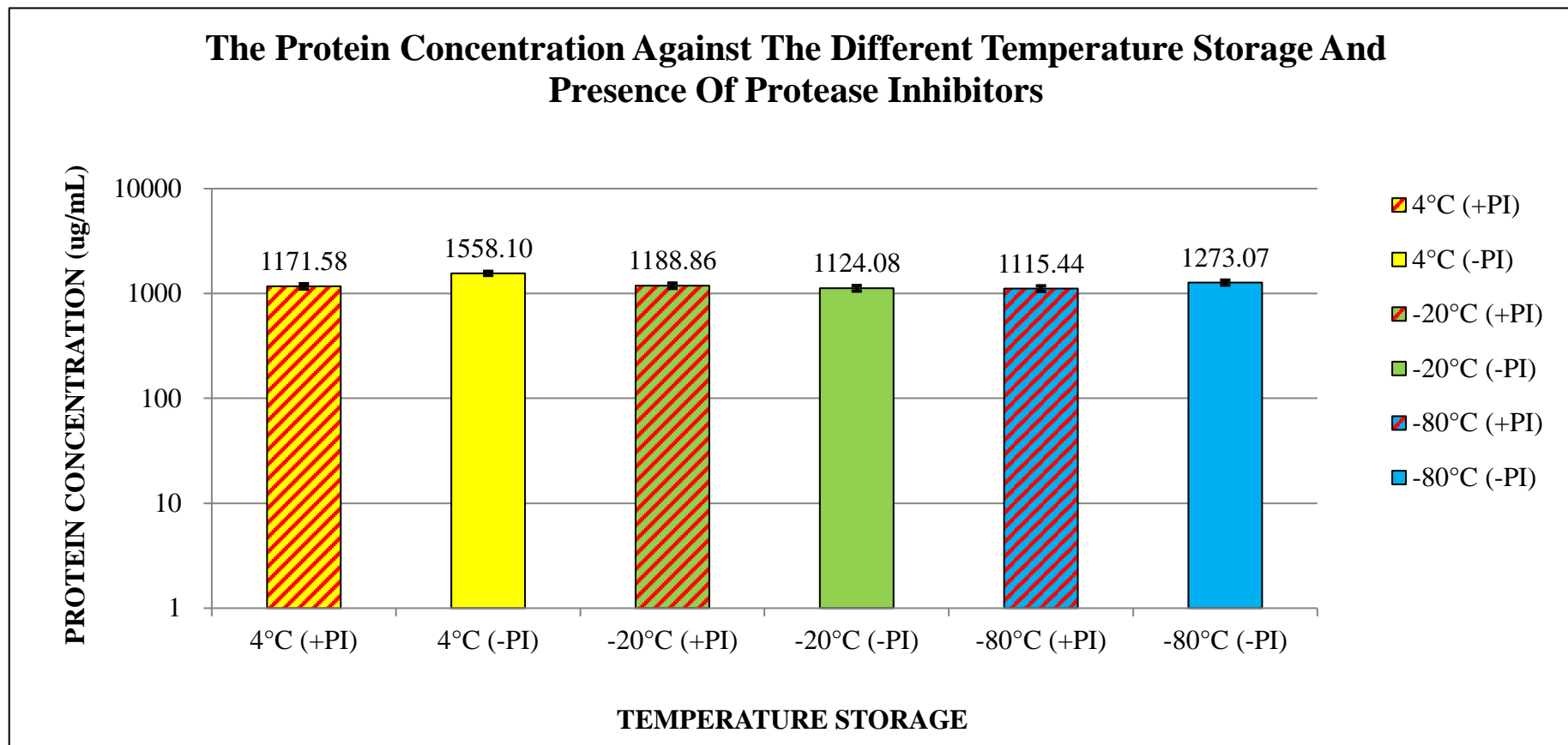
*(+PI) indicates samples with addition of protease inhibitor; (-PI) indicates samples without protease inhibitor

Figure 3.11: The chart of the protein concentration against the different temperature and presence of protease inhibitors with no significant difference. (Data represent the mean value ± SEM; EXCEL 2016: Statistical Inference for Two-variable Regression Analysis, $p > 0.05$).

3.3.2 Establishment of Human salivary exosomes Storage Condition

The results showed that there was no effect of protease inhibitor on the human salivary exosomes. There was also no effect of different temperature storage on the human salivary exosomes. Details of the effect of both conditions on the samples are as follows:

(a) Effect of Protease Inhibitor

The sample result for protein assay (Figure 3.11) showed no significant difference ($p > 0.05$) on the concentration value, regardless of the presence of protease inhibitors. The SDS-PAGE analysis of Comassie blue solution (Figure 3.6) and Western blot analysis of CD63 (Figure 3.7) showed that there was no significant difference in the intensity of the signals or bands, regardless of the protease inhibitors addition. The intensity of the bands was also correlated to the protein concentration of exosome samples. The expression of CD63 in all samples showed the exosomes are intact, with or without addition of protease inhibitor.

(b) Effect of Different Temperature Storage

The protein concentration for all exosomes samples (Figure 3.11) from protein assay showed no significant difference on the concentration value regardless of the storage temperature ($p > 0.05$). SDS-PAGE analysis of target protein (Figure 3.6) and Western blot analysis of CD63 (Figure 3.7) showed that there was no significant difference in the intensity of the signals or bands, regardless of the different temperature storage. All exosomes samples expressed CD63, hence showing that exosomes were still intact and not affected by the temperature storage.

3.4 DISCUSSIONS

SEM image viewed under 30,000x magnifications (Figure 3.3) showed crowded exosomes. This may be due to the high concentration of exosomes in the sample suspension. Even without fixation method, the exosomes were still distinct enough for observation and viewing. This therefore supports that the exosome is a stable component. The image obtained from SEM supported the presence of exosomes by showing the fine shape of exosome which were round, with a size range in between 10 nm-100 nm (Figure 3.3, Figure 3.4 and Figure 3.5).

The NTA results showed that the sizes calculated were quite inconsistent with the variation in the sizes that were captured (Figure 3.8 and Table 3.9). The published range of exosomes size was within 30-120 nm (Keller *et al.*, 2006, Sharma *et al.*, 2010). The mean size obtained from NTA was 203 nm, showing a larger particle captured. The standard deviation was 90.8 ± 7.0 nm, which also showed the huge difference in sizes range. Since NTA was not able to manually separate particles, the larger size detected was probably due to the clumping of exosomes themselves. Therefore, even under the 100x dilutions, the exosomes concentration calculated was high and if the clumping of exosomes was put into consideration, the actual concentration of exosomes could be higher where exosomes are in a single form. Notwithstanding, this showed that human salivary exosomes could be yielded even with low amount of human saliva.

As observed, the clumping of exosomes as seen under SEM and showed by NTA results still manifested even though the steps to prevent it from occurring had been carried out before all the tests were done. The same exosomes clumping matter had been

encountered by other previous researches as well. The clumping of exosomes is primarily due to the shearing forces of the exosomes during the preparation process (Schneider and Simons, 2013) and exosome aggregation (Hood *et al.*, 2014). NTA managed to give us the concentration of the exosomes isolated, however, due to the clumping of the exosomes, we believe it was more reliable to use exosomes protein concentration from protein assay result (Section 3.3.2) for treatment of cells *in vitro*.

All samples were detected to express CD63, the exosomes protein marker by SDS-PAGE and Western blot analysis. All samples showed significant bands on the membrane. This finding not only confirmed the presence of exosomes in the isolated human saliva via protein markers, but also proved that the exosomes were intact and in good quality for further tests.

Protease inhibitors are protein molecules that inhibit the function of enzyme protease from performing proteolysis, which is the catabolism of protein by hydrolysis of the peptide bonds that link amino acids together in a polypeptide chain. Due to the ability of inhibiting the proteolysis, protease inhibitor can act as a preservative of biological fluid and samples from the degradation of proteins. Our results showed that the addition of protease inhibitor into the saliva samples yielded no significant difference ($p > 0.05$) on the exosomes protein concentration, the intensity of signal on the SDS-PAGE membranes and CD63 detection on Western blot. These findings contradicted with the results published by Zhou *et al*., (2006) which showed that urinary exosomes samples without protease inhibitors had no signal or decreased signal compared to the samples with protease inhibitor. Therefore, they suggested that protease inhibitors are necessary to prevent the degradation of urinary exosomes protein (Zhou *et al.*, 2006). However, our

results showed that human saliva-derived exosome is stable and do not need any preservation; this suggests that human saliva may contain important substances which prevent the degradation of exosomes that need further investigation.

Our findings showed there was no effect of different temperature storages on the exosomes protein concentration, the intensity of signal on the SDS-PAGE membranes and CD63 detection on Western blot results for all samples. These findings were supported by another finding by Ge *et al*., (2014). Their result on plasma exosomes tested also showed no significant influence on the exosomal miRNA despite the different storage conditions, except for short term storage at 4ºC (Ge *et al.*, 2014). When compared with the results obtained from Zhou *et al.,* (2006), urinary exosomes showed a major loss of proteins due to the freezing at -20ºC from their Bicinchoninic Acid (BCA) protein assay, gel-electrophoresis and Comassie-Blue staining tests results. However, their result showed that freezing at -80ºC preserved all the specific urinary exosome-associated protein samples. In contrast, human salivary exosomes in our study showed stability at each temperature (4°C, -20°C and -80°C) tested.

Mechanism that controls exosomes stability has not yet being studied in detail. However, from previous study by Ogawa *et al.,* (2011) on proteomic analysis of exosomes from human saliva, we can suggest that the proteins contained in exosomes may play a significant role in regulating their stability. One of the proteins that may influence the stability of the exosomes is heat shock protein (Hsp) 70. Hsp70 has been proven to be present in human salivary exosomes and has been listed as one of the exosomal biomarker (Ogawa *et al.*, 2011). In general, heat shock protein functions as chaperone for other cellular proteins in assisting the folding and the establishment of protein shapes and

prevent protein aggregation as well as helping in stabilize unfolded proteins (Buchner and Walter, 2002). Keller *et al.,* (2011) study on Hsp70 presence in exosomes from three different body fluids (amniotic fluid, saliva and urine) supported our result too. Compared to salivary exosomes, only three out of 12 sucrose density fractions of urinary exosomes were detected by Western blot analysis, meanwhile Hsp70 were detected in all 12 fractions salivary exosomes. The higher level of Hsp70 detected in salivary exosome from that result supported our results that salivary exosomes therefore have higher stability compared to urinary exosomes. The most recent study done on exosome's recovery yield and stability by various storage condition and from all the proteins investigated; only Hsp70 shows the minimum loss even for the long storage in room temperature .

3.5 CONCLUSION

Exosomes from human saliva has successfully isolated and their presence was confirmed from its morphology, correct size and protein markers. The results show no significant difference in the quantity and quality of the exosomes whether with and without the addition of protease inhibitors or under different temperature storage. Hence, proving that human saliva-derived exosome is a stable and consistent biological fluid sample.

CHAPTER IV

MORPHOLOGY AND PROLIFERATION OF HUMAN PERIODONTAL

LIGAMENT FIBROBLAST IN THE PRESENCE OF EXOSOMES

4.1   INTRODUCTION

The previous chapter reports on the preparation of human salivary exosomes. Exosomes were successfully isolated, confirmed and subsequently, the establishment of exosomes storage condition was also achieved. In this chapter, the effect of isolated human salivary exosomes on morphology and proliferation of (HPdLF) cells were studied. As discussed in the literature review, there are many functions of exosomes that have been enumerated; however, the study of the effect of human salivary exosomes on periodontal cells proliferation and regeneration is still has not yet been established.

For this study, the concentration of exosomes that was applied onto HPdLF cells to study the effect on gene expression was decided to be 10 µg/ml. A few other researches on exosomes effect had been using this concentration as one of the dose concentration range or as minimum concentration that managed to give effect on the targeted cells studied (Clayton *et al.*, 2007, Liu *et al.*, 2010, Silverman *et al.*, 2010, Christianson *et al.*, 2013, Xiao *et al.*, 2013).

The morphology of HPdLF will be examined under inverted light microscope and SEM while the proliferation assay (cell count) will be performed by trypan blue staining. Normal fibroblast shows the filopodia, lamellipodia, cytoplasmic vesicles and the cytoskeleton as the basic cell morphology. Under SEM, these criteria can be observed in detail and the average sizes of the cells can be measured and compared.

Two of the components of basic cell morphology are lamellipodia and filopodia. Lamellipodia are flat extensions with thickness of 0.1-0.5 µm meanwhile filopodia are cylindrical or conical processes, usually 10-20 µm long with small diameter (Al-Hisayat *et al.*, 2012). Lamellipodia are projections which can be found in the leading edge of the cells by the assembly of focal adhesions when cell membranes are in contact with the substratum, consequently make the cells able to migrate forward. Lamellipodia contain mikrospikes (the ribs of actin) (Small *et al.*, 2002). The extension of mikrospikes will create filopodia (frontier lamellipodium) that protrude into antennae-like shape to the surrounding environment. These slender cytoplasmic projections that extend beyond the leading edge of lamellipodia are initiated and elongated by the polymerization, convergence and crosslinking of actin filaments (Mattila and Lappalainen, 2008). As with lamellipodia, filopodia's main function also involve in cell migration and wound healing.

Cytoplasmic vesicles are membrane-limited structures derived from the plasma membrane or various intracellular membranes which function as storage, transport or in metabolism. Cytoskeleton function is to maintain the shape and internal organization of the cell, as well as to provide mechanical support (Alberts *et al.*, 2008). With this in mind, both cytoplasmic vesicles and cytoskeleton will also be observed as it is viewable especially under SEM.

The cells morphology criterions are referred to the differential interference contrast (DIC) image of HeLa cell as shown in Figure 4.1. HeLa cell image is used as reference since HPdLF cell reference image for SEM is not currently available. However, HeLa cell is a reliable reference as it is the oldest and the most used human cell line and because the criteria is similar to that of fibroblast cells.

This chapter will mainly focus on the results of the human salivary exosomes effect on the HPdLF cells, especially in morphology changes and the proliferation rate.
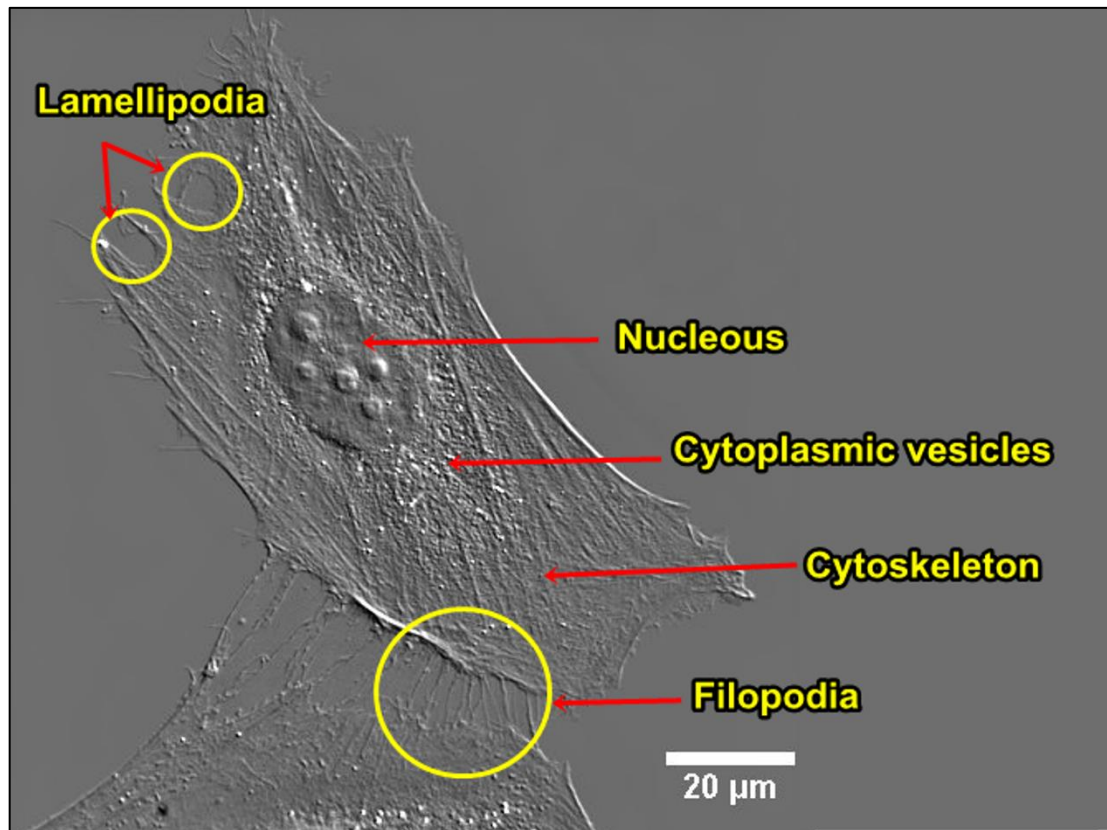
Figure 4.1: The DIC image of HeLa cell. This image shows the cell morphology criterion labels that were used as the references for HPdLF cell observation. [Image courtesy of Dave Mason (Sée and Lévy Labs)]

4.2 METHODOLOGY

4.2.1 Cell Culture

Human Periodontal Ligament Fibroblast (Cryopreserved) (CC-7049) cell line used from LONZA Clonetics[TM] Human Fibroblast Cell Systems (LONZA, Switzerland). The growth medium used was Stromal Cell Medium BulletKit[TM] (CC-3205) which contains Stromal Cell Basal Medium (CC-3204) and growth supplements such as hFGF-B, Insulin, FBS and GA-1000.

Cell culture procedures were performed using Reagent Pack[TM] (CC-5034) which contains Trypsin/EDTA, Trypsin Neutralizing Solution and HEPES Buffered Saline Solution. All methods were done by following the instruction manuals. For cell maintenance, cells were cultured in HyClone[TM] Minimum Essential Medium (MEM) Alpha Modification with L-glutamine, ribo- and deoxyribonucleotides (SH30265.01). Sample tests were done in biological triplicates for both control and treatment samples.

Throughout this process, all cells were cultured at 37°C with 5% CO_2. HPdLF cells were cultured in T75 flasks until confluent and later were re-seeded into 6 wells plate with 90,000 cells and 2 ml of media per well. The plate was incubated for 24 hours for cell attachment. The images of the cells growth were taken (Figure 4.3).

4.2.2   HPdLF Treatment with Human Salivary Exosomes

After 24 hours of incubation, cells were treated with 10 µg/ml of exosomes (Xiao *et al.*, 2013) suspended in medium solution for three wells (B1, B2 and B3) and the rest of the three wells (A1, A2 and A3) were treated with regular basic medium (α-MEM) as control (Figure 4.2). The cells were left to grow for another 24 hours at the same incubation condition (37°C with 5% $CO_{2)}$, then, the images of the cells were recaptured to look for any changes in the morphology and proliferation activity (Figure 4.4). The cells were then proceeded for cell counting and RNA extraction process.
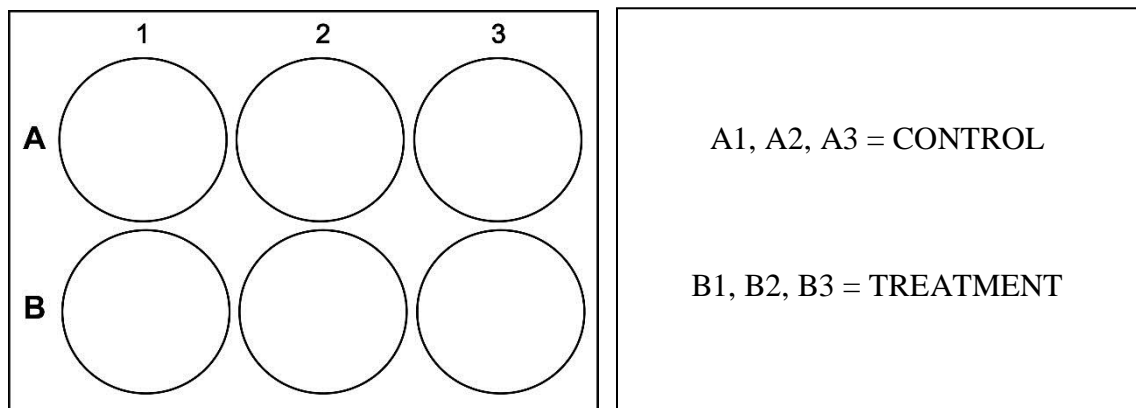
Figure 4.2: The diagrammatic presentation of experiment in 6 well plate. Control group: A1, A2, A3; treatment group: B1, B2, B3.

4.2.3   Cell Image Viewing

Cell images were captured after 24 hours of culturing in 6 well plates (Figure 4.3) and recaptured after 24 hours of treatment (Figure 4.4). Comparisons of images were done under inverted microscope (Carl Zeiss, Germany) with same magnifications and light intensity. The area of observation was chosen randomly as in the best to represent the average of whole well.

4.2.4   Cell Count

Cell counts were carried out to compare the proliferation activity before and after intervention. This method was done using Trypan Blue Solution (0.4%) (Sigma-Aldrich, United States). About 10 µl of cell suspension (after cells detachment and resuspended in 1 ml medium) was mixed with 10 µl of trypan blue and spread onto hemocytometer slide. The cells were counted under inverted microscope. Calculation steps are shown in Appendix 8.

4.2.5   Scanning Electron Microscopy

For this part, another set of samples were cultured on poly-L-lysine glass slides that undergone the same procedure of cell culture and treatment as mentioned in Section 4.2.1 and Section 4.2.2. Both control and treatment samples were then undergone to SEM viewing to observe for any morphological changes on the cells after exosomes treatment. Procedure of cells fixation was based on Al-Hisayat *et al.* (2012) protocol and "General Sample Preparation for Scanning Electron Microscope Protocol" produced by Scanning Electron Microscope Laboratory, School of Health Sciences, Universiti Sains Malaysia,

(Appendix 9) with a slight alteration to suit the type of cell. Reagents used for this procedure were from Bio-Rad (United States).

After 24 hours of treatment period, all media was aspirated out from both control and treated cells. Samples were fixed with 1 ml of 2.5% glutaraldehyde for 30 minutes and then washed with PBS three times for 10 minutes each before continuing with the dehydration process. A dehydration series of 30%, 50%, 70% and 90% of ethanol were used for all samples for 30 minutes each. Samples then fixed twice in 100% ethanol for 30 minutes each time. Samples were finally fixed in 1:1 of Hexamethyldisilazane (HMDS) and 100% ethanol for 15 minutes and 100% HMDS for another 15 minutes. The samples underwent drying process by incubation in air-dryer for overnight before being mounted on aluminum stub and coated with gold coating for viewing (Al-Hisayat *et al.*, 2012).

The samples were viewed under a FEI Quanta 450 Scanning Electron Microscope (FEI, United States) at 5.00 kV of high-voltage (HV) and 10.6 mm of working distance (WD). Images were captured under 200x, 5,000x, and 100,000x magnifications and the changes in morphology for both groups were observed.

4.3 RESULTS

4.3.1 Cell Morphology (Inverted Microscope)
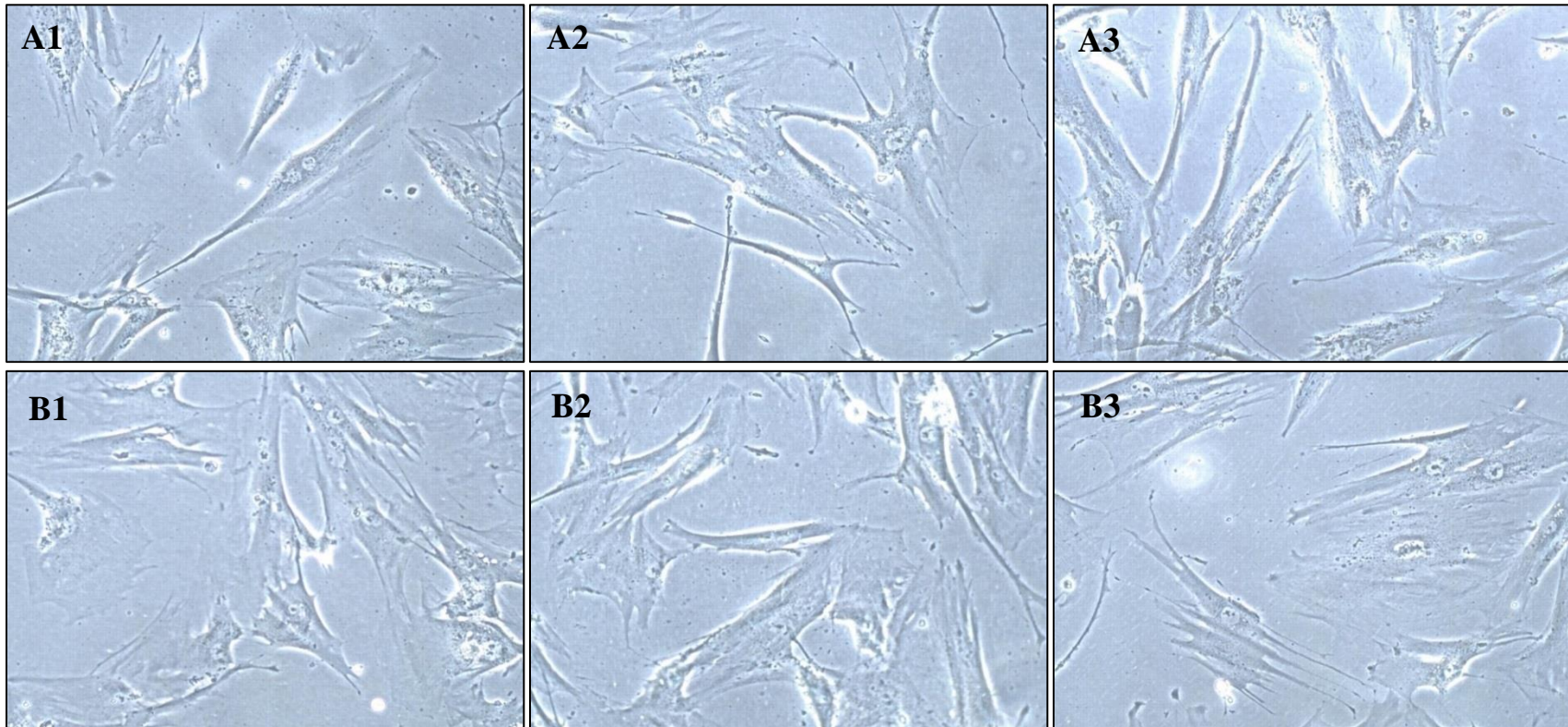
Figure 4.3: The HPdLF cells 24 hours' post seeding under 10x magnifications. The morphology of HPdLF cells were viewed under inverted microscope. The elongated shape of the cells was perfectly shown and there was no difference in the morphology for all wells. All wells also had the same confluence percentage at this time.
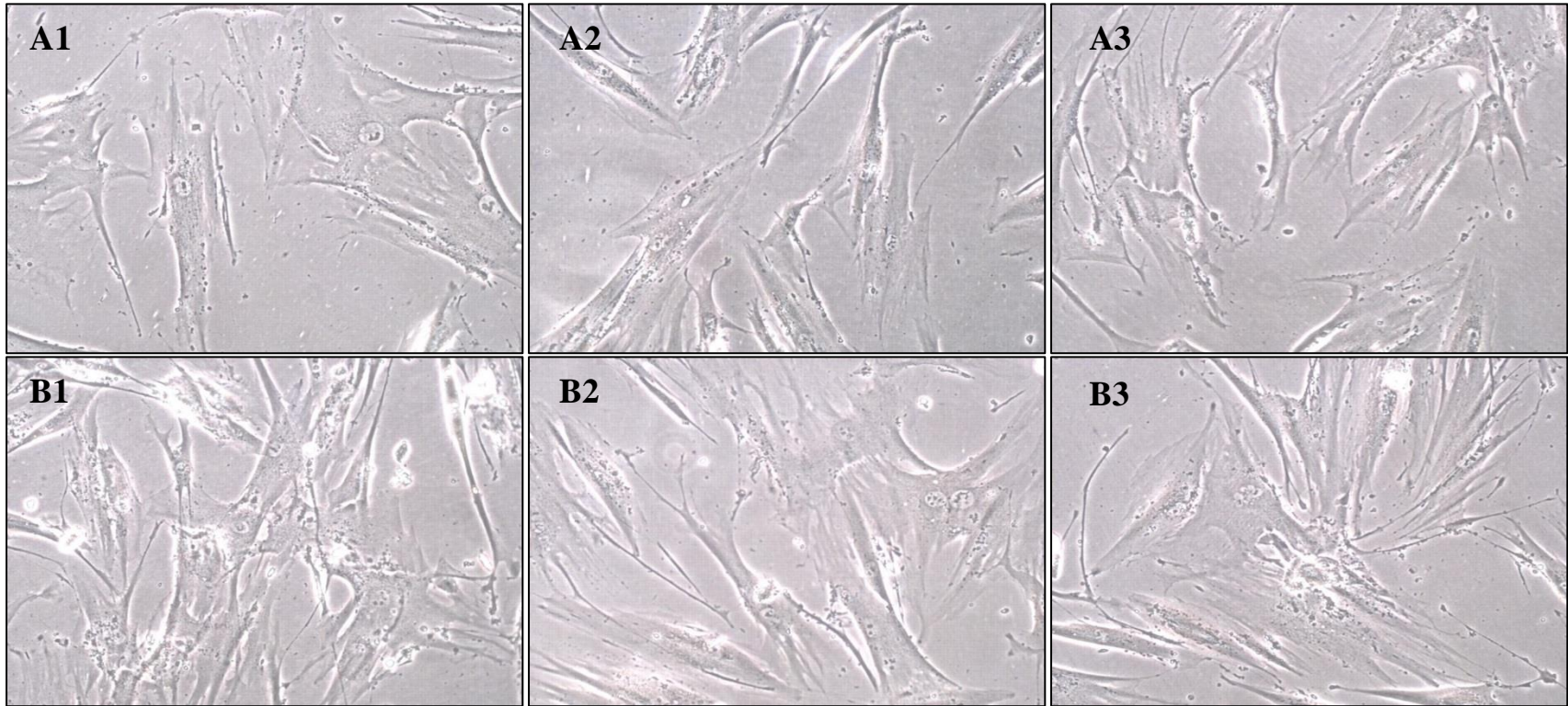
Figure 4.4: The HPdLF cells 24 hours' post treatment with exosomes under 10x magnifications. The morphology of HPdLF cells were viewed under inverted microscope after 24 hours of A1, A2 and A3 and exosomes treatment B1, B2 and B3. The A line wells acted as the control meanwhile the B line wells were treated with 10 µg exosomes. The HPdLF cells showed elongated and spindle shape morphology in all groups. Both groups also showed same confluence percentage.

4.3.2 Cell Proliferation
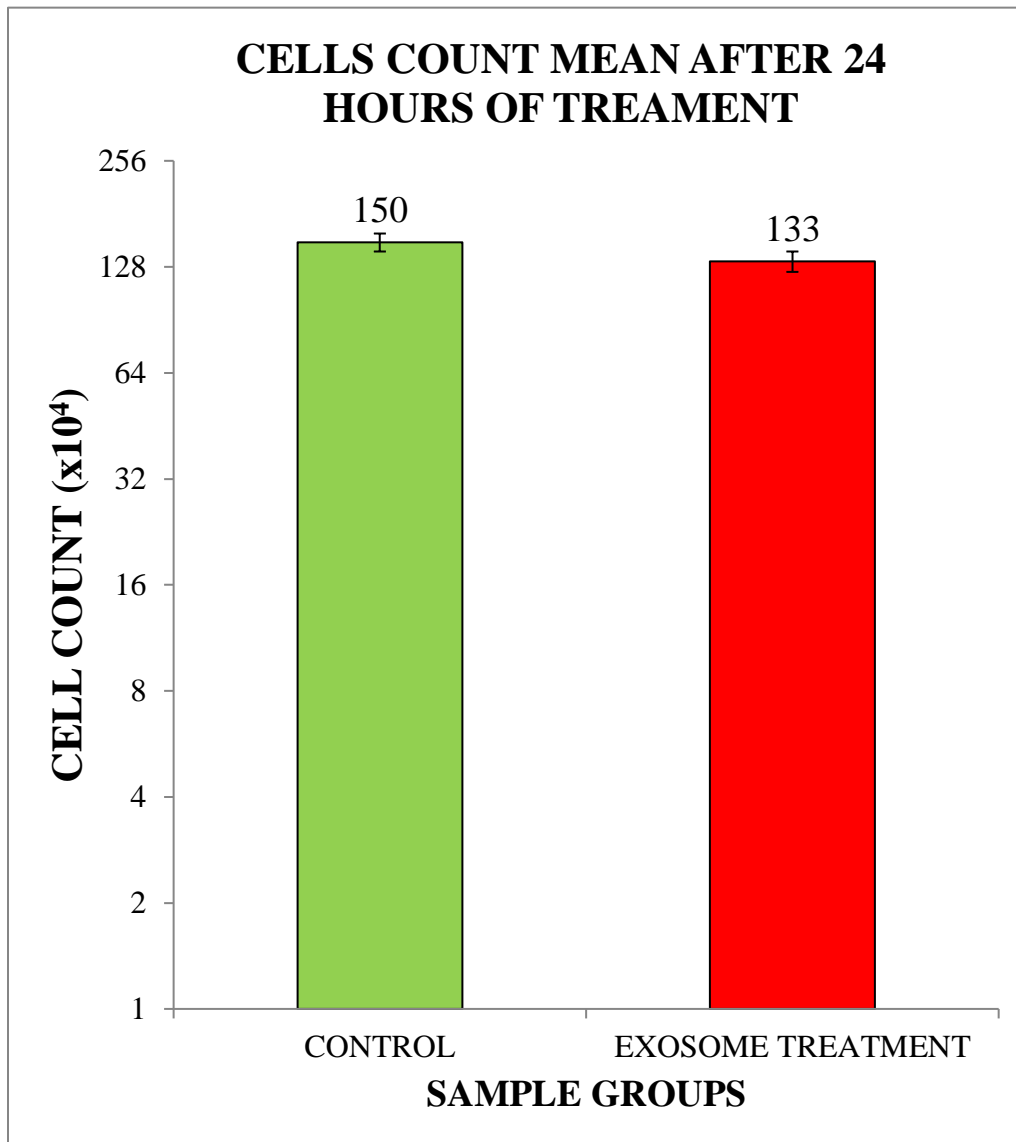
Figure 4.5: The graph of the cell counts after 24 hours' post treatment with exosomes. The HPdLF cell counts were done manually with Trypan Blue staining under inverted microscope. (Data represent the mean value ± SEM; EXCEL 2016: ANOVA: Single Factor Statistical Analysis, p > 0.05).

4.3.3　Cell Morphology (SEM)

The images of the control after 24 hours of HPdLF cells with exosomes treatment under 200x magnification (Figure 4.6), 5,000x magnifications (Figure 4.7), and 100,000x magnifications (Figure 4.8 and Figure 4.9) showed some of comparable cell features. The elongated shape of the cells was perfectly shown for both control and treated cells. However, cell treated with exosomes appeared to be rougher and wider in size. Cytoplasm showing more abundant cytoplasmic vesicles protruded on the treated cells (Figure 4.7). The roughness of the fibroblast cytoplasm (shown in Figure 4.7) was due to the cytoplasmic vesicles or vacuoles protruding as buds. Those vacuoles appeared larger in the cell treated with exosomes (Figure 4.8). The lamellipodia and filopodia were observed. As shown on Figure 4.7, the features of lamellipodia and filopodia were more distinct in the cell treated with exosomes (Figure 4.9).
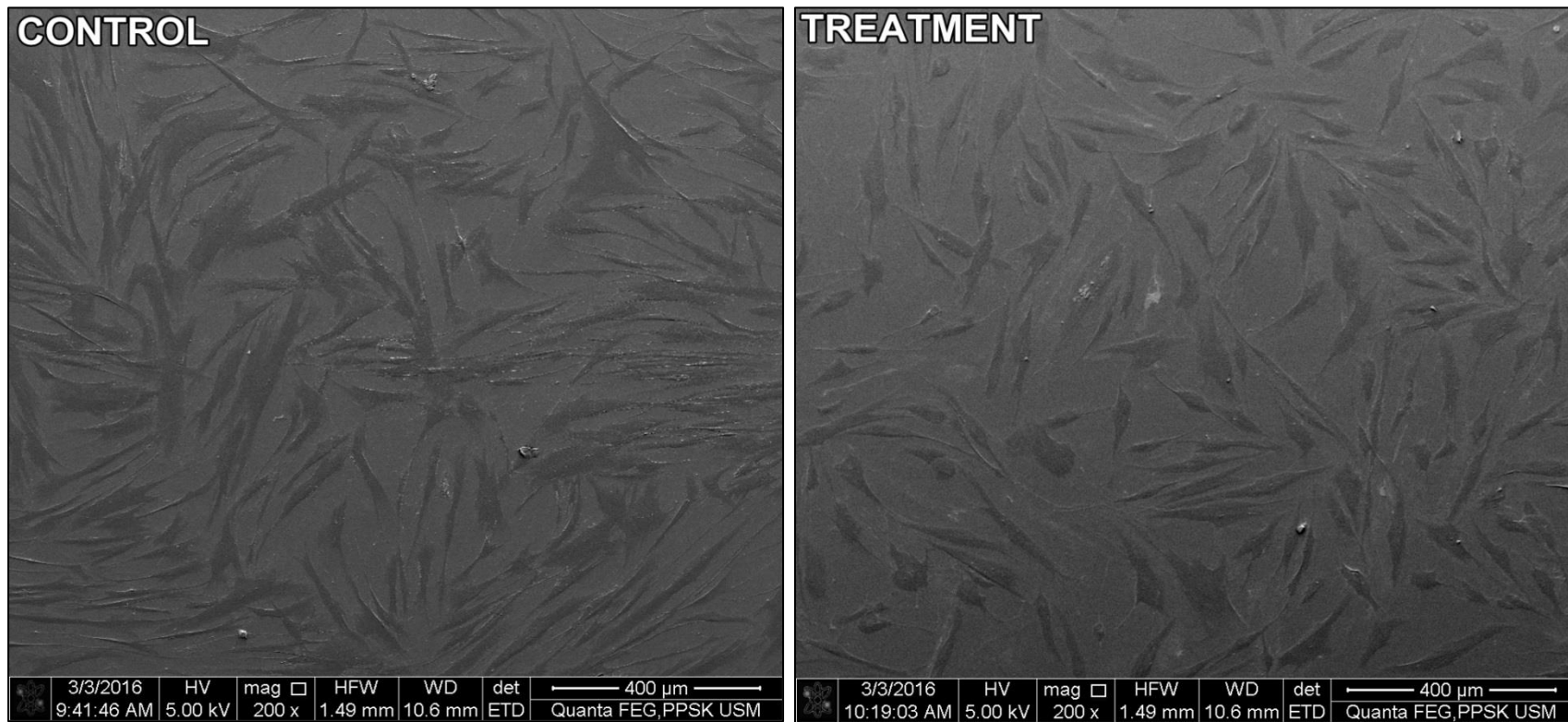
Figure 4.6: The representative images of HPdLF cells 24 hours after exosomes treatment under 200x magnifications. Both control and treatment show no distinct difference in morphology. The elongated shape of the cells was perfectly shown for both control and treated cells.
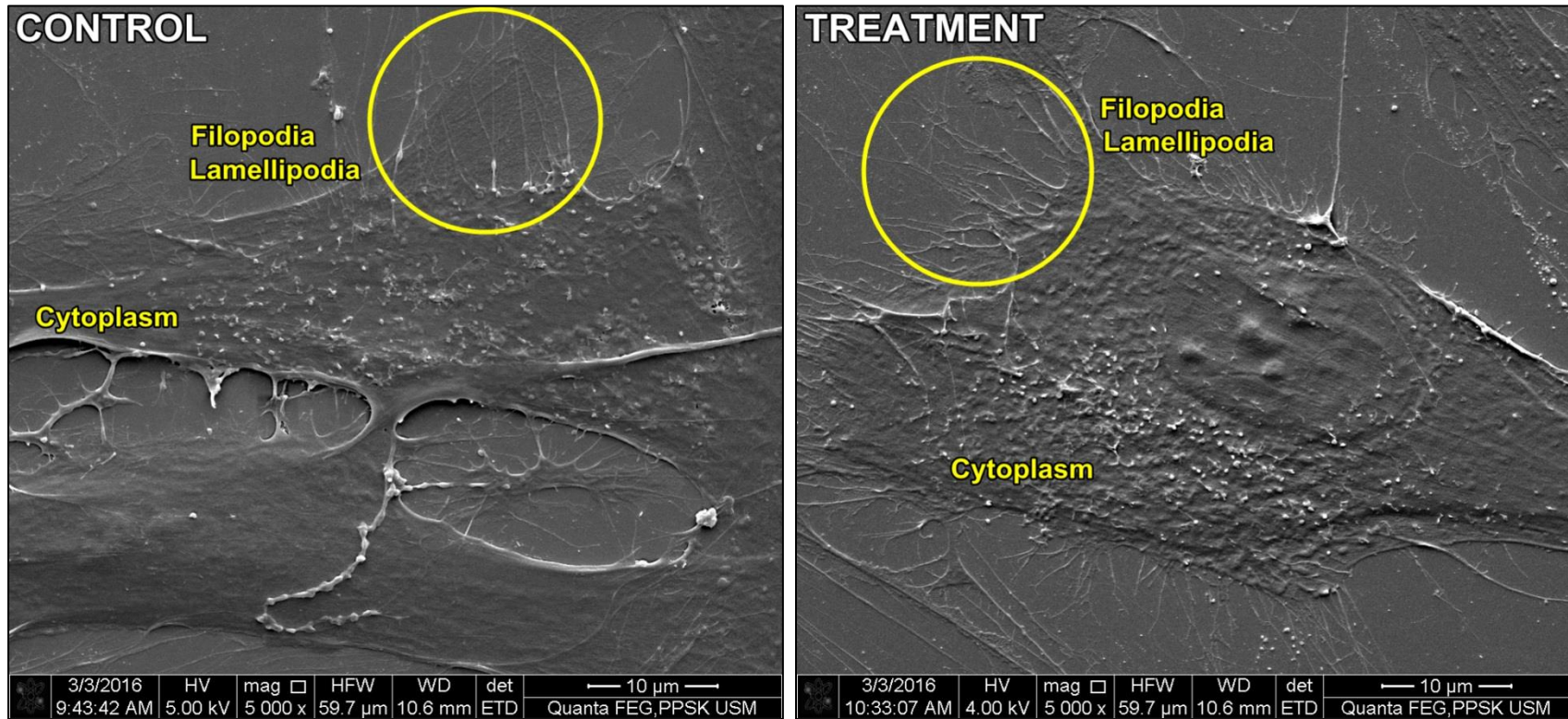
Figure 4.7: The representative images of HPdLF cells 24 hours after exosomes treatment under 5,000x magnifications. The filopodia and lamellipodia were more abundant in cell treated with exosomes. The surface of HPdLF cells treated with exosomes appeared to be rougher and wider in size. Cytoplasm showing more abundant cytoplasmic vesicles protruded on the treated cells.

.
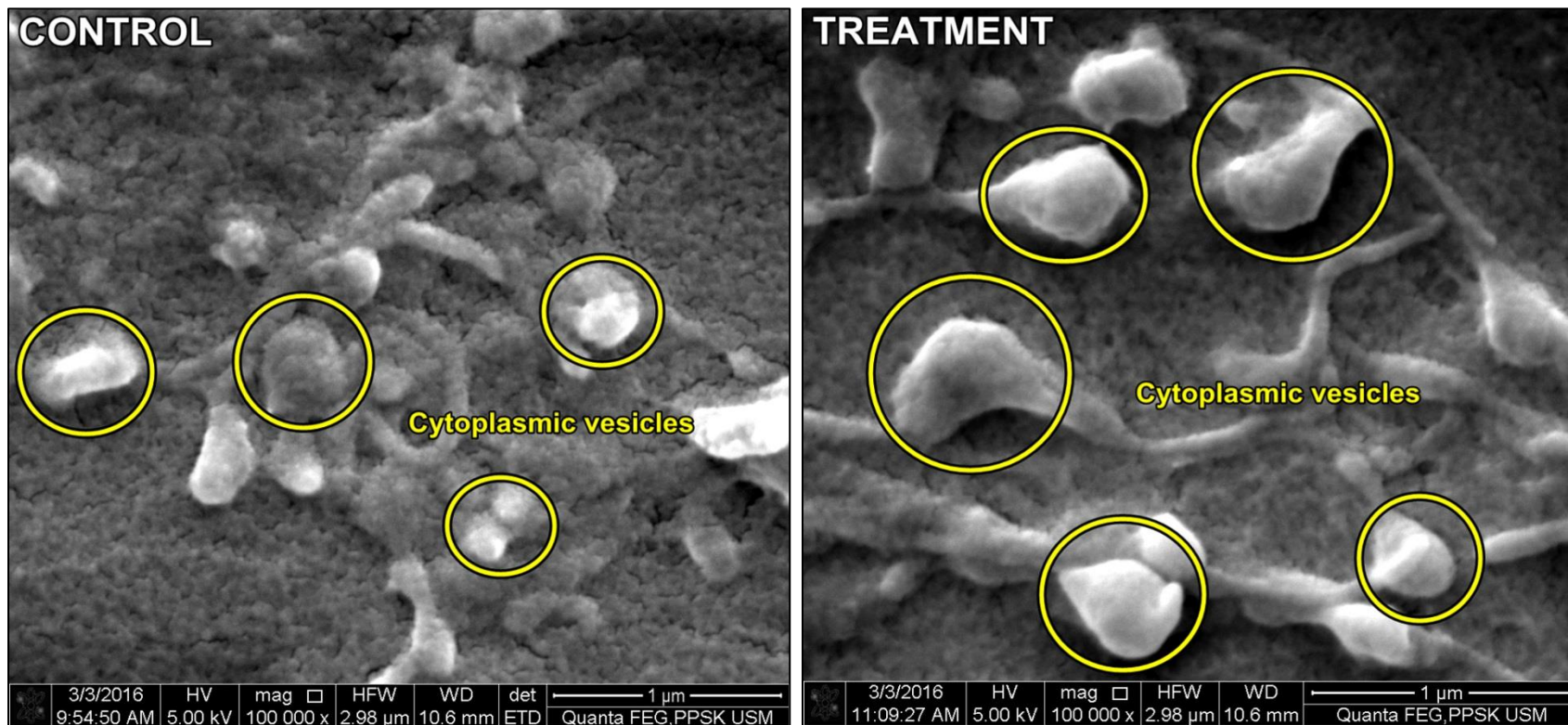
Figure 4.8: The representative images of HPdLF cells 24 hours after exosomes treatment under 100,000x magnifications. The roughness of the fibroblast cytoplasm (shown in Figure 4.7) was due to the cytoplasmic vesicles or vacuoles protruding as buds. Those vacuoles appeared larger in the cell treated with exosomes.
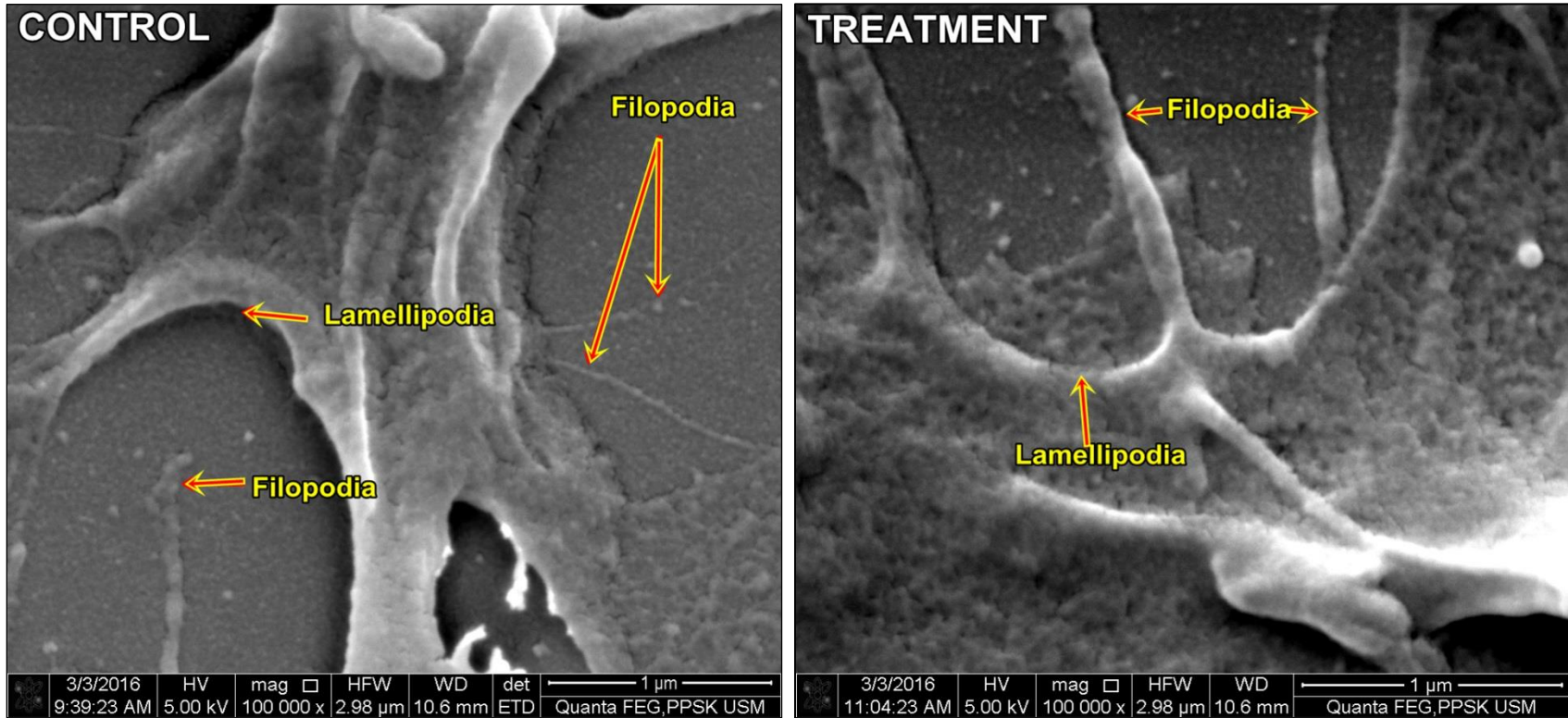
Figure 4.9: The representative images of HPdLF cells 24 hours after exosomes treatment under 100,000x magnifications. The lamellipodia and filopodia were observed. As shown on Figure 4.7, the features of lamellipodia and filopodia were more distinct in the cell treated with exosomes.

4.4   DISCUSSIONS

From the observation of cells under inverted microscope after 24 hours of treatment, human salivary exosomes showed no distinct effect on the morphology of the HPdLF cells. The cells still maintain their basic fibroblast shape; elongated and spindle-like shape and there are no changes in the size as well (Figure 4.3 and Figure 4.4). Cell count also revealed no significant changes ($p > 0.05$) in cell number (Figure 4.5). These suggest that human salivary exosomes probably gave no effect on the growth and proliferation of cells.

Further analysis was carried out by SEM to look at the ultrastructural changes of the cell surface. SEM showed that under 100,000x magnifications, the sample treated with exosomes showed minimal differences that can be observed with the morphology criteria. The treated sample showed more distinct and richer filopodia and lamellipodia. Both filopodia and lamellipodia are involved in cell growth and proliferation as they function in cell migration (Small *et al.*, 2002, Mattila and Lappalainen, 2008). The protrusion of filopodia is a method for cells to respond to the outer materials of the cells or as the inner response of the cells themselves (Mattila and Lappalainen, 2008).

Since filopodia and lamellipodia extended from the actin cytoskeleton of the cells, the increase number of their formations showed a higher level in actin contents and actin meshwork. Actin basically functions in intracellular transport. The contractility of the actin-based parts of the cells control the cell shape changes and direct involvement of cells from cell division to cell migration and wound healing process (Pollard and Cooper, 2009).

Figure 4.7 showed the abundance of filopodia and lamellipodia in cell treated with exosomes. The higher number of filopodia and lamellipodia may also increase the effectiveness of the fibroblast attachment to surfaces. Therefore, from Figure 4.9, we can see the better attachment of the cells onto the surface in the treated sample. This criterion is important especially in relation to the quality of wound healing and tissue regeneration. Cells are required to attach onto the root surfaces in the process of healing and regeneration of periodontal tissue (Ramseier *et al.*, 2000).

In endodontic surgery, the fibroblast migration attachment and orientation are vital for the healing process as it initiates the cellular functions (Weston *et al.*, 1999). Anchorage dependent cell such as HPdLF itself requires cell adhesion and attachment formation for survival. It is either adhesion to neighboring cells and to an extracellular matrix (ECM) or to protein absorbed onto a substrate (Baxter *et al.*, 2002).

SEM also showed the lumpier surface on the cytoplasm of the treated cells due to the cytoplasmic vesicles or vacuoles (Figure 4.7). As the magnification for observation increased, the treated cells showed abundant of vesicles and the cells appeared larger in treated exosomes sample compared to control sample (Figure 4.8). The size of the cells can be compared based on the SEM scales provided on the images. The formation of the cytoplasmic vesicles could be due of the phagocytosis process. During this process, filopodia folded to embrace the foreign materials around which then followed by invagination of the enclosed plasma membrane (Masci *et al.*, 2015). During this phase, the cells were capturing or in contact with exosomes particles from the surrounding and phagocyte them into the cells. The larger sizes of the vesicles showing the increase materials ensnared by the filopodia and in this case, might be exosomes themselves. This

theory is supported by a research done by Heusermann *et al.* (2016) on the exosomes uptake by cells. Their research managed to prove the recruitment of exosomes (conditioned medium originated exosomes) into cell body (human primary fibroblast) by surfing on filopodia as well as by the grabbing and pulling motions of filopodia (Heusermann *et al.*, 2016).

In addition, the fibroblast cytoplasm itself is filled with vacuoles containing varied materials with different consistency and density. Some of the materials in the vacuoles is related to the actual continuity to collagen fibril (Masci *et al.*, 2015). Therefore, this also proposes that the particular phase visualize the moment where the vacuoles are conveying the inner complex endogenous material from the cells to the extracellular matrix environment. The cytoplasmic vesicles are likely to be the Golgi-associated vesicles delivering the materials such as hydrolytic enzymes into the collagen containing vacuoles for additional processing (Masci *et al.*, 2015). However, the larger size of the vesicles could indicate that the cell has received or contained more endogenous materials.

4.5 CONCLUSION

The minor differences showed by the SEM images may not suffice to account for the effect of human salivary exosomes on HPdLF. However, within 24 hours of culturing of the cells with human salivary exosomes, the samples already shown some respective changes that could suggest that exosomes contain materials that can enhance the cell proliferation. To further investigate the distinct effect of human salivary exosomes on the HPdLF cells, gene expression analysis of specific protein was carried out.

CHAPTER V

THE EFFECT OF EXOSOMES ON THE GENE EXPRESSION OF HUMAN PERIODONTAL LIGAMENT FIBROBLAST

5.1   INTRODUCTION

The previous chapter showed human salivary exosomes might have very little influences on the HPdLF cells proliferation. The minor changes seen morphologically from SEM observation can be further confirmed by investigating the gene expression level of the genes involve in cells proliferation. The gene expression is the most fundamental level at which the genotype gives rise to phenotype (Chiba-Falek, 2013). Therefore, this chapter aims to investigate the effect of exosomes on HPdLF gene expression by Quantitative Reverse Transcription Polymerase Chain Reaction (RT-qPCR) method from qualified extracted RNA. This method is the most established technique for quantifying mRNA in biological samples over the conventional methods used due to its sensitivity in measuring RNA, large dynamic range and high throughout potential of accurate quantification (Huggett *et al.*, 2005).

.   As previously explained in Chapter II (Subchapter 2.4), the genes of interest for this study are the bFGF and COL1 as both are the genes responsible for the proliferation of HPdLF cells. Glyceraldehyde-3-phosphate dehydrogenase (GAPDH) was used as

reference gene. Other than GAPDH, beta-actin, hypoxanthine-guanine phosphoribosyl transferase (HPRT) and 18S ribosomal RNA are also commonly used as gene references. GAPDH has been used as reference for many years in Northern blots, RNase protection assays and conventional RT-PCR assays due to the high expression levels expressed in all cells, making them the ideal internal controls (Huggett *et al.*, 2005).

5.2   METHODOLOGY

5.2.1   RNA Extraction

The cells prepared as explained in Chapter V (Subchapter 5.1) was proceeded with RNA extraction. This procedure was done using RNeasy Plus Universal Kits (QIAGEN, Germany) and all methods done as provided in the protocol manuals.

Precautions for RNA handling were done thoroughly all along the experiment to avoid RNA degradation and contamination. Gloves were changed frequently as the protocol progresses from cured extract to purified material and all disposable plasticware used were sterile and typically RNase-free. All reagents and chemicals purchased were guaranteed to be RNase-free and aseptic techniques were properly conducted. All RNA samples work on bench was kept on ice and closed lid all the time. All work surfaces benches and safety cabinets were sterilized with 100% ethanol and RNase decontamination solution each time before and after working with RNA samples.

About 300 µl QIAzol Lysis Reagent was added into each well after the media was aspirated. The cells and reagents were mixed properly until a sticky mixture was formed. The mixture was let to sit at room temperature (15-25°C) for 5 minutes then transferred into different 1.5 ml micro centrifuge tubes. About 50 µl of genomic DNA (gDNA) Eliminator Solution was added to all tubes and the mixture was vigorously shaken for 15 seconds. About 60 µl of chloroform was added and the mixture was shaken for another 15 seconds then was let to sit at room temperature (15-25°C) for 2-3 minutes.

The tubes then centrifuged at 12,000xg or 15 minutes at 4°C. After centrifugation, the samples were separated into 3 phases; an upper, colorless, aqueous phase containing RNA; a white interphase; and a lower, red, organic phase (Figure 5.1). The volume of aqueous phase should be approximately 150-200 µl.

For each tube, only the upper aqueous RNA phase (about 200 µl) was transferred to a new micro centrifuge tube. 1 volume (1:1 to aqueous volume) of 70% ethanol (200 µl) was added and mixed thoroughly by pipetting it up and down. Up to 400 µl of the sample was transferred to an RNeasy Mini spin column placed in a 2 ml collection tube. The lid was gently closed, centrifuged for 15 seconds at >8,000xg at room temperature (15-25°C).
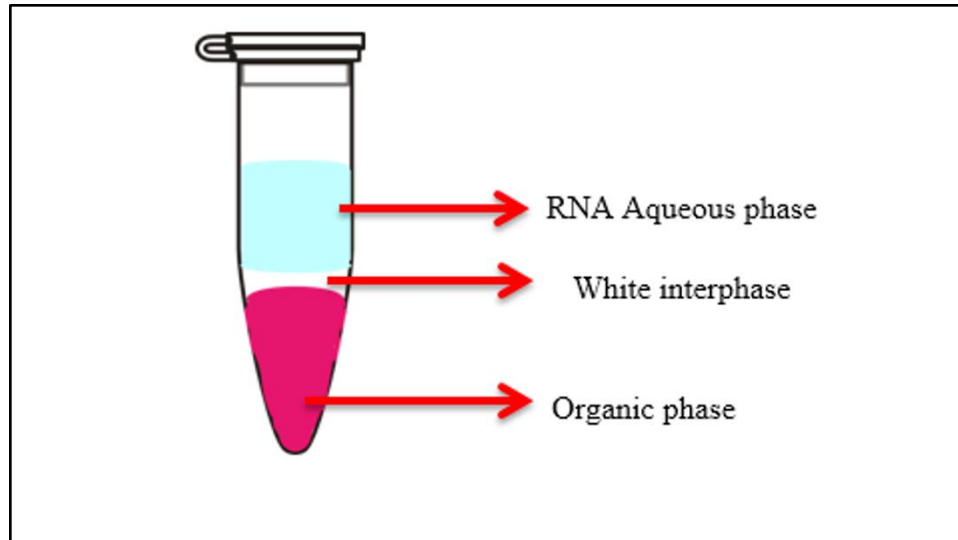
Figure 5.1: The diagram of RNA centrifugation 3 phases.
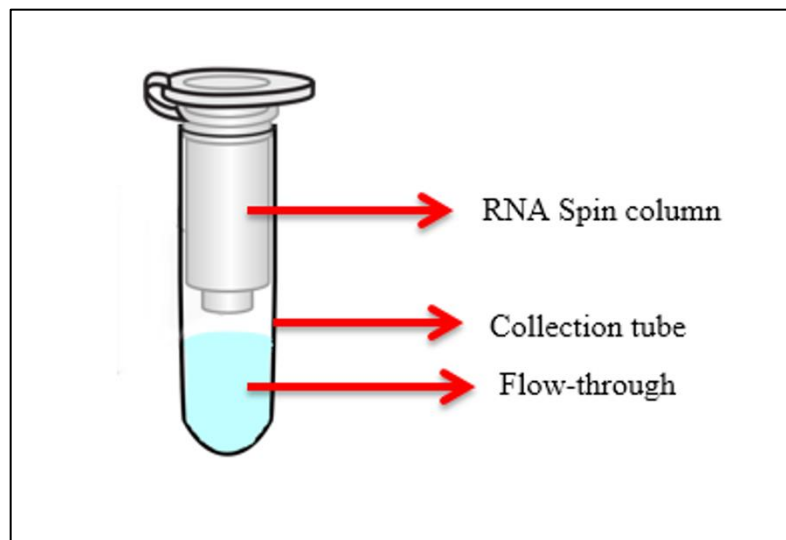
Figure 5.2: The diagram of RNA spin column in the collection tube.

The flow-through was then discarded (Figure 5.2). After each centrifugation step, the RNeasy spin column was carefully removed from the collection tube so that the column does not contact with the flow-through. About 250 µl of Buffer RWT was added to the RNeasy spin column. The lid was gently closed, and once again proceeded to centrifuge for 15 seconds at >8,000xg at room temperature (15-25°C). The flow-through was discarded.

About 170 µl of Buffer RPE was added to the RNeasy spin column. The lid was gently closed and centrifuged for 15 second at >8,000xg and the flow-through was discarded. Second volume of 170 µl of Buffer RPE was added to the RNeasy spin column and proceeded to centrifuge again for 2 minutes at >8,000xg to wash the membrane. Both flow-through and the collection tube were discarded and the RNeasy spin column was replaced in a new 1.5 ml collection tube.

About 20 µl of RNase-free water was added directly to the spin column membrane. The lid was gently closed. To elute the RNA, the tube was centrifuged for one minute at >8,000xg. Previous step was repeated using another volume of RNase-free water or using the eluate from last step (if high RNA concentration is needed). The purified RNA samples were stored at -80°C until used. Full method summary is shown in Appendix 10.

5.2.2 RNA Quantification

The purity and the concentration of the total RNA extracted were analyzed using the BioPhotometer. The samples were diluted by 1:50 dilution in RNase-free water. The RNA concentration was quantified by measuring the optical density (OD) at 260 nm wavelength and the purity at 260/280 nm. Values obtained were tabulated (Table 5.10).

5.2.3   RNA Integrity

All RNA samples undergone gel electrophoresis on 1% agarose gel to check their integrity. The reagents and materials used for this method were from Bio-Rad (United States). About 0.4 g of agarose powder was mixed with 40 ml of LB Buffer and 5.0 µl of SYBR Safe (integrated agent). The mixture was dissolved in the microwave for one minute. All mixture then was poured into the gel case and the comb was inserted. The gel was let to solidify for about 30 minutes. The samples were prepared by mixing 3 µl of RNA sample with 3 µl of loading dye and about 5 µl was loaded into each well. The gel was run at 70 Volts for 50 minutes and viewed under Gel Doc™ XR+ Gel Documentation System (Bio-Rad, United States). Quantification of protein bands densitometry was carried out using ImageJ 1.50i software by Wayne Rasband (National Institutes of Health, USA). The bands intensity values were resulted in peak area unit of pixel.

5.2.4   Quantitative Reverse Transcriptase Polymerase Chain Reaction (RT-qPCR)

The complementary DNA (cDNA) conversion kit used was QuantiTect™ Reverse Transcription Kit (QIAGEN, Germany). Real-time PCR was done by using PowerUp™ SYBR™ Green Master Mix (Thermo Fisher Scientific, United States) and reverse and forward primers of gene interest from Integrated DNA Technologies (IDT, United States). The primers used were GAPDH (R), GAPDH (F), bFGF (R), bFGF (F), COL1 (R), and COL1 (F) and the gene sequence details are shown Table 5.3. The gene expression of bFGF and COL1 were done by RT-qPCR Two-Step method (Appendix 11) by converting RNA samples to cDNA (RT) (Appendix 12) and run on real-time PCR (qPCR) analysis.

Table 5.3: Primer Gene Sequences

Genes		Sequences	NCBI Reference Sequence	Origins	References
bFGF	F	5' TTCTTCCTGCGCATCCAC 3'	NM_002006.4	121	(Liao *et al.*, 2013)
	R	5' TGCTTGAAGTTGTAGCTTGATGT 3'			
COL1	F	5' GACATGTTCAGCTTTGTGGACCTC 3'	NM_000088.3	121	(Nagai *et al.*, 2007)
	R	5' CCGTTCTGTACGCAGGTGATTG 3'			
GAPDH	F	5' AGCCACATCGCTCAGACAC 3'	NM_002046.4	541	(Liao *et al.*, 2013)
	R	5' GCCCAATACGACCAAATCC 3'			

(a) Reverse Transcriptase (RT) cDNA Conversion

The illustration of this procedure is as shown in Appendix 5.4. The RNA samples were thawed on ice. The gDNA Wipeout Buffer, Quantiscript® Reverse Transcriptase, Quantiscript RT Buffer, RT Primer Mix, and RNase-free water were thawed at room temperature (15-25°C). Each solution was mixed by flicking the tubes and briefly centrifuged to collect residual liquid from the sides of the tubes, then being kept on ice.

About 400 ng of total RNA from each sample were reverse transcribed to standardized final concentration of cDNA into 20 ng/µl using the kit according to the manufacturer's instructions. The RNA to cDNA calculation was based on $M_1V_1=M_2V_2$ method shown in Appendix 11. The cDNA conversion of RNA was divided into Step A and Step B. Step A is the genomic DNA elimination reaction prepared by adding gDNA Wipeout Buffer, template RNA (from RNA extraction sample, Section 5.2.1) and RNase-free water, accordingly to Table 5.4, mixed and kept on ice. From the gDNA elimination reaction, the Step A mixture was incubated for 2 minutes at 42°C and then placed immediately on ice. Step B is the preparation of the reverse-transcriptase reaction components, accordingly to Table 5.5. The reverse-transcriptase master mix contains all components [except template RNA (Step A mixture)] required for first-strand cDNA synthesis were mixed and placed on ice. Step A mixture (14 µl) was then lastly added to each tube containing reverse-transcription master mix. It was then mixed and stored on ice. The Step B mixture was incubated for 15 minutes at 42°C. The mixture then was incubated more for 3 minutes at 95°C to inactivate Quantiscript Reverse Transcriptase. The reverse-transcription reaction was placed on ice and then proceeded directly with real-time PCR (qPCR) or stored at -20°C.

Table 5.4: The genomic DNA elimination reaction components (Step A)

Component	Volume / Reaction
gDNA Wipeout Buffer, 7x	2.0 µl
Template RNA, (400 ng) *	Variable (Appendix 11)
RNase-free water	Variable
Total reaction volume (Step A mixture)	**14.0 µl**

*This amount corresponds to the entire amount of RNA present, including any rRNA, mRNA, viral RNA and carrier RNA present, and regardless of the primers used or cDNA analyzed.

Table 5.5: Reverse-transcription reaction components (Step B)

Component	Volume / Reaction
Reverse-transcription master mix	
Quantiscript Reverse Transcriptase	1.0 µl
Quantiscript RT Buffer, 5x	4.0 µl
RT Primer Mix	1.0 µl
Template RNA (Step A mixture)	
Entire genomic DNA elimination reaction	14.0 µl
Total reaction volume (Step B mixture)	**20.0 µl**

(b)   Standard curve reaction

From cDNA prepared from control sample A1 (A1) (Appendix 11), a standard curve of five serial dilution points of cDNA [5.2.3(a)] with two-fold dilution (1:2) factor (10 ng/µl, 5 ng/µl, 2.5 ng/µl, 1.25 ng/µl and 0.625 ng/µl) were prepared. The serial dilutions were made as shown in Figure 5.5 and the calculation was based on $M_1V_1 = M_2V_2$ method. About 10 µl of cDNA sample from A1 (20 ng/µl) was transferred to another tube and added with 10 µl of RNase-free water, then mixed by pipetting up and down. Steps were repeated until five series of dilutions were prepared. All the standard curves serial dilution samples were labeled with SC (SC1, SC2, SC3, SC4 and SC5) accordingly and to their respective concentrations (Figure 5.6).

The preparation of standard curve reaction mix was done following the manufacturer's instruction and was run in duplicate for every cDNA dilution for each gene. The standard curve reaction was prepared in a final volume of 10 µl per reaction. Each standard curve reaction mix contained 5 µl PowerUp™ SYBR™ Green Master Mix (2X), 0.5 µl of 500 nM forward primers and 0.5 µl of 500 nM reverse primers, 3 µl of RNase-free water and 1 µl of cDNA template for each cDNA dilution (SC1, SC2, SC3, SC4 and SC5) accordingly (Table 5.7). The standard curve reaction strips were then run using Quantitation-Standard Curve test, in duplicate with the thermal cycling condition as shown in Table 5.8.
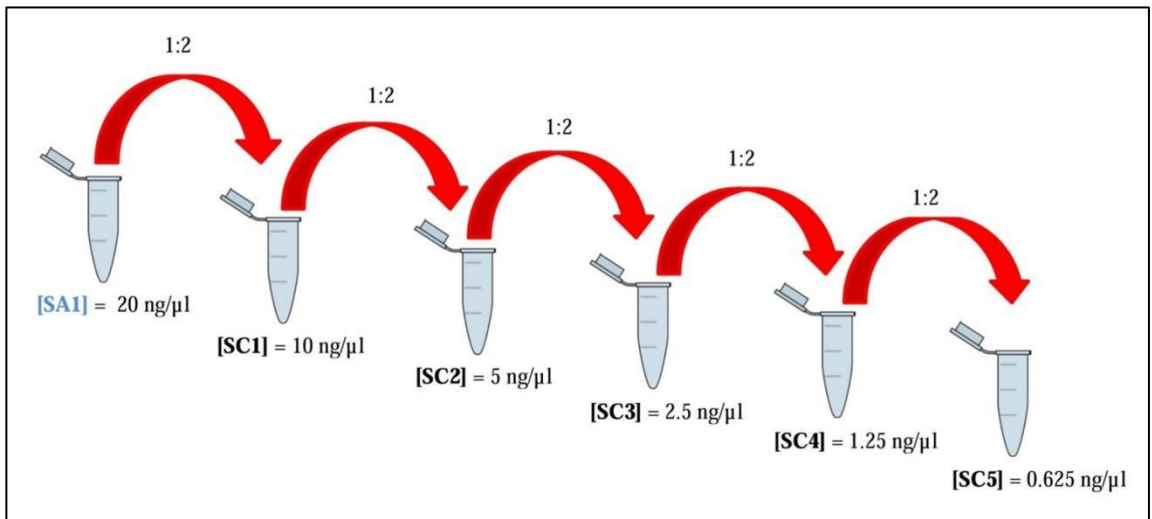
Figure 5.6: The standard curve serial dilution procedure.

(c)   qPCR reaction samples

The qPCR reaction samples include the calibrator samples, control samples and experimental samples. The qPCR reaction sample was prepared in a final volume of 10 µl per reaction. Each reaction mix contained 5 µl PowerUp^{TM} SYBR^{TM} Green Master Mix (2X), 0.5 µl of 500 nM forward primers and 0.5 µl of 500 nM reverse primers, 3 µl of RNase-free water and 1 µl of 5 ng/µl cDNA template (Table 5.7). The concentration of cDNA template (5 ng/µl) was standardized for all reactions and was in the standard curve serial dilution concentration range (10 ng/µl, 5 ng/µl, 2.5 ng/µl, 1.25 ng/µl and 0.625 ng/µl).

The mixture components were thoroughly mixed, sealed and centrifuged briefly to spin down the contents and eliminate any air bubbles. Samples then were run in the real-time PCR instrument using Quantitation-Comparative C_T test, in triplicates with the thermal cycling conditions used as shown in Table 5.8.

Table 5.7: Real-time PCR reactions mixture

Component	10 µl/well
PowerUp^{TM} SYBR^{TM} Green Master Mix (2X)	5.0 µl
Forward Primer (500 nM)	0.5 µl
Reverse Primer (500 nM)	0.5 µl
RNase-free water	3.0 µl
cDNA template	1.0 µl
Total Volume	**10.0 µl**

Table 5.8: Standard Cycling Mode Primer $T_m < 60°C$

Standard Cycling Mode Primer $T_m < 60°C$			
Step	**Temperature**	**Duration**	**Cycles**
UDG Activation	50°C	2 minutes	Hold
Dual-Lock^{TM} DNA Polymerase	95°C	2 minutes	Hold
Denature	95°C	15 seconds	
Anneal	56°C	15 seconds	40
Extend	72°C	1 minute	

* Anneal temperature was set to the average melting point of the primers.
* The thermal cycling conditions were set using the default PCR-thermal-cycling condition specified according to the instrument cycling parameters and the melting temperature of the primers (Tm < 60°C). The instrument was set to perform a default dissociation step.
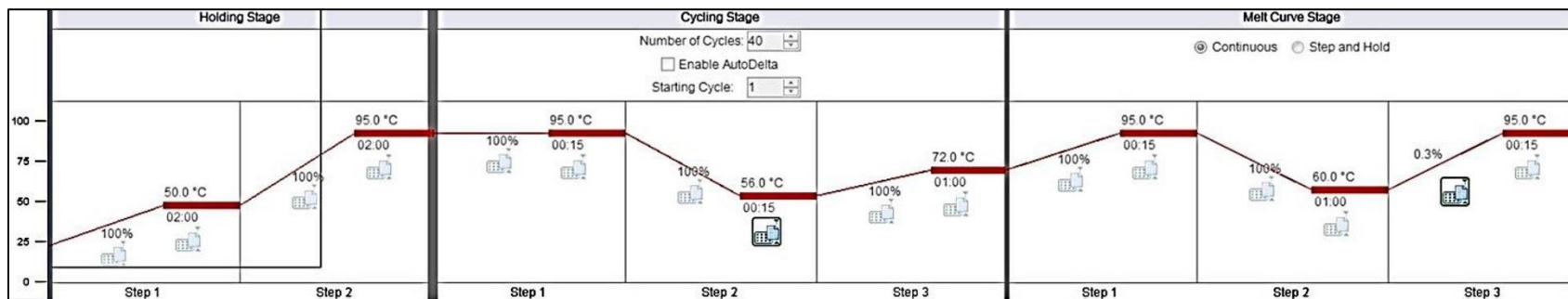
Figure 5.9: The dissociation set up.

(a) Data analysis

The software used for the analysis is the StepOnePlus Version 2.2.2. For standard curve, data was analyzed and the performance were evaluated based on the R^2 (correlation coefficient) and efficiency (%). The R^2 should be > 0.99 and the efficiency (%) should be between 90-110% based on the manufacturer's instructions. The efficiency values and R^2 values were automatically calculated and given by the software.

There are two common methods to analyze real-time, quantitative PCR experiments data which are the absolute quantification and relative quantification. Absolute quantification method relates the PCR signal to a standard curve to determine the input copy number. Meanwhile, relative quantification ($2^{-(\Delta\Delta C_T)}$)) method relates to the PCR signal of the target transcript in a treatment group to untreated control groups. The $2^{-(\Delta\Delta C_T)}$ method is a convenient way to analyze the relative changes in gene expression for this research (Livak and Schmittgen, 2001). Therefore, for qPCR reaction samples, the amplification plot was viewed and the relative quantification ($\Delta\Delta C_T$) values obtained were tabulated (Table 5.12). Relative quantity of gene expression ($2^{-(\Delta\Delta C_T)}$) of each gene was calculated to determine the fold change in expression and the analyzed results is shown in Table 5.12 and graphed (Figure 5.13).

5.3   RESULTS

5.3.1   RNA Concentration Values

The purity and the concentration of the total RNA extracted for all samples were as reported below (Table 5.10). Sample A1, A2 and A3 contained 90 µg/ml, 110 µg/ml and 131 µg/ml of total RNA, respectively. Sample B1, B2 and B3 contained 89 µg/ml, 145 µg/ml and 85 µg/ml of total RNA, respectively. All sample optical density reading (OD) value were above 1.70 and the readings of A340nm were 0.0.

Table 5.10: Total RNA extracted concentrations and purity

SAMPLE (Wells)	TOTAL RNA (µg/ml)	260/280 OPTICAL DENSITY READING (OD)
A1	90.00	1.71
A2	110.00	1.84
A3	131.00	1.85
B1	89.00	1.82
B2	145.00	2.05
B3	85.00	1.90

.

5.3.2 RNA Gel Electrophoresis

RNA Gel electrophoresis showed that all samples had a good quality RNA as shown by Figure 5.11. The 28S band should be approximately twice as intense as the 18S band. As shown in the figure, the ratio 2:1 (28S:18S) indicates that the RNA is completely intact. From ImageJ analysis, the value peak area of pixel for band intensities also showed the ratio of 2:1 for all samples (Appendix 14). All bands were also in sharp appearance (no smear), showing the RNA samples were not degraded in any forms.
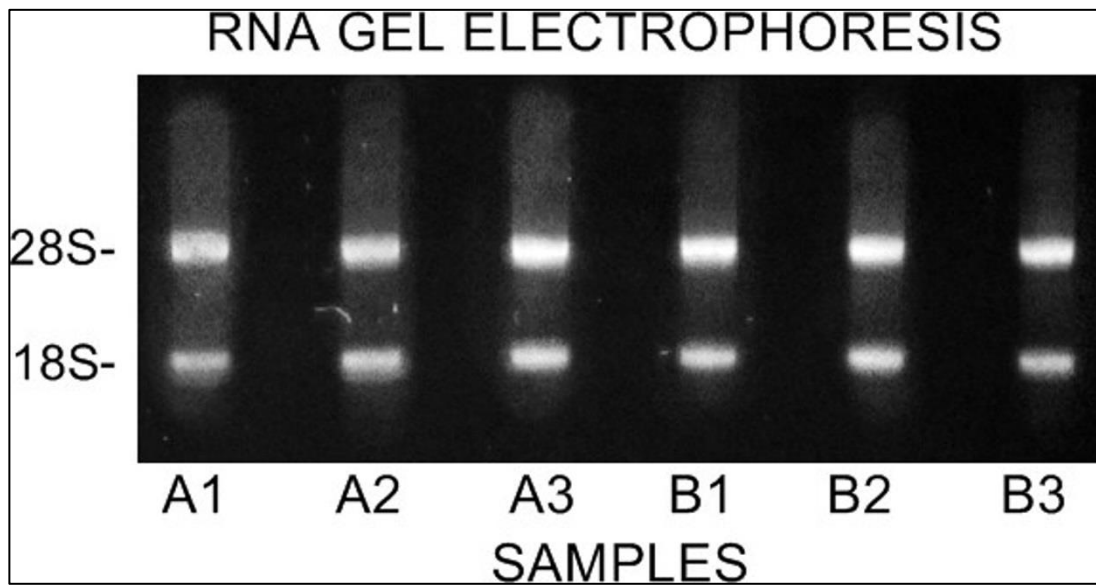
Figure 5.11: The RNA gel electrophoresis. This image shows the bands of all the samples, hence, confirming the intact of the RNA samples for further investigation.

5.3.3 Gene Expression Analysis

This research used the relative quantification analysis method of $2^{-\Delta\Delta C_T}$ calculation (Comparative C_T) (Livak and Schmittgen, 2001). The threshold cycle (C_T) values obtained from real-time PCR instrumentation were imported into a spreadsheet and tabulated as shown in Table 5.12. The change in expression of the bFGF and COL1 target genes normalized to GAPDH was monitored from corresponding cDNA synthesized from each sample. The C_T values of the gene of interest (GOI) (bFGF and COL1 genes) in both the experimental sample (s) and calibrator (c) (control sample) were adjusted in relation to a normalizer (norm) gene's (internal control gene, GAPDH) C_T from the same two samples. The resulting $\Delta\Delta C_T$ value is incorporated to determine the fold changes in expression (Livak and Schmittgen, 2001).

The analysis equations used is shown as follows:

$$\Delta C_{T\ \text{sample}} = C_{T\ \text{GOI}}\ s - C_{T\ \text{norm}}\ s$$

$$\Delta C_{T\ \text{calibrator}} = C_{T\ \text{GOI}}\ c - C_{T\ \text{norm}}\ c$$

$$\Delta\Delta C_T = \Delta C_T\ s - \Delta C_T\ c$$

$$\textbf{Fold change} = 2^{-\Delta\Delta C_T}$$

The technical replicates of PCRs were averaged to get the mean of C_T data before performing the $2^{-\Delta\Delta C_T}$ (Table 5.12) and the mean fold change ($2^{-\Delta\Delta C_T}$) of both COL1 and bFGF gene expression were graphed in Figure 5.13. The data were analyzed using Excel Analysis ToolPack of statistical Two Samples Student's T-Test to find the p value of data using C_T Mean value of samples (Table 5.12).

The real-time PCR analysis endpoint is determined by a log linear plot of the PCR signal versus the cycle number, the threshold cycle (C_T). In log-scale of $\Delta\Delta C_T$ values, positive value suggests up-regulation and the negative value suggests down-regulation. Since all C_T values are normalized to calibrator and internal control gene, GAPDH, the comparative analysis of $2^{-(\Delta\Delta C_T)}$ value higher than 1.000 showing the upregulation of GOI.

Table 5.12 shows the data summary and calculation using C_T Mean value of samples. All values were calculated and presented as mean values from technical replicates of each samples. Final values of fold change ($2^{-(\Delta\Delta C_T)}$) were presented in graph bars to show the differences of end results. From the chart (Figure 5.13), the values of fold change ($2^{-(\Delta\Delta C_T)}$) shows an increased pattern for the exosomes treated (experiment) samples for both COL1 and bFGF genes. However, there is only small difference for COL1 fold change values between control and treated samples, compared to bFGF fold change values. Therefore, to support this result, all samples data were analyzed statistically to determine the significant values and only bFGF gene showed a significant value ($p < 0.05$) (Figure 5.13).

Table 5.12: Data summary and calculation using C_T Mean value of samples.

Gene of Interest (GOI)		Avg. $C_{T\ GOI}$ Mean		Avg. $C_{T\ GAPDH}$ Mean		ΔC_T	$\Delta\Delta C_T$	$2^{-\Delta\Delta C_T}$
COL 1	Control samples (Calibrator, c)	22.575		22.924				
		20.336		22.744				
		20.367		22.265		-1.551 ± 0.776		
		Average	21.093 ± 0.741	Average	22.644 ± 0.197			
							-0.109 ± 0.545	1.078 (0.9-1.1)
	Experiment samples (Unknown, s)	18.447		21.797				
		17.045		20.864				
		23.121		20.932		-1.660 ± 0.830		
		Average	19.538 ± 1.84	Average	21.198 ± 0.300			
bFGF	Control samples (Calibrator, c)	29.078		26.919				
		27.616		27.617				
		29.831		26.287		6.197 ± 3.099		
		Average	28.842 ± 0.650	Average	26.941 ± 0.384			
							-1.905 ± 0.953	3.732 (3.5-3.9)
	Experiment samples (Unknown, s)	18.447		21.797				
		17.045		20.864				
		23.121		20.932		4.292 ± 3.872		
		Average	19.538 ± 1.84	Average	21.198 ± 0.300			

- Avg. $C_{T\ GOI}$ Mean = Average of C_T Mean values from technical triplicates of sample
- Avg. $C_{T\ GAPDH}$ Mean = Average of GAPDH C_T Mean values (normalizer) from technical triplicates of sample
- ΔC_T = Average of (Avg. $C_{T\ GOI}$ Mean) – Average of (Avg. $C_{T\ GAPDH}$ Mean)
- $\Delta\Delta C_T$ = ΔC_T Control Samples - ΔC_T Experiment samples
- $2^{-\Delta\Delta C_T}$ = Mean of fold changes of gene expressions
- Internal control gene, GAPDGH $2^{-\Delta\Delta C_T}$ = 1.000

Mean Fold Change of Gene Expressions in Control and Human salivary exosomes Treated HPdLF cells.
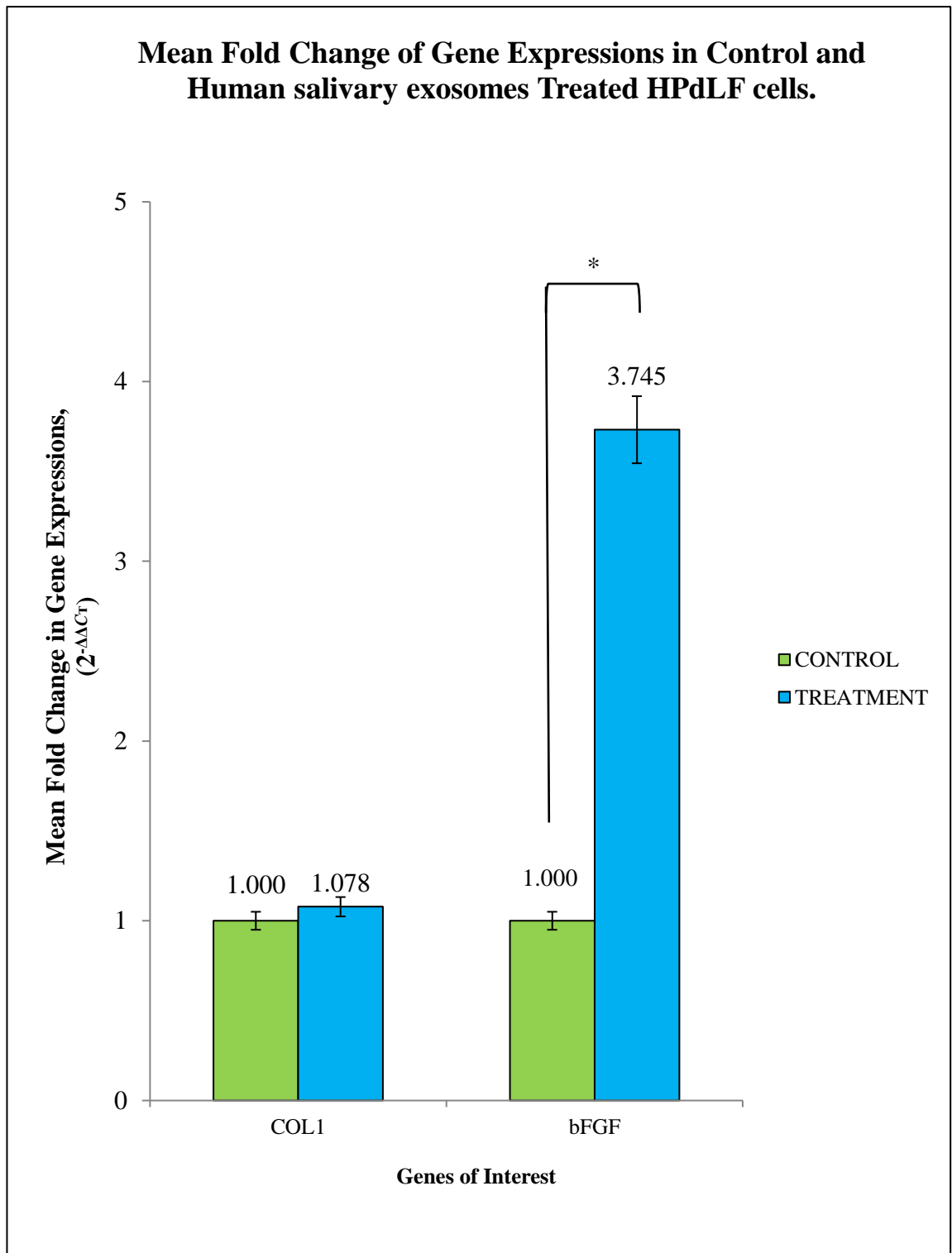
*p < 0.05, significant

Figure 5.13: The chart of mean fold change in gene expression ($2^{-\Delta\Delta C_T}$) values of the control versus treatment of the interest genes. (Data represent the mean value ± SEM; EXCEL 2016; T-Test: Two-Sample Assuming Equal Variances Statistical Analysis).

5.4   DISCUSSION

The values of RNA concentration obtained were reliable as the ratio of 260/280 from optical density reading were in the range for RNA purity, which is about 1.7 to around 2.0. For all samples, the readings of A340nm were 0.0, therefore indicating that the samples did not contain any particulate matter. All bands appeared for both 28S and 18S based on the RNA gel electrophoresis, showing all RNA were intact and in good quality for further testing.

The insignificant value of COL1 gene expression ($p > 0.05$) shown by this research is suggested to be due to the short incubation time. As published by other researches, collagen induction by other factors such as hormones, only gave significant result after for more than 24 hours of cell incubations. A research on the collagen production stimulated by transforming growth factor-beta 1 (TGF-β1) on fibroblast and myofibroblast cells on time-dependence (2-48 hours) showed that there was no increase in collagen production after long incubation (24-28 hours) at low concentrations (< 1 ng/ml), or after short incubation (2-4 hours) at high concentrations (1-15 ng/ml). Even though the collagen production increased after a long incubation at high concentration, the maximal increase was only observed after 48 hours (Lijnen and Petrov, 2002). Another study using TGF-β1-containing exosomes from injured epithelial cells on fibroblasts showed the COL1 expression was significantly increase after 24 hours and 48 hours of cell incubations (Borges *et al.*, 2013). This report supports our findings that collagen gene might not give significant difference within just only 24 hours of exosomes treatment.

Despite the insignificant increase of COL1 gene expression level, our study was able to prove the significant increase of bFGF gene level within just 24 hours. Hence, these findings are still reliable to suggest that exosomes may influence the cell proliferation and it might indirectly be involved in wound healing. The results of human salivary exosomes affecting the genes of interests (bFGF and COL1) obtained from our study were concurrent with the results obtained from other studies that used exosomes from other sources. As far as we are concerned, this is the first study that considers the effect of human salivary exosomes on HPdLF cells. Therefore, regardless of the exosome's origins (sources), their general effects on genes expressions (downregulate or upregulate) are used to support our findings. As an example, oligodendroglial exosomes affect the gene expression in neuron cells by downregulated the immediate early response 3 (Ier3), VGF nerve growth factor inducible (Vgf), and brain-derived neurotrophic factor (Bdnf) on transduction pathways in neurons after exosome treatment (Fröhlich *et al.*, 2014). Another study done on the exosomes from human monocytes resulted in the increase of the gene expression of the osteogenic markers runt-related transcription factor 2 (RUNX2) and bone morphogenetic protein-2 (BMP-2) (Ekström *et al.*, 2013). Meanwhile, tumor derived exosomes and other type of body fluids derived exosomes; (amniotic fluid exosomes, liver cirrhosis ascites exosomes, and malignant ascites exosomes of ovarian cancer patients) were analyzed to give effect on the THP-1 cells gene expression as well (Bretz *et al.*, 2013).

The effects shown by exosomes on the gene expressions of cells proved the involvement of exosomes in intercellular communication and RNA/mRNA/miRNA information transfer, despite the different origins of the exosomes. (Simpson *et al.*, 2009, Palanisamy *et al.*, 2010). There is cell to cell signaling and information transfer

between exosomes and cells. Some of the exosomes effect on the gene expression may involve in cell maturation and differentiation (Ekström *et al.*, 2013, Fröhlich *et al.*, 2014) or associated with immunosuppressive mechanisms induction (Bretz *et al.*, 2013). Likewise, for the results obtained from this study, we suggest that human salivary exosomes may give effect on periodontal regeneration and involve in wound healing as positively shown by the upregulation of the genes studied.

5.5   CONCLUSION

Human salivary exosomes give effect on the gene expression of bFGF and COL1 in HPdLF cells by showing the upregulation of the genes. Therefore, suggesting the involvement of exosomes in the periodontal cells regeneration.

CHAPTER VI

CONCLUSION AND RECOMMENDATIONS

6.1   GENERAL CONCLUSION

In general, we managed to show the effect of human salivary derived exosomes on the gene expression of HPdLF cells. Specifically, we had isolated, confirmed and established the storage condition of the human salivary exosomes (Chapter III). We managed to confirm the presence of exosomes in human saliva using Scanning Electron Microscope (SEM), Western blot and Nanoparticle Tracking Analysis (NTA). With the results from SDS-PAGE analysis, Western blot and protein assay reported, it showed that human saliva-derived exosome is a very stable sample regardless of the presence of protease inhibitor or the different storage temperature condition. We also studied and discussed the morphology and the proliferation of HPdLF in presence and absence of exosomes. It demonstrated that the exosomes treatment had showed influence on the morphology changes and proliferation of the cells (Chapter IV). We also determined the gene expression level of bFGF and COL1 in HPdLF cell in the presence and absence of exosomes (Chapter V). From the results obtained, it showed that human salivary exosomes treatment on the cell cultured effecting the proliferation of the cells by the upregulation of bFGF gene.

Exosome from human saliva is a biomaterial component which can be extracted easily and with less cost needed. This study has shown the effect of human salivary exosomes on the proliferation of the cells. Observation of the exosome's effect can be generally observed under SEM. Even though the effect was only shown by two types of genes in the gene expression analysis, this still could be an indicator for further in-depth study. This study was done under 24 hours of exosomes treatment; however, the effects have already can be observed and analyzed.

The results showed by this research is a positive sign for researchers to continue revealing the potential of human salivary exosomes. As the main focus of this research is to develop new method or procedure in periodontal tissue regeneration and healing with the usage of human salivary exosomes, the results may contribute as a base for a more in-depth study that can be taken from here.

6.2   LIMITATIONS AND FUTURE RECOMMENDATIONS

The findings acquired from this research are essential for the progression of the periodontal regeneration development. However, there are several limitations to this study that should be addressed and expounded with relevant recommendations to guide future research.

In Chapter IV, clumping of exosomes had been detected through SEM analysis and NTA. This finding did not affect this study directly, however, to provide for a more reliable end results, the concentration of exosomes treatment was decided to be based on protein concentration (protein assay) instead of concentration based on number of exosome particles (NTA). Therefore, for future research, we would like to

recommend for the usage of exosomes concentration based on the number of particles by the newly develop method, NTA. It will be an innovative approach of determining the concentration as NTA gives the yield of exosomes isolation in particle numbers.

We also would like to highlight that this research did not intend on using either specific type of exosomes (Exosome I and Exosome II) (Ogawa *et al.*, 2011); instead, human salivary exosomes samples used were believed to include both of the types. All samples expressed CD63, and CD63 is the protein marker for both type of exosomes. The identification methods of exosomes were done in overall basis and according to their general characteristics only. However, since there are new researches on the specifications and difference properties of exosomal types, we suggest the future research to work on which type of exosomes involved majorly in the proliferation of HPdLF cells, so more detailed information can be collected and reported.

From Chapter VI, we reported that COL1 gene expression was insignificant, therefore, no upregulation of this gene by the exosomes treatment. As discussed, (Subchapter 5.4), this could be due to the short incubation time for COL1 to be express significantly. Therefore, we would recommend for next research to extend the treatment period to more than 24 hours.

The development of human salivary derived exosomes research can improve the cell-based tissue engineering for periodontal regeneration. On the other hand, this study is one of the pioneer researches that opened a new door to the development of human salivary-derived exosomes. The mechanism of exosomes regulating genes expression and its role in exosome-induced proliferation requires further in-depth investigation. Recently, exosomes labelling kit has been developed and marketed. However, the use of this kit on human salivary exosomes has not been reported. This

technique will be done by applying the fluorescently-label isolated exosomes RNAs and proteins which can be used to track the cellular interaction and cargo delivery of exosomes contents into cultured cells. Consequently, we propose for next research to explore deeper into the mechanisms and specifications of the intercellular interaction of these human salivary-derived exosomes.

There are more parts of human salivary exosomes that still need additional and progressing research in the future. From this study, we hope it can be the foundation for next comprehensive discovery of human salivary exosomes, including their functions, mechanisms, characteristics, and much more.
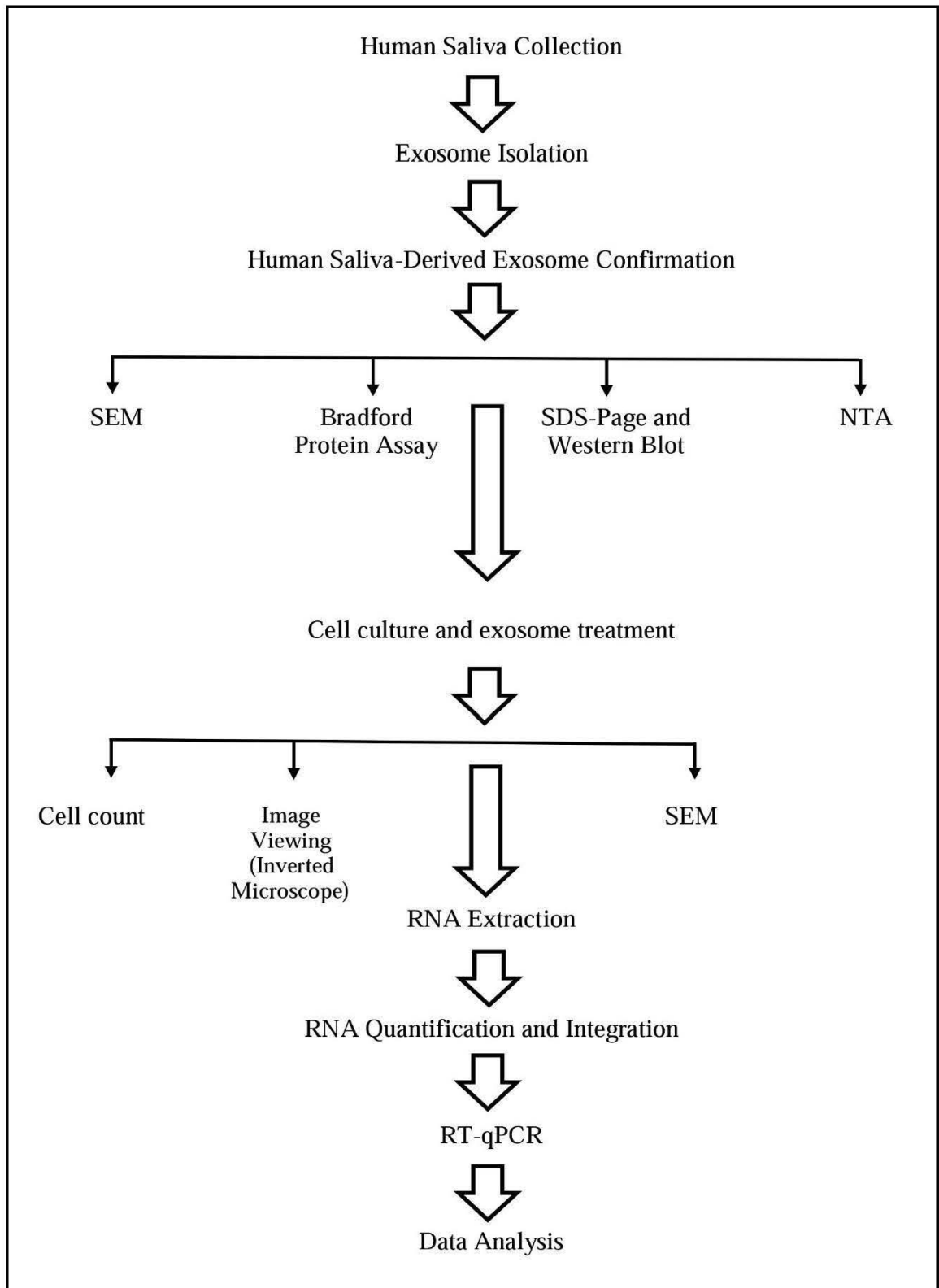
Figure 6.1: Flow chart of the summary for the research methodologies.

REFERENCES

Aframian, D. J., Davidowitz, T. & Benoliel, R. 2006. The distribution of oral mucosal pH values in healthy saliva secretors. *Oral Diseases,* 12**,** 420-423.

Al-Hisayat, A. S., Al-Sa'eed, O. R. & Darmani, H. 2012. Quality of cellular attachment to various root-end filling materials. *Journal of Applied Oral Science,* 20.

Al-Jehani, Y. A. 2014. Risk factors of periodontal disease: Review of the literature. *International Journal of Dentistry***,** 1-9.

Alberts, B., Johnson, A., Lewis, J., Raff, M., Roberts, K. & Walter, P. 2008. *Molecular biology of the cell,* New York.

Alves, L. B., Mariguela, V. C., Grisi, M. F. d. M., Sérgio Luiz Scaombatti de Souza, Junior, A. B. N., Junior, M. T., Oliveira, P. T. d. & Palioto, D. B. 2014. Expression of osteoblastic phenotype in periodontal ligament fibroblasts cultured in three-dimensional collagen gel. *Journal of Applied Oral Science,* 23**,** 206-214.

Bartold, P. M. 2015. Group C Initiator Paper Periodontal Regeneration - fact or fiction? *Journal of the International Academy of Periodontology,* 17.

Bath-Balogh, M. & Fehrenbach, M. J. 2011. *Illustrated dental embryology, histology, and anatomy*, Elsevier.

Baxter, L. C., Frauchiger, V., Textor, M., Gwynn, I. a. & Richards, R. G. 2002. Fibroblast and osteoblast adhesion and morphology on calcium phosphate surfaces. *European Cells and Materials,* 4**,** 1-17.

Bendandi, M. 2010. Hybridoma-Derived Idiotype Vaccine for Lymphoma: Approval Must Wait. *Pharmaceuticals,* 3**,** 667-678.

Bennett, N. T. & Schultz, G. S. 1993. Growth factors and wound healing: biochemical properties of growth and their receptors. *American Journal of Surgery,* 165**,** 728-737.

Borges, F. T., Melo, S. A., Özdemir, B. C., Kato, N., Revuelta, I., Miller, C. A., II, V. H. G., LeBleu, V. S. & Kalluri, R. 2013. TGF-β1-containing exosomes from injured epithelial cells activate fibroblasts to initiate tissue regenerative responses and fibrosis. *Journal of The American Society of Nephrology,* 24**,** 385-392.

Braden, B. C., Dall'Acqua, W., Eisenstein, E., Fields, B. A., Goldbaum, F. A., Malchiodi, E. L., Mariuzza, R. A., Schwarz, F. P., Ysern, X. & Poljak, R. J. 1995. Protein motion and lock and key complementarity in antigen-antibody reactions. *Pharmaceutica Acta Helvetiae,* 69**,** 225-230.

Bretz, N. P., Ridinger, J., Rupp, A.-K., Rimbach, K., Keller, S., Rupp, C., Marmé, F., Umansky, L., Umansky, V., Eigenbrod, T., Sammar, M. & Altevogt, P. 2013. Body fluid exosomes promote secretion of inflammatory cytokines in monocytic cells via toll-like receptor signaling. *Journal of Biological Chemistry,* 288.

Buchner, J. & Walter, S. 2002. Molecular chaperones–cellular machines for protein folding. *Angewandte Chemie,* 41**,** 1098-1113.

Caton, J. G., DeFuria, E. L., Polson, A. M. & Nyman, S. 1987. Periodontal regeneration via selective cell repopulation. *Jounal of Periodontology,* 58.

Cheruvanky, A., Zhou, H., Pisitkun, T., Kopp, J. B., Knepper, M. A., Yuen, P. S. T. & Star, R. A. 2007. Rapid isolation of urinary exosomal biomarkers using a nanomembrane ultrafiltration concentrator. *American Journal of Physiology - Renal Physiology,* 292**,** F1657-F1661.

Chiba-Falek, O. 2013. Gene Expression. *In:* GELLMAN, M. D. & TURNER, J. R. (eds.) *Encyclopedia of Behavioral Medicine.* New York, NY: Springer New York.

Christianson, H. C., Svensson, K. J., van Kuppevelt, T. H., Li, J.-P. & Belting, M. 2013. Cancer cell exosomes depend on cell-surface heparan sulfate proteoglycans for their internalization and functional activity. *Proceedings of the National Academy of Sciences,* 110**,** 17380-17385.

Clayton, A., Mitchell, J. P., Court, J., Mason, M. D. & Tabi, Z. 2007. Human Tumor-Derived Exosomes Selectively Impair Lymphocyte Responses to Interleukin-2. *Cancer Research,* 67**,** 7458.

Crewe, A. V. 1974. Scanning transmission electron microscopy. *Journal of Microscopy,* 100**,** 247-259.

Dabra, S., Chhina, K., Soni, N. & Bhatnagar, R. 2012. Tissue engineering in periodontal regeneration: A brief review. *Dental Research Journal,* 9**,** 671-680.

Dangaria, S. J., Ito, Y., Luan, X. & Diekwisch, T. G. H. 2011. Successful periodontal ligament regeneration by periodontal progenitor preseeding on natural tooth root surfaces. *Stem Cells and Development,* 20**,** 1659-1668.

Dawes, C. 2008. Salivary flow patterns and the health of hard and soft tissues. *Journal of American Dental Association,* 139**,** 18-25.

Díaz-Martín, V., Manzano-Román, R., Valero, L., Oleaga, A., Encinas-Grandes, A. & Pérez-Sánchez, R. 2013. An insight into the proteome of the saliva of the argasid tick Ornithodoros moubata reveals important differences in saliva protein composition between the sexes. *Journal of Proteomics,* 80**,** 216-235.

Docheva, D., Padula, D., Popov, C., Weishaupt, P., Prägert, M., Miosge, N., Hickel, R., Böcker, W., ClausenSchaumann, H. & Schieker, M. 2011. Establishment of immortalized periodontal ligament progenitor cell line and its behavioural analysis on smooth and rough titanium surfaces. *European Cells and Materials,* 19**,** 228-241.

Edgar, M., Dawes, C. & O'Mullane, D. 2013. *Saliva and oral health*, Nature Publishing Group.

Edwards, P. C. & Kanjirath, P. 2010. Recognition and management of common acute conditions of the oral cavity resulting from tooth decay, periodontal disease, and trauma: An update for the family physician. *Journal of The American Board of Family Medicine,* 23**,** 285-294.

Ekström, J., Khosravani, N., Castagnola, M. & Messana, I. 2012. Saliva and the Control of Its Secretion. *In:* EKBERG, O. (ed.) *Dysphagia: Diagnosis and Treatment.* Berlin, Heidelberg: Springer Berlin Heidelberg.

Ekström, K., Omar, O., Granéli, C., Wang, X., Vazirisani, F. & Thomsen, P. 2013. Monocyte exosomes stimulate the osteogenic gene expression of mesenchymal stem cells. *Exosomes Communicate Osteogenic Responses,* 8.

Ellegaard, B., Kauring, T. & Löe, H. 1974. New periodontal attachment procedure based on retardation of epithelial migration. *Journal of Clinical Periodontology,* 1**,** 75-88.

Fröhlich, D., Kuo, W. P., Frühbeis, C., Sun, J.-J., Zehendner, C. M., Luhmann, H. J., Pinto, S., Toedling, J., Trotter, J. & Krämer-Albers, E.-M. 2014. Multifaceted effects of oligodendroglial exosomes on neurons: Impact on neuronal firing rate, signal transduction and gene regulation. *Philosophical Transactions of the Royal Society B: Biological Sciences,* 369.

Fuentes, P., Garrett, S., Nilvéus, R. & Egelberg, J. 1993. Coronally positioned flap with or without citric acid root conditioning in class II defects. *Journal of Clinical Periodontology,* 20**,** 425-430.

Gallo, A., Tandon, M., Alevizos, I. & Illei, G. G. 2012. The majority of microRNAs detectable in serum and saliva is concentrated in exosomes. *PLoS ONE,* 7**,** 1-5.

Ganapathy, N., Venkataraman, S. S., Daniel, R., Aravind, R. J. & Kumarakrishnan, V. B. 2012. Molecular biology of wound healing. *Journal of Pharmacy & Bioallied Sciences,* 4**,** S334-S337.

Ge, Q., Zhou, Y., Lu, J., Bai, Y., Xie, X. & Lu, Z. 2014. miRNA in plasma exosome is stable under different storage conditions. *Molecules,* 19**,** 1568-1575.

Gonzalez-Begne, M., Lu, B., Han, X., Hagen, F. K., Hand, A. R., Melvin, J. E. & Yates, J. R. 2009. Proteomic analysis of human parotid gland exosomes by multidimensional protein identification technology (MudPIT). *Journal of Proteome Research,* 8**,** 1304-1314.

Greening, D. W., Xu, R., Ji, H., Tauro, B. J. & Simpson, R. J. 2015. A Protocol for Exosome Isolation and Characterization: Evaluation of Ultracentrifugation, Density-Gradient Separation, and Immunoaffinity Capture Methods. *In:* POSCH, A. (ed.) *Proteomic Profiling: Methods and Protocols.* New York, NY: Springer New York.

Gröschl, M. 2009. The physiological role of hormones in saliva. *BioEssays,* 31**,** 843-852.

Han, X. & Amar, S. 2002. Identification of genes differentially expressed in cultured human periodontal ligament fibroblasts vs. human gingival fibroblasts by DNA microarray analysis. *Journal of Dental Research,* 81**,** 399-405.

He, M., Crow, J., Roth, M., Zeng, Y. & Godwin, A. K. 2014. Integrated immunoisolation and protein analysis of circulating exosomes using microfluidic technology *Lab on a Chip,* 14**,** 3773-3780.

Heintze, U., Birkhed, D. & Björn, H. 1983. Secretion Rate and Buffer Effect of Resting and Stimulated Whole Saliva as a Function of Age and Sex. *Swedish Dental Journal,* 7**,** 227-238.

Heusermann, W., Hean, J., Trojer, D., Steib, E., von Bueren, S., Graff-Meyer, A., Genoud, C., Martin, K., Pizzato, N., Voshol, J., Morrissey, D. V., Andaloussi, S. E. L., Wood, M. J. & Meisner-Kober, N. C. 2016. Exosomes surf on filopodia to enter cells at endocytic hot spots, traffic within endosomes, and are targeted to the ER. *The Journal of Cell Biology,* 213**,** 173-184.

Hoffman, W., Lakkis, F. G. & Chalasani, G. 2016. B Cells, Antibodies, and More. *Clinical Journal of the American Society of Nephrology : CJASN,* 11**,** 137-154.

Hofman, L. F. 2001. Human saliva as a diagnostic specimen. *Journal of Nutrition***,** 1621-1625.

Hood, J. L., Scott, M. J. & Wickline, S. A. 2014. Maximizing exosome colloidal stability following electroporation. *Analytical Biochemistry,* 448**,** 41-49.

Huggett, J., Dheda, K., Bustin, S. & Zumla, A. 2005. Real-time RT-PCR normalisation; strategies and considerations. *Genes and Immunity,* 6**,** 279-284.

Humphrey, S. P. & Williamson, R. T. 2001. A review of saliva: Normal composition, flow and function. *The Journal of Prosthetic Dentistry,* 85**,** 162-169.

Ishikawa, Y., Pieczonka, T. D. & Bragiel, A. M. 2014. Membrane transporters in salivary exosomes and microvesicles as biomarkers of systemic or oral disease. *Journal of Oral Biosciences,* 56**,** 110-114.

Ivanovski, S., Li, H., Haase, H. R. & Bartold, P. M. 2001. Expression of bone associated macromolecules by gingival and periodontal ligament fibroblasts. *Journal of Periodontal Research,* 36**,** 131-141.

Iwata, T., Yamato, M., Ishikawa, I., Ando, T. & Okano, T. 2014. Tissue engineering in periodontal tissue. *The Anatomical Record,* 297**,** 16-25.

Kalra, H., Drummen, G. P. C. & Mathivanan, S. 2016. Focus on Extracellular Vesicles: Introducing the Next Small Big Thing. *International Journal of Molecular Sciences,* 17**,** 170.

Kawas, S. A., Rahim, Z. H. A. & Ferguson, D. B. 2012. Potential uses of human salivary protein and peptide analysis in the diagnosis of disease. *Archives of Oral Biology,* 57**,** 1-9.

Keller, S., Sanderson, M. P., Stoeck, A. & Altevoqt, P. 2006. Exosomes: From biogenesis and secretion to biological function. *Immunology Letters,* 107**,** 103-108.

Kern, B., Shen, J., Starbuck, M. & Karsenty, G. 2001. Cbfa1 contributes to the osteoblast-specific expression of type I collagen genes. *Journal of Biological Chemistry,* 276**,** 7101-7107.

Lagerlof, F. & Dawes, C. 1984. The Volume of Saliva in the Mouth Before and After Swallowing. *Journal of Dental Research,* 63**,** 618-621.

Lai, R. C., Arslan, F., Lee, M. M., Sze, N. S. K., Choo, A., Chen, T. S., Salto-Tellez, M., Timmers, L., Lee, C. N., El Oakley, R. M., Pasterkamp, G., de Kleijn, D. P. V. & Lim, S. K. 2010. Exosome secreted by MSC reduces myocardial ischemia/reperfusion injury. *Stem Cell Research,* 4**,** 214-222.

Lai, R. C., Yeo, R. W. Y., Tan, K. H. & Lim, S. K. 2012. Exosomes for drug delivery - A novel application for the mesenchymal stem cell. *Biotechnology Advances,* 31**,** 534-551.

Lallier, T. E. 2005. Transcript profiling of periodontal fibroblasts and osteoblasts. *Jounal of Periodontology,* 76**,** 1044-1055.

Lässer, C., Eldh, M. & Lötvall, J. 2012. Isolation and characterization of RNA-containing exosomes. *Journal of Visualized Experiments*.

Lee, C. H., Shin, H. J., Cho, I. H., Kang, Y.-M., Kim, I. A., Park, K.-D. & Shin, J.-W. 2005. Nanofiber alignment and direction of mechanical strain affect the ECM production of human ACL fibroblast. *Biomaterials,* 26**,** 1261-1270.

Lee, K., Shao, H., Weissleder, R. & Lee, H. 2015. Acoustic Purification of Extracellular Microvesicles. *ACS Nano,* 9**,** 2321-2327.

Lee, M., Ban, J., Im, W. & Kim, M. 2016. Influence of storage condition on exosome recovery. *Biotechnology and Bioprocess Engineering,* 21**,** 299-304.

Li, P., Kaslan, M., Lee, S. H., Yao, J. & Gao, Z. 2017. Progress in Exosome Isolation Techniques. *Theranostics* 7**,** 789-804.

Liao, W., Okada, M., Sakamoto, F., Okita, N., Inami, K., Nishiura, A., Hashimoto, Y. & Matsumoto, N. 2013. In vitro human periodontal ligament-like tissue formation with porous poly-L-lactide matrix. *Material Science and Engineering C,* 33**,** 3273-3280.

Liddell, E. 2013. Chapter 3.1 - Antibodies A2 - Wild, David. *The Immunoassay Handbook (Fourth Edition).* Oxford: Elsevier.

Lijnen, P. & Petrov, V. 2002. Transforming growth factor-beta 1-induced collagen production in cultures of cardiac fibroblasts is the result of the appearance of myofibroblasts. *Methods and Findings in Experimental and Clinical Pharmacology,* 24**,** 333-344.

Liu, Y., Xiang, X., Zhuang, X., Zhang, S., Liu, C., Cheng, Z., Michalek, S., Grizzle, W. & Zhang, H.-G. 2010. Contribution of MyD88 to the Tumor Exosome-Mediated Induction of Myeloid Derived Suppressor Cells. *The American Journal of Pathology,* 176**,** 2490-2499.

Livak, K. J. & Schmittgen, T. D. 2001. Analysis of Relative Gene Expression Data Using Real-Time Quantitative PCR and the $2^{-\Delta\Delta CT}$ Method. *Methods,* 25**,** 402-408.

Mahmood, T. & Yang, P.-C. 2012. Western Blot: Technique, Theory, and Trouble Shooting. *North American Journal of Medical Sciences,* 4**,** 429-434.

Major, C. V., Read, S. E., Coates, R. A., Francis, A., McLaughlin, B. J., Millson, M., Shepherd, F., Fanning, M., Calzavara, L., MacFadden, D., Johnson, J. K. & O'Shaughnessy, M. V. 1991. Comparison of saliva and blood for human immunodeficiency virus prevalence testing. *Journal of Infection Disease,* 163.

Malloy, A. 2011. Count. size and visualize nanoparticles. *Materials Today,* 14**,** 170-173.

Manoranjan, S. J., Faizuddin, M., Hemalatha, M. & Ranganath, V. 2012. The effect of platelet derived growth factor-AB on periodontal ligament fibroblasts: An in vitro study. *Journal of Indian Society of Periodontology,* 16**,** 49-53.

Masci, V. L., Taddei, A. R., Gambellini, G., Giorgi, F. & Fausto, A. M. 2015. Ultrastructural investigation on fibroblast interaction with collagen scaffold. *Journal of Biomedical Materials Research Part A,* 00A**,** 1-11.

Mathew, M. M., Joseph, J. & Vineetha, V. C. 2014. Periodontitis–Disease and treatment – A Review. *International Journal of Pharmaceutical and Chemical Sciences,* 3**,** 791-800.

Mathivanan, S., Ji, H. & Simpson, R. J. 2010. Exosomes: Extracellular organelles important in intercellular communication. *Journal of Proteomics,* 73**,** 1907-1920.

Mattila, P. K. & Lappalainen, P. 2008. Filopodia: Molecular architecture and cellular functions. *Nature Reviews Molecular Cell Biology,* 9**,** 446-454.

Maverakis, E., Kim, K., Shimoda, M., Gershwin, M. E., Patel, F., Wilken, R., Raychaudhuri, S., Ruhaak, L. R. & Lebrilla, C. B. 2015. Glycans in the immune system and The Altered Glycan Theory of Autoimmunity: A critical review. *Journal of Autoimmunity,* 57**,** 1-13.

McCulloch, C. A. G., Lekic, P. & McKee, M. D. 2000. Role of physical forces in regulating the form and function of the periodontal ligament. *Periodontology 2000,* 24**,** 56-72.

Merchant, M. L., Rood, I. M., Deegens, J. K. J. & Klein, J. B. 2017. Isolation and characterization of urinary extracellular vesicles: implications for biomarker discovery. *Nature Reviews Nephrology,* 13**,** 731.

Mese, H. & Matsuo, R. 2007. Salivary secretion, taste and hyposalivation. *Journal of Oral Rehabilitation,* 34**,** 711-723.

Michael, A., Bajracharya, S. D., Yuen, P. S. T., Zhou, H., Star, R. A., Illei, G. G. & Alevizos, I. 2010. Exosomes from human saliva as a source of microRNA biomarkers. *Oral Disease,* 16 (1)**,** 1-10.

MOH 2013. Periodontal disease amongst Malaysian. Malaysia: Ministry of Health, Malaysia.

Mumford, J. H., Carnes, D. L., Cochran, D. L. & Oates, T. W. 2001. The effects of platelet-derived growth factor-BB on periodontal cells in an in vitro wound model. *Jounal of Periodontology,* 72**,** 331-340.

Murakami, Y., Kojima, T., Nagasawa, T., Kobayashi, H. & Ishikawa, I. 2003. Novel isolation of alkaline phosphatase positive subpopulation from periodontal ligament fibroblasts. *Jounal of Periodontology,* 74**,** 780-786.

Muralidharan-Chari, V., Clancy, J., Plou, C., Romao, M., Chavrier, P., Raposo, G. & D'Souza-Schorey, C. 2009. ARF6-Regulated Shedding of Tumor Cell-Derived Plasma Membrane Microvesicles. *Current Biology,* 19**,** 1875-1885.

Nagai, N., Mori, K., Satoh, Y., Takahashi, N., Yunoki, S., Tajima, K. & Munekata, M. 2007. In vitro growth and differentiated activities of human periodontal fibroblast cultured on salmon collagen gel. *Wiley InterScience*.

Nanci, A. 2013. *Ten Cate's oral histology*, Elsevier.

Nanci, A. & Bosshardt, D. D. 2006. Structure of periodontal tissues in health and disease. *Periodontology 2000,* 40**,** 11-28.

Nield-Gehrig, J. S. & Willmann, D. 2007. *Foundation of periodontics for the dental hygienist,* Philadelphia, Lippincott Williams & Wilkins.

Nomura, Y., Ishikawa, M., Yashiro, Y., Sanggarnjanavanich, S., Yamaguchi, T., Arai, C., Noda, K., Takano, Y., Nakamura, Y. & Hanada, N. 2012. Human periodontal ligament fibroblasts are the optimal cell source for induced pluripotent stem cells. *Histochemistry and Cell Biology,* 137**,** 719-732.

Nyman, S., Gottlow, J., Lindhe, J., Karring, T. & Wennstrom, J. 1987. New attachment formation by guided tissue regeneration. *Journal of Periodontal Research,* 22**,** 252-254.

Nyman, S., Lindhe, J., Karring, T. & Rylander, H. 1982. New attachment following surgical treatment of human periodontal disease. *Journal of Clinical Periodontology,* 9**,** 290-296.

Oates, T. W., Mumford, J. H., Carnes, D. L. & Cochran, D. L. 2001. Characterization of proliferation and cellular wound fill in periodontal cells using an in vitro wound model. *Jounal of Periodontology,* 72**,** 324-330.

Oates, T. W., Rouse, C. A. & Cochran, D. L. 1993. Mitogenic effects of growth factors on human periodontal ligament cells in vitro. *Journal of Periodontology,* 64**,** 142-148.

Ogawa, Y., Miura, Y., Harazono, A., Kanai-Azuma, M., Akimoto, Y., Kawakami, H., Yamaguchi, T., Toda, T., Endo, T., Tsubuki, M. & Yanoshita, R. 2011. Proteomic analysis of two types of exosomes in human whole saliva. *Biological and Pharmaceutical Bulletin,* 34**,** 13-23.

Ornitz, D. M. & Itoh, N. 2001. Fibroblast growth factors. *Genome Biology,* 2**,** 1-12.

Palanisamy, V., Sharma, S., Deshpande, A., Zhou, H., Gimzewski, J. & Wong, D. T. 2010. Nanostructural and transcriptomic analyses of human saliva-derived exosome. *PLoS ONE,* 5**,** 1-11.

Pandit, N., Malik, R. & Philips, D. 2011. Tissue engineering: A new vista in periodontal regeneration. *Journal of Indian Society of Periodontology,* 15**,** 328-337.

Pant, S., Hilton, H. & Burczynski, M. E. 2012. The multifaceted exosome: Biogenesis, role in normal and aberrant cellular function, and frontiers for pharmacological and biomarker opportunities. *Biochemical Pharmacology,* 83.

Pollard, T. D. & Cooper, J. A. 2009. Actin, a central player in cell shape and movement. *Science,* 326**,** 1208-1212.

Popova, C., Dosseva-Panova, V. & Panov, V. 2013. Microbiology of Periodontal Disease, A Review. *Biotechnology & Biotechnological Equipment,* 27**,** 3754-3759.

Prichard, J. 1957. The infrabony technique as a predictable procedure. *Journal of Periodontology,* 28**,** 202-216.

Raja, S., Byakod, G. & Pudakalkatti, P. 2009. Growth factors in periodontal regeneration. *International Journal of Dental Hygiene,* 7**,** 82-89.

Ramseier, C. A., Rasperini, G., Batia, S. & Giannobile, W. V. 2000. Advanced regenerative technologies for periodontal tissue repair. *Periodontology 2000,* 59**,** 185-202.

Read, G. F. 1989. Hormones in saliva. *Human Saliva: Clinical Chemistry and Microbiology,* 2**,** 147-176.

Reviews, C. 2016. *21st Century Chemistry*, Cram101.

Reynolds, M. A., Aichelmann-Reidy, M. E., Branch-Mays, G. L. & Gunsolley, J. C. 2003. The efficacy of bone replacement grafts in the treatment of periodontal osseous defects. A systematic review. *Annals of Periodontology,* 8**,** 227-265.

Sato, Y., Kikuchi, M., Ohata, N., Tamura, M. & Kuboki, Y. 2004. Enhanced cementum formation in experimentally induced cementum defects of the root surface with the application of recombinant bFGF in collagen gel in vivo. *Journal of Periodontology,* 75**,** 243-248.

Schenkels, L. C. P. M., Veerman, E. C. I. & Amerongen, A. V. N. 1995. Biochemical composition of human saliva in relation to other mucosal fluids. *Critical Reviews in Oral Biology and Medicine,* 6**,** 161-175.

Schneider, A. & Simons, M. 2013. Exosomes: Vesicular carriers for intercellular communication in neurodegenerative disorders. *Cell Tissue Research,* 352**,** 33-47.

Schwartz, K. & Bochkariov, D. 2017. Novel chemiluminescent Western blot blocking and antibody incubation solution for enhanced antibody-antigen interaction and increased specificity. *Electrophoresis,* 38**,** 2631-2637.

Shahidan, W. N. S. 2011. *MicroRNA analysis in saliva.* Doctoral (Academic) Doctoral (Academic) thesis, The University of Tokushima Graduate School.

Sharma, S., Rasool, H. I., Palanisamy, V., Mathisen, C., Schmidt, M., Wong, D. T. & Gimzewski, J. K. 2010. Structural-mechanical characterization of nano-particles-exosomes in human saliva, using correlative AFM, FESEM and force spectroscopy. *ACS Nano,* 40**,** 1-11.

Silverman, J. M., Clos, J., Horakova, E., Wang, A. Y., Wiesgigl, M., Kelly, I., Lynn, M. A., McMaster, W. R., Foster, L. J., Levings, M. K. & Reiner, N. E. 2010. Leishmania Exosomes Modulate Innate and Adaptive Immune Responses through Effects on Monocytes and Dendritic Cells. *The Journal of Immunology,* 185**,** 5011.

Simpson, R. J., Lim, J. W. E., Moritz, R. L. & Mathivanan, S. 2009. Exosomes: proteomic insights and diagnostic potential. *Expert Reviews Proteomics,* 6**,** 267-283.

Small, J. V., Stradal, T., Vignal, E. & Rottner, K. 2002. The lamellipodium: where motility begins. *Trends in Cell Biology,* 12**,** 112-120.

Sokolova, V., Ludwig, A.-K., Hornung, S., Rotan, O., Horn, P. A., Epple, M. & Giebel, B. 2011. Charaterization of exosomes derived from human cells by nanoparticle tracking analysis and scanning electron microscopy. *Colloids and Surfaces B: Biointerfaces,* 87**,** 146-150.

Spielman, N. & Wong, D. T. 2011. Saliva: Diagnostics and therapeutic perspectives. *Oral Diseases,* 17**,** 345-354.

Stein, J. M. & Luzio, J. P. 1991. Ectocytosis caused by sublytic autologous complement attack on human neutrophils. The sorting of endogenous plasma-membrane proteins and lipids into shed vesicles. *Biochemical Journal,* 274**,** 381-386.

Szajnik, M., Derbis, M., Lach, M., Patalas, P., Michalak, M., Drzewiecka, H., Szpurek, D., Nowakowski, A., Spaczynski, M., Baranowski, W. & Whiteside, T. L. 2013. Exosomes in plasma of patients with ovarian carcinoma: Potential biomarkers of tumor progression and response to therapy. *Gynecology & Obstetrics***,** 1-5.

Takashiba, S., Naruishi, K. & Murayama, Y. 2003. Perspective of cytokine regulation for periodontal treatment: Fibroblast biology. *Journal of Periodontology,* 74**,** 103-110.

Takayama, S., Murakami, S., Ikezawa, K., Tasaka, S., Asano, T. & Okada, H. 1997. Effect of basic fibroblast growth factor in human periodontal ligament cells. *Journal of Periodontal Research,* 32**,** 667-675.

Taylor, R. C., Cullen, S. P. & Martin, S. J. 2008. Apoptosis: controlled demolition at the cellular level. *Nature Reviews Molecular Cell Biology,* 9**,** 231.

Thakur, B. K., Zhang, H., Becker, A., Matei, I., Huang, Y., Costa-Silva, B., Zheng, Y., Hoshino, A., Brazier, H., Xiang, J., Williams, C., Rodriguez-Barrueco, R., Silva, J. M., Zhang, W., Hearn, S., Elemento, O., Paknejad, N., Manova-Todorova, K., Welte, K., Bromberg, J., Peinado, H. & Lyden, D. 2014. Double-stranded DNA in exosomes: a novel biomarker in cancer detection. *Cell Research,* 24**,** 766-769.

Théry, C., Amigorena, S., Raposo, G. & Clayton, A. 2006. Isolation and Characterization of Exosomes from Cell Culture Supernatants and Biological Fluids. *Current Protocols in Cell Biology.* John Wiley & Sons, Inc.

Van Der Pol, E., Hoekstra, A. G., Sturk, A., Otto, C., Van Leeuwen, T. G. & Nieuwland, R. 2010. Optical and non-optical methods for detection and characterization of microparticles and exosomes. *Journal of Thrombosis and Haemostasis,* 8**,** 2596-2607.

van Oss, C. J., Good, R. J. & Chaudhury, M. K. 1986. Nature of the antigen-antibody interaction. Primary and secondary bonds: optimal conditions for association and dissociation. *J Chromatogr,* 376**,** 111-9.

Vernon-Parry, K. D. 2000. Scanning electron microscope: An introduction. *Analysis,* 13**,** 40-44.

Wang, H. L., Greenwell, H., Fiorellini, J., Giannobile, W., Offenbacher, S., Salkin, L., Townsend, C., Sheridan, P. & Genco, R. J. 2005. Position paper: Periodontal regeneration. *Journal Of Periodontology,* 76**,** 1601-1622.

Wang, K., Zhang, S., Weber, J., Baxter, D. & Galas, D. J. 2010. Export of microRNAs and microRNA-protective protein by mammalian cells. *Nucleic Acids Research,* 38**,** 7248-7259.

Wang, Z., Wu, H.-j., Fine, D., Schmulen, J., Hu, Y., Godin, B., Zhang, J. X. J. & Liu, X. 2013. Ciliated micropillars for the microfluidic-based isolation of nanoscale lipid vesicles. *Lab on a chip,* 13**,** 2879-2882.

Weston, G. D., Moule, A. J. & Bartold, P. M. 1999. A comparison *in vitro* of fibroblast attachment to resected root-ends. *Internation Endodontic Journal,* 32**,** 444-449.

WHO 2012. Oral health. April 2012 ed.: World Health Organization.

Williams, D. B. & Carter, C. B. 1996. *Transmission electron microscopy*, Springer US.

Woof, J. M. & Burton, D. R. 2004. Human antibody–Fc receptor interactions illuminated by crystal structures. *Nature Reviews Immunology,* 4**,** 89.

Wu, Y., Deng, W. & Klinke, D. J. 2015. Exosomes: Improved methods to characterize their morphology, RNA content, and surface protein biomarkers. *Analyst,* 140**,** 6631-6642.

Xiao, W., Dong, W., Zhang, C., Saren, G., Geng, P., Zhao, H., Li, Q., Zhu, J., Li, G., Zhang, S. & Ye, M. 2013. Effects of the epigenetic drug MS-275 on the release and function of exosome-related immune molecules in hepatocellular carcinoma cells. *European Journal of Medical Research,* 18.

Yagi, K. 1987. Reflection electron microscopy. *Journal of Applied Crystallography,* 20**,** 147-160.

Yamada, T., Inoshima, Y., Matsuda, T. & Ishiguro, N. 2012. Comparison of methods for isolating exosome from bovine milk. *Journal of Veterinary Medical Science,* 74**,** 1523-1525.

Yang, Q., Diamond, M. P. & Al-Hendy, A. 2016. The emerging role of extracellular vesicle-derived miRNAs: Implication in cancer progression and stem cell related diseases. *Journal of Clinical Epigenetics,* 2**,** 1-10.

Yu, N., Oortgiesen, D. A. W., Bronckers, A. L., Yang, F., Walboomers, X. F. & Jansen, J. A. 2013. Enhanced periodontal tissue regeneration by periodontal cell implantation. *Journal of Clinical Periodontology,* 40**,** 698-706.

Yun, S. J., Kim, B. O., Yun, J. H., Kang, D. W. & Jang, H. S. 2006. Profiling of genes in healthy hGF, aging hGF, healthy hPDLF and inflammatory hPDLF by DNA microarray. *Journal of Peridontal & Implant Science,* 36**,** 767-782.

Zarovni, N., Corrado, A., Guazzi, P., Zocco, D., Lari, E., Radano, G., Muhhina, J., Fondelli, C., Gavrilova, J. & Chiesi, A. 2015. Integrated isolation and quantitative analysis of exosome shuttled proteins and nucleic acids using immunocapture approaches. *Methods,* 87**,** 46-58.

Zelles, T., Purushotham, K. R., Macauley, S. P., Oxford, G. E. & Humphreys-Beher, M. G. 1995. Saliva and growth factors: The fountain of youth resides in us all. *Journal of Dental Research,* 74**,** 1825-1832.

Zeringer, E., Barta, T., Li, M. & Vlassov, A. V. 2015. Strategies for Isolation of Exosomes. *Cold Spring Harbor Protocols***,** 319-324.

Zhou, H., Yuen, P. S. T., Pisitkun, T., Gonzales, P. A., Yasuda, H., Dear, J. W., Gross, P., Knepper, M. A. & Star, R. A. 2006. Collection, storage, preservation, and normalization of human urinary exosomes for biomarker discovery. *Kidney International,* 69**,** 1461-1476.

APPENDICES

Appendix 1: Copy of Human Ethics Approval Letter

UNIVERSITI SAINS MALAYSIA

Jawatankuasa Etika Penyelidikan Manusia USM (JEPeM)
Human Research Ethics Committee USM (HREC)

Our. Ref. : USM/JEPeM/272.4.(1.2)
Date : 21st November 2013

Dr. Wan Nazatul Shima Shahidan
School of Dental Sciences
Universiti Sains Malaysia
16150 Kubang Kerian, Kelantan.

Universiti Sains Malaysia
Kampus Kesihatan,
16150 Kubang Kerian,
Kelantan. Malaysia.
T: 609 - 767 3000 *samb.* 2352 / 2362
F: 609 - 767 2351
E: jepem.usm@gmail.com
www.research.usm.my

The Human Research Ethics Committee, Universiti Sains Malaysia (FWA Reg. No: 00007718; IRB Reg. No: 00004494) has approved in principle the study mentioned below:

Title	Effect of Human Saliva Derived Exosome on the Proliferation and Differentiation of Human Periodontal Ligament Stem Cells Cell Line – An *In Vitro* Study.		
Protocol No	-	**Principle Investigator**	Dr. Wan Nazatul Shima Shahidan
Date of approval Protocol received Reviewed by Committee Received Amended Protocol	21st November 2013 24th March 2013 9th October 2013 -	**Co-Investigator(s)**	Dr. Azlina Ahmad Dr. Khairani Idah Mokhtar @ Makhtar Dr. Zurairah Berahim
Research Center	School of Dental Sciences, Universiti Sains Malaysia.	**Date of study start**	December 2013 – November 2015
Financial Support	-	**Number of Samples**	5 subjects

The following item (✓) have been received and reviewed:-

- (✓) **Ethical Approval Application Form**
- (✓) **Research Proposal**
- (✓) **Participant Information Sheet and Consent Form**

Investigator(s) are required to:
a) follow instructions, guidelines and requirements of the Human Research Ethics Committee, Universiti Sains Malaysia (JEPeM)
b) report any protocol deviations/violations to Human Research Ethics Committee (JEPeM)
c) comply with International Conference on Harmonization – Guidelines for Good Clinical Practice (ICH-GCP) and the Declaration of Helsinki
d) note that Human Research Ethics Committee (JEPeM) may audit the approved study.

PROFESSOR DR. HANS AMIN VAN ROSTENBERGHE
Chairman
Human Research Ethics Committee

Appendix 2: Consent Form

MAKLUMAT KAJIAN

Tajuk Kajian:	**Kesan eksosom dalam air liur manusia terhadap proliferasi sel fibroblast periodontal ligamen manusia (HPdLF) - Kajian *in vitro***

Nama Penyelidik: **Dr.Wan Nazatul Shima Shahidan**
                              Dr.Azlina Ahmad
                              Dr.Khairani Idah Mokhtar@Makhtar
                              Dr.Zurairah Berahim

No. Pendaftaran MMC :   **3215** （**Dr.Zurairah Berahim** ）

PENGENALAN

Anda dipelawa untuk menyertai satu kajian penyelidikan secara sukarela yang melibatkan eksosom dalam air liur manusia. Eksosom merupakan vesikel berukuran 40-100 nm yang disekresikan oleh berbagai jenis sel mamalia. Eksosom boleh terhasil dari vesikel endosom intralumenal (MVB) ketika dilepas ke media ekstrasel. Eksosom kini telah ditemui didalam cairan badan seperti darah, urin, air liur dan sebagainya. Eksosom ini dipercayai mempunyai kesan perubatan dan juga alat diagnostic. Walaubagaimanapun kesan eksosom dalam air liur manusia terhadap penambahan dan pembezaan stem sel periodontium masih tidak jelas. Sebelum anda bersetuju untuk menyertai kajian penyelidikan ini, adalah penting anda membaca dan memahami borang ini. Sekiranya anda menyertai kajian ini, anda akan menerima satu salinan borang ini untuk disimpan sebagai rekod anda.

Penyertaan anda di dalam kajian ini hanyalah sekali semasa pengumpulan air liur. Seramai lima sukarela akan menyertai kajian ini.

TUJUAN KAJIAN

Kajian ini bertujuan adalah untuk menentukan sama ada eksosom dalam air liur berpotensi untuk menggiatkan pertumbuhan dan pembezaan stem sel periodontium.

KELAYAKAN PENYERTAAN

Doktor yang bertanggungjawab dalam kajian ini atau salah seorang kakitangan kajian telah membincangkan kelayakan untuk menyertai kajian ini dengan anda. Adalah penting anda berterus terang dengan doktor dan kakitangan tersebut tentang sejarah kesihatan anda. Anda tidak seharusnya menyertai kajian ini sekiranya anda tidak memenuhi semua syarat kelayakan.

Beberapa **keperluan** untuk menyertai kajian ini adalah –

- Sihat tubuh badan

- Anda mesti berumur diantara 20 hingga 40 tahun.

- Tidak merokok

Anda **tidak boleh** menyertai kajian ini sekiranya –

- Anda sedang mempunyai sejarah malignansi, periodontitis, kekurangan imun, hepatitis atau jangkitan HIV.

PROSEDUR-PROSEDUR KAJIAN

Pada hari anda bersetuju untuk diambil air liur, anda akan diminta memberi maklumat tentang sejarah perubatan dan kesihatan gigi diperiksa oleh doktor gigi yang bertauliah. Setelah memenuhi kelayakan anda dilarang makan, minum atau mengunakan produk bahan kumur sekurang kurangnya sejam sebelum pengumpulan air liur itu. Pengumpulan air liur itu juga hendaklah dilakukan dalam masa setengah jam atau sehingga 5 ml dapat dikumpulkan.

RISIKO

Pengumpulan air liur ini tidak akan menimbulkan apa-apa risiko kepada subjek.

Jika apa-apa maklumat penting yang baru dijumpai semasa kajian ini yang mungkin mengubah persetujuan anda untuk terus menyertai kajian ini, anda akan diberitahu secepat mungkin.

PENYERTAAN DALAM KAJIAN

Penyertaan anda dalam kajian ini adalah secara sukarela. Anda berhak menolak untuk menyertai kajian ini atau anda boleh menamatkan penyertaan anda pada bila-bila masa, tanpa sebarang hukuman atau kehilangan manfaat yang sepatutnya anda perolehi.

Penyertaan anda juga mungkin boleh diberhentikan oleh doktor yang terlibat dalam kajian ini tanpa persetujuan anda. Sekiranya anda berhenti menyertai kajian ini, doktor yang terlibat di dalam kajian ini atau salah seorang kakitangan akan berbincang dengan anda mengenai apa-apa isu perubatan berkenaan dengan pemberhentian penyertaan anda.

MANFAAT YANG MUNGKIN [Manfaat terhadap Individu, Masyarakat, Universiti]

Prosedur kajian ini akan diberikan kepada anda tanpa kos. Anda mungkin menerima maklumat tentang kesihatan gigi anda daripada pemeriksaan yang dilakukan dalam kajian ini. Hasil atau maklumat kajian ini diharapkan, dapat memberi manfaat kepada pesakit-pesakit pada masa hadapan. Anda tidak akan menerima sebarang pampasan kerana menyertai kajian ini. Namun sebarang keperluan perjalanan berkaitan dengan penyertaan ini akan diberi.

PERSOALAN

Sekiranya anda mempunyai sebarang soalan mengenai prosedur kajian ini atau hak-hak anda, sila hubungi;

Dr. Wan Nazatul Shima Shahidan
Pusat pengajian Sains Pergigian
USM Kampus Kesihatan
Tel: 09-7675806

Sekiranya anda mempunyai sebarang soalan berkaitan kelulusan Etika atau sebarang pertanyaan dan masalah berkaitan kajian ini, sila hubungi;

Puan Mazlita Zainal Abidin
Setiausaha Jawatankuasa Etika Penyelidikan (Manusia) USM
Pelantar Penyelidikan Sains Klinikal, USM Kampus Kesihatan.
No. Tel: 09-767 2355 / 09-767 2352
Email : jepem@kk.usm.my

KERAHSIAAN

Maklumat perubatan anda akan dirahsiakan oleh doktor dan kakitangan kajian. Ianya tidak akan didedahkan secara umum melainkan jika ia dikehendaki oleh undang-undang.

Data yang diperolehi dari kajian yang tidak mengenalpasti anda secara perseorangan mungkin akan diterbitkan untuk tujuan memberi pengetahuan baru.

Rekod perubatan anda yang asal mungkin akan dilihat oleh pihak penyelidik, Lembaga Etika kajian ini dan pihak berkuasa regulatori untuk tujuan mengesahkan prosedur dan/atau data kajian klinikal. Maklumat perubatan anda mungkin akan disimpan dalam komputer dan diproses dengannya.

Dengan menandatangani borang persetujuan ini, anda membenarkan penelitian rekod, penyimpanan maklumat dan pemindahan data seperti yang dihuraikan di atas.

TANDATANGAN

Untuk dimasukkan ke dalam kajian ini, anda atau wakil sah anda mesti menandatangani serta mencatatkan tarikh halaman tandatangan (Lihat contoh Borang Keizinan Pesakit di **LAMPIRAN S** atau **LAMPIRAN G (untuk sampel genetik)** atau **LAMPIRAN P**).

Borang Keizinan Pesakit/ Subjek
(Halaman Tandatangan)

Tajuk Kajian: **Kesan eksosom dalam air liur manusia terhadap proliferasi sel fibroblast periodontal ligamen manusia (HPdLF) - Kajian** *in vitro*

Nama Penyelidik: **Wan Nazatul Shima Shahidan**

Untuk menyertai kajian ini, anda atau wakil sah anda mesti menandatangani mukasurat ini. Dengan menandatangani mukasurat ini, saya mengesahkan yang berikut:

- Saya telah membaca semua maklumat dalam Borang Maklumat dan Keizinan Pesakit ini **termasuk apa-apa maklumat berkaitan risiko yang ada dalam kajian** dan saya telah pun diberi masa yang mencukupi untuk mempertimbangkan maklumat tersebut.

- Semua soalan-soalan saya telah dijawab dengan memuaskan.

- Saya, secara sukarela, bersetuju menyertai kajian penyelidikan ini, mematuhi segala prosedur kajian dan memberi maklumat yang diperlukan kepada doktor, para jururawat dan juga kakitangan lain yang berkaitan apabila diminta.

- Saya boleh menamatkan penyertaan saya dalam kajian ini pada bila-bila masa.

- Saya telah pun menerima satu salinan Borang Maklumat dan Keizinan Pesakit untuk simpanan peribadi saya.

Nama Pesakit	**Nama Singkatan & No. Pesakit**
No. Kad Pengenalan Pesakit (Baru)	**No. K/P** (Lama)
Tandatangan Pesakit atau Wakil Sah	**Tarikh** (dd/MM/yy) (Masa jika perlu)
Nama & Tandatangan Individu yang Mengendalikan Perbincangan Keizinan	**Tarikh** (dd/MM/yy)
Nama Saksi dan Tandatangan	**Tarikh** (dd/MM/yy)

Nota: i) Semua subjek/pesakit yang mengambil bahagian dalam projek penyelidikan ini tidak dilindungi insuran.

Appendix 3: Table of Sample Labels

SAMPLES LABEL	TEMPERATURE STORAGE	STORAGE PERIOD	ADDITION OF PROTEASE INHIBITOR
4°C (+PI)	4°C	1 hour	Yes
4°C (-PI)	4°C	1 hour	No
-20°C (+PI)	-20°C	1 week	Yes
-20°C (-PI)	-20°C	1 week	No
-80°C (+PI)	-80°C	1 month	Yes
-80°C (-PI)	-80°C	1 month	No

Appendix 4: The Flow Chart of Isolation of Exosome

THE FLOW CHART OF ISOLATION OF EXOSOME

Saliva samples collection

Centrifugation, 6000xg for 20 minutes

Supernatant allocation to new tubes

With protease inhibitor

Without protease inhibitor

A 4°C (1 hour)

B -20°C (1 week)

C -80°C (1 month)

Ultracentrifugation. 100 000xg for 2 hours, 4°C

Exosome pellet (Suspended in 1 ml PBS)
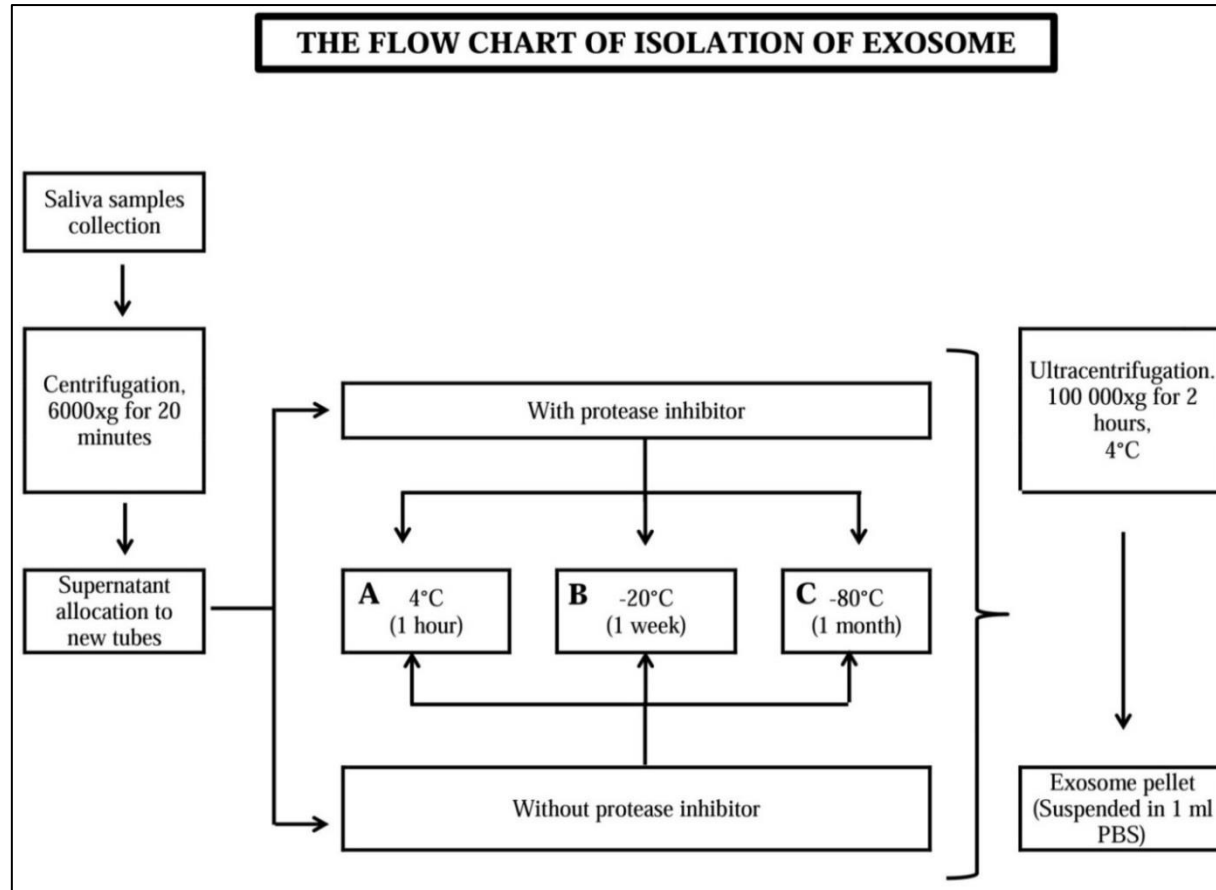
Appendix 5: SDS-PAGE and Western Blot Preparation

I. Resolving Buffer

a. Solution 1 (Tris Base)

Components	Volume/Mass
Tris	72.68 g
Sodium Dodecyl Sulfate (SDS) (0.4%)	1.60 g
Distilled water (dH$_2$O)	400.00 ml

b. Solution 2 (Tris HCl)

Components	Volume/Mass
Tris Hydrochloride (HCl)	23.65 g
Sodium Dodecyl Sulfate (SDS) (0.4%)	0.40 g
Distilled water (dH$_2$O)	100.00 ml

c. Resolving Buffer Solution

Components	Ratio	Volume
Solution 1 (Tris)	80%	400.00 ml
Solution 2 (Tris HCl)	20%	100.00 ml

i. Buffer needs to be adjust to pH 9.3
ii. Buffer needs to be filtered using Grade 1 filter paper
iii. Storage at 4°C
iv. Warm at 37°C before usage

II. Stacking Buffer

Components	Volume/Mass
Tris	6.050 g
Sodium Dodecyl Sulfate (SDS)	0.400 g
Distilled water (dH$_2$O)	100.000 ml

    i.   Buffer needs to be adjust to pH 6.8
    ii.   Buffer needs to be filtered using Grade 1 filter paper
    iii.   Storage at 4°C
    iv.   Warm at 37°C before usage

III. Transfer Buffer

Components	Volume/Mass
Glycine	14.4 g
Tris	3.0 g
Distilled water (dH$_2$O)	1000.0 ml

IV. Sample Buffer

Components	Volume/Mass
Tris Base	0.76 g
Glycerol	10.00 g
Sodium Dodecyl Sulfate (SDS)	1.00 g
Distilled water (dH$_2$O)	50.00 ml

    i.   Buffer needs to be adjust to pH 6.8
    ii.   Buffer needs to be filtered using Grade 1 filter paper
    iii.   Storage at 4°C
    iv.   Warm at 37°C before usage

V. Ammonium Persulfate (10%)

$$\frac{Mass\ of\ AP\ (g)}{10} \times 100 = Distilled\ Water\ (dH2O)\ volume\ needed$$

i.   Store in dark storage (Keep away from light)
ii. Freshly prepare for every use or storage at -20°C (last 6 months)

VI. Running Buffer

Components	Volume/Mass
Tris	30.0 g
Glycine	144.0 g
Sodium Dodecyl Sulfate (SDS)	10.0 g
Distilled water (dH$_2$O)	1000.0 ml

i.   Mix all components
ii. Stir until all the components dissolve completely

VII. Working Running Buffer

Reagents	Volume
Running buffer (1x)	100.0 ml
Distilled water (dH$_2$O)	900.0 ml

VIII. Loading Buffer

Components	Ratio
Sample Buffer	9
2-mercapthoethanol	1
*A tip of blue dye	(1.0 µl)

*Each sample diluted with loading buffer in 1:1 ratio

IX. Preparation of Resolving Gel (2 small gels)

Reagents	Volume
30% acrylamide/bis-acrylamide	4.500 ml
Resolving buffer	2.813 ml
Distilled water (dH$_2$O)	3.938 ml
Ammonium Persulfate (APS)	0.075 ml
Tetramethylethylenediamine (TEMED)	0.015 ml

X. Preparation of Stacking Gel

Reagents	Volume
30% acrylamide/bis-acrylamide	0.325 ml
Stacking buffer	0.625 ml
Distilled water (dH$_2$O)	1.525 ml
Ammonium Persulfate (APS)	0.025 ml
Tetramethylethylenediamine (TEMED)	0.005 ml

XI. Preparation of De-Staining Solution

Reagents	Volume
Acetic Acid	100.0 ml
Isopropanol	100.0 ml
Distilled water (dH$_2$O)	800.0 ml

XII. Preparation of Blocking Buffer

Reagents	Weight or Volume
Skimmed milk (Non-fat dry milk)	1.5 g
Phosphate Buffer Saline with Tween-20 (PBST)	30.0 ml

XIII. Preparation of Phosphate Buffer Solution

Reagents	Weight or Volume
Tablet	1814.5 – 2005.5 mg/tablet
Purified water	200.0 ml

XIV. Preparation of 12% resolving gel

Solution	Volume (µl)
30% Acrylamide + 0.8% bis-acrylamide	4500
Resolving Buffer (4xTris/SDS), pH 9.3	2813
Distilled water	3938
10% Ammonium persulfate (APS)	75
Tetramethylethylenediamine (TEMED)	10

*TEMED was added last

* Preparation was for two small gels

XV. Preparation of 12% stacking gel

Solution	Volume (µl)
30% Acrylamide + 0.8% bis-acrylamide	325
Stacking Buffer (4xTris-Cl/SDS), pH 6.8	625
Distilled water	1525
10% Ammonium persulfate (APS)	25
Tetramethylethylenediamine (TEMED)	5

*TEMED was added last
* Preparation was for two small gels

XVI. Copy of anti-CD63 datasheet

ThermoFisher
SCIENTIFIC

Performance guaranteed
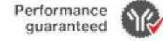
CD63 Monoclonal Antibody (MEM-259)

Catalog Number   MA1-19281

Product data sheet

Details	
Size	100 µg
Host/Isotope	Mouse / IgG1
Class	Monoclonal
Type	Antibody
Clone	MEM-259
Immunogen	T cell line HPB-ALL.
Conjugate	Unconjugated
Form	Liquid
Concentration	1 mg/ml
Purification	Protein A
Storage buffer	PBS, pH 7.4
Contains	15mM sodium azide
Storage Conditions	4° C, do not freeze

Species Reactivity	
Tested species reactivity	Human

Tested Applications	Dilution *
Flow Cytometry (Flow)	2µg/ml
Immunocytochemistry (ICC)	Assay Dependent
Immunofluorescence (IF)	Assay-dependent
Immunohistochemistry (Paraffin) (IHC (P))	10 µg/ml
Immunoprecipitation (IP)	Assay Dependent

* Suggested working dilutions are given as a guide only. It is recommended that the user titrate the product for use in their own experiment using appropriate negative and positive controls.

Background/Target Information

CD63 (LAMP-3, lysosome-associated membrane protein-3), a glycoprotein of tetraspanin family, is present in late endosomes, lysosomes and secretory vesicles of various cell types. It is also present in the plasma membrane, usually following cell activation. Hence, it has become an widely used basophil activation marker. In mast cells, however, CD63 exposition does not need their activation. CD63 interacts with integrins and affects phagocytosis and cell migration, it is also involved in H/K-ATPase trafficking regulation of ROMK1 channels. CD63 also serves as a T-cell costimulation molecule. Expression of CD63 can be used for predicting the prognosis in earlier stages of carcinomas.

For Research Use Only. Not for use in diagnostic procedures. Not for resale without express authorization.

XVII. Copy of anti-β-actin datasheet

ThermoFisher
SCIENTIFIC

Website: thermofisher.com
Customer Service (US): 1 800 955 6288 ext. 1
Technical Support (US): 1 800 955 6288 ext. 441
thermofisher.com/contactus

Performance
guaranteed

beta Actin Monoclonal Antibody (AC-15)

Catalog Number   MA1-91399   **Product data sheet**

Details	
Size	100 µL
Host/Isotope	Mouse / IgG1
Class	Monoclonal
Type	Antibody
Clone	AC-15
Immunogen	synthetic peptide DDDIAALVIDNGSGL conjugated to KLH, corresponding to amino acids 1-14 of Xenopus laevis Actin (beta).
Conjugate	Unconjugated
Form	Liquid
Storage buffer	Ascites
Contains	15mM sodium azide
Storage Conditions	-20° C, Avoid Freeze/Thaw Cycles

Species Reactivity	
Tested species reactivity	Bovine, Dog, Fruit fly, Cat, Fish, Guinea pig, Human, Mouse, Sheep, Pig, Rabbit, Rat, Xenopus
Published species reactivity	Bovine, Zebrafish, Human, Mouse, Not Applicable

Tested Applications	Dilution *
Dot blot (DB)	Assay dependent
ELISA (ELISA)	Assay dependent
Immunocytochemistry (ICC)	1:1000
Immunofluorescence (IF)	1:100-1:2000
Immunohistochemistry (Frozen) (IHC (F))	Assay dependent
Immunohistochemistry (Paraffin) (IHC (P))	Assay dependent
Immunomicroscopy (IM)	Assay dependent
Western Blot (WB)	1:5000-1:10,000

Published Applications	
Western Blot (WB)	See 6 publications below
Miscellaneous PubMed (MISC)	See 4 publications below

* Suggested working dilutions are given as a guide only. It is recommended that the user titrate the product for use in their own experiment using appropriate negative and positive controls.

Product specific information

MA1-91399 detects beta Actin from Xenopus laevis, fish, Drosophila melanogaster, canine, bovine, feline, guinea pig, human, mouse, porcine, rabbit, rat and ovine samples.

MA1-91399 has been successfully used in immunocytochemistry, immunofluorescence, immunohistochemistry (frozen tissue), immunomicroscopy, Western blot, ELISA, dot blot and immunohistochemistry (paraffin tissue) applications. Positive control of cultured human or chicken fibroblasts suggested.

The MA1-91399 immunogen is synthetic peptide; DDDIAALVIDNGSGL, conjugated to KLH, corresponding to amino acids 1-14 of Xenopus laevis Actin (beta).

Background/Target Information

This gene encodes one of six different actin proteins. Actins are highly conserved proteins that are involved in cell motility, structure, and integrity. This actin is a major constituent of the contractile apparatus and one of the two nonmuscle cytoskeletal actins.

For Research Use Only. Not for use in diagnostic procedures. Not for resale without express authorization.

Thermo Fisher Scientific
3747 N. Meridian Road
Rockford, IL 61105 USA

thermofisher.com/contactus

ThermoFisher
SCIENTIFIC

XVIII. Copy of secondary antibody datasheet

ThermoFisher SCIENTIFIC

Website: thermofisher.com
Customer Service (US): 1 800 955 6288 ext. 1
Technical Support (US): 1 800 955 6288 ext. 441
thermofisher.com/contactus

Performance guaranteed
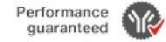
Goat anti-Mouse IgG (H+L) Secondary Antibody, HRP

Catalog Number   31430

Product data sheet

Details

Size	2 mL
Host/Isotope	Goat / IgG
Class	Polyclonal
Type	Secondary Antibody
Target Class	IgG
Conjugate	HRP
Form	Lyophilized
Concentration	0.8 mg/ml
Purification	Antigen affinity chromatography
Storage buffer	PBS, pH 7.6, with 15mg/ml BSA, 50mM sucrose
Contains	no preservative
Storage Conditions	4° C

Species Reactivity

Tested species reactivity	Mouse
Published species reactivity	Not Applicable

Tested Applications

	Dilution *
ELISA (ELISA)	1:10,000-1:25,000
Immunohistochemistry (IHC)	1:5,000 - 1:100,000
Immunoprecipitation (IP)	1:500 - 1:5,000
Western Blot (WB)	1:5,000 - 1:200,000

Published Applications

Western Blot (WB)	See 62 publications below
Immunohistochemistry (Paraffin) (IHC (P))	See 1 publications below
ELISA (ELISA)	See 1 publications below
Immunocytochemistry (ICC)	See 2 publications below
Immunohistochemistry (IHC)	See 3 publications below
Miscellaneous PubMed (MISC)	See 1 publications below

* Suggested working dilutions are given as a guide only. It is recommended that the user titrate the product for use in their own experiment using appropriate negative and positive controls.

Product specific information

Product # 31430 has been successfully used in Western blot, IHC and IP applications.

Product # 31430 reacts with the heavy chains of mouse igg and with the light chains common to most mouse immunoglobulins, but does not react against non-immunoglobulin serum proteins. However, this antibody may cross-react with immunoglobulins from other species.

Store product at 4°C until opened. To extend the shelf-life of this product, add an equal volume of glycerol to make a final concentration of approximately 50% glycerol and store at -20°C.

Reconstitute with 2.0 ml of distilled water (0.8 mg/ml after restoration).

Background/Target Information

Thermo Scientific Anti-Mouse secondary antibodies are affinity-purified antibodies with well-characterized specificity for mouse immunoglobulins and are useful in the detection, sorting or purification of its specified target. Secondary antibodies offer increased versatility enabling users to use many detection systems (e.g. HRP, AP, fluorescence). They can also provide greater sensitivity through signal amplification as multiple secondary antibodies can bind to a single primary antibody. Most commonly, secondary antibodies are generated by immunizing the host animal with a pooled population of immunoglobulins from the target species and can be further purified and modified (i.e. immunoaffinity chromatography, antibody fragmentation, label conjugation, etc.) to generate highly specific reagents.

For Research Use Only. Not for use in diagnostic procedures. Not for resale without express authorization.

For Research Use Only. Not for use in diagnostic procedures. Not for resale without express authorization.

Products are warranted to operate or perform substantially in conformance with published Product specifications in effect at the time of sale, as set forth in the Production documentation, specifications and/or accompanying package inserts ("Documentation"). No claim of suitability for use in applications regulated by FDA is made. The warranty provided herein is valid only when used by properly trained individuals. Unless otherwise stated in the Documentation this warranty is limited to one year from date of shipment when the Product is subjected to normal, proper and intended usage. This warranty does not extend to anyone other than the Buyer. Any model or sample furnished to Buyer is merely illustrative of the general type and quality of goods and does not represent that any Product will conform to such model or sample.

NO OTHER WARRANTIES EXPRESS OR IMPLIED ARE GRANTED INCLUDING WITHOUT LIMITATION IMPLIED WARRANTIES OF MERCHANTABILITY, FITNESS FOR ANY PARTICULAR PURPOSE OR NON INFRINGEMENT. BUYER'S EXCLUSIVE REMEDY FOR NON CONFORMING PRODUCTS DURING THE WARRANTY PERIOD IS LIMITED TO REPAIR, REPLACEMENT OF OR REFUND FOR THE NON-CONFORMING PRODUCT(S) AT SELLER'S SOLE OPTION. THERE IS NO OBLIGATION TO REPAIR, REPLACE OR REFUND FOR PRODUCTS AS THE RESULT OF (i) ACCIDENT, DISASTER OR EVENT OF FORCE MAJEURE, (ii) MISUSE, FAULT OR NEGLIGENCE OF OR BY BUYER, (iii) USE OF THE PRODUCTS IN A MANNER FOR WHICH THEY WERE NOT DESIGNED, OR (iv) IMPROPER STORAGE AND HANDLING OF THE PRODUCTS. Unless otherwise expressly stated on the Product or in the documentation accompanying the Product, the Product is intended for research only and is not to be used for any other purpose, including without limitation, unauthorized commercial uses, in vitro diagnostic uses, ex vivo or in vivo therapeutic uses, or any type of consumption by or application to humans or animals.

Thermo Fisher Scientific
3747 N. Meridian Road
Rockford, IL 61105 USA

thermofisher.com/contactus

ThermoFisher SCIENTIFIC

Appendix 6: Human Salivary Exosomes Targeted Protein Western Blot Bands Intensity ImageJ Analysis Result

Storage Condition	Band intensity of targeted proteins (peak area, pixel)	
	CD63	**β-actin**
4°C (with protease inhibitor)	1013.477	1031.648
4°C (without protease inhibitor)	6204.326	1812.497
-20°C (with protease inhibitor)	302.263	423.092
-20°C (without protease inhibitor)	328.092	640.749
-80°C (with protease inhibitor)	1177.355	2080.083
-80°C (with protease inhibitor)	1809.598	3720.397

Appendix 7: Preparation of Diluted Bovine Serum Albumin (BSA) Standards

Vial	Volume of Diluent	Volume and Source of BSA	Final BSA Concentration
A	0	300 µl of Stock	2000 µg/ml
B	125 µl	375 µl of Stock	1500 µg/ml
C	325 µl	325 µl of Stock	1000 µg/ml
D	175 µl	175 µl of vial B dilution	750 µg/ml
E	325 µl	325 µl of vial C dilution	500 µg/ml
F	325 µl	325 µl of vial E dilution	250 µg/ml
G	325 µl	325 µl of vial F dilution	125 µg/ml
H	400 µl	100 µl of vial G dilution	25 µg/ml
I	400 µl	0	0 µg/ml = Blank

*Working Range = 100-1500 µg/ml

Appendix 8: Cell Counts Calculation

I.   **Cell Count (View under microscope, stained with Trypan Blue Solution)**
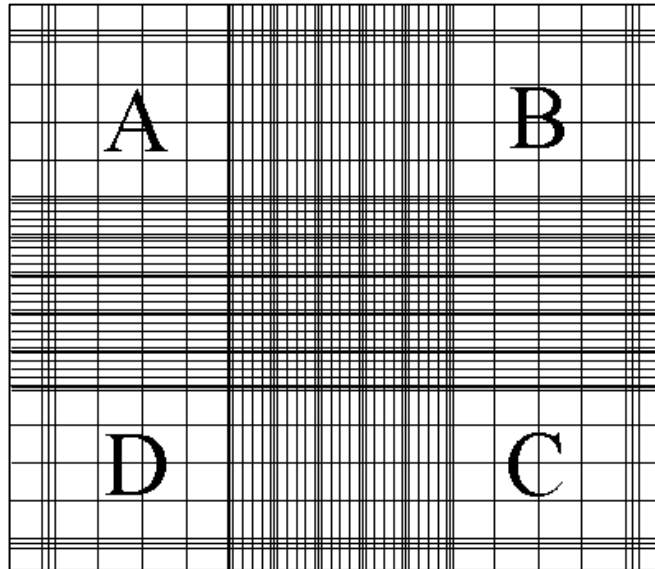
Image I: Gridlines on hemocytometer slide. (Image source: Google Image)
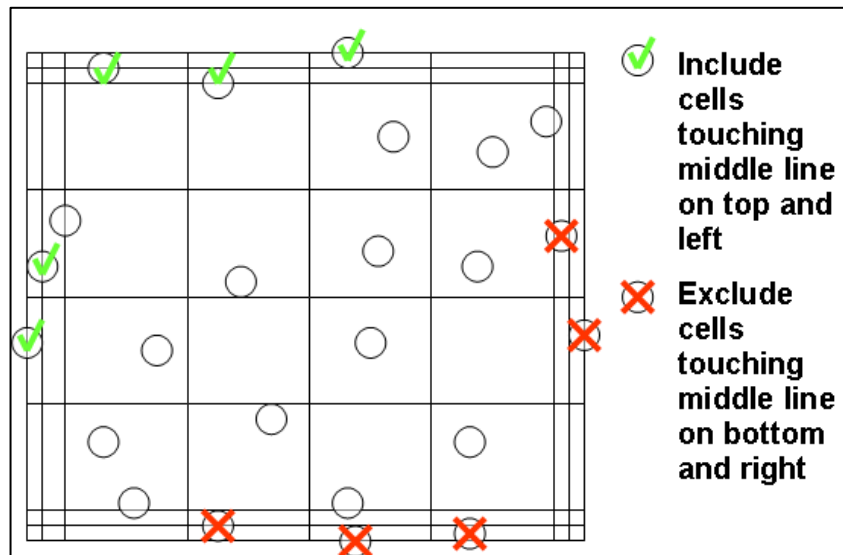
Image II: The cells were counted within the large square and those crossing the edge on two out of the four sides. (Image source: Google Image)

Cell Count Formula

$$\left[\frac{A + B + C + D}{4}\right] \times 2 \times 10^4$$

Dilution factor
(10 ul Trypan Blue + 10 ul sample)

II. Cell seeding counts

HPdLF cells recommendation seeding number

    i. 3,500 cells/cm^2

    ii. Cell culture flask T25 is 87,500 cells

    iii. Cell culture flask T75 is 262,500 cells

    iv. Cell culture 6 well plate is 33,600 cells (For normal growth period)

    v. Cell culture 6 well plate is 90,000-100,000 (For 24 hours of growth)

Appendix 9: Scanning Electron Microscope Sample Fixation Method

GENERAL SAMPLE PREPARATION FOR SCANNING ELECTRON MICROSCOPE

		Plant (CPD)	Tissue (CPD)	Tissue (HMDS)	Bacteria (HMDS)
Primary Fixation	McDowel Trump fixative (4°C)	24 hrs	24 hrs	24 hrs	*2 hrs
Wash	PBS Buffer (0.1 M)	30 min (3x)	10 min (3x)	10 min (3x)	*(2x)
Secondary Fixation	1% Osmium tetroxide (4°C)	2 hrs	1-2 hrs	1-2 hrs (RT)	*1 hrs
Wash	Distilled water / PBS Buffer (0.1 M)	PBS 30 min (3x)	PBS 10 min (2x)	DH2O 10 min (2x)	DH2O *(2x)
Dehydration	35% Acetone	30 min	10 min	-	-
	50% Acetone	30 min	10 min	15 min	*10 min
	75% Acetone	30 min	10 min	15 min	*10 min
	95% Acetone	30 min	10 min (2x)	15 min (2x)	*10 min
	100% Acetone	60 min (3x)	15 min (3x)	20 min (3x)	*10 min (2x)
HMDS	HMDS/Acetone (1:1)	-	-	15 min	-
	100% HMDS	-	-	15 min (3x)	*10 min (2x)
		Continue to CPD	Continue to CPD	Air dry overnight	Air dry overnight
Mount the specimen onto SEM sample stub					
Coat the sample with gold					
View under FESEM					

*Centrifuge the resuspended sample first. Then, discard the supernatant and resuspended the pellet with the chemical.
All centrifuge in this technique should be at 2000g for 10 minutes. (setting for the Hettich Micro 120 Centrifuge is 4560 rpm).

*Courtesy of Scanning Electron Microscope Laboratory, School of Health Sciences, Universiti Sains Malaysia.
*CPD – Critical Point Drying
*HMDS - Hexamethyldisilazane

Appendix 10: RNA Extraction Protocol Summary
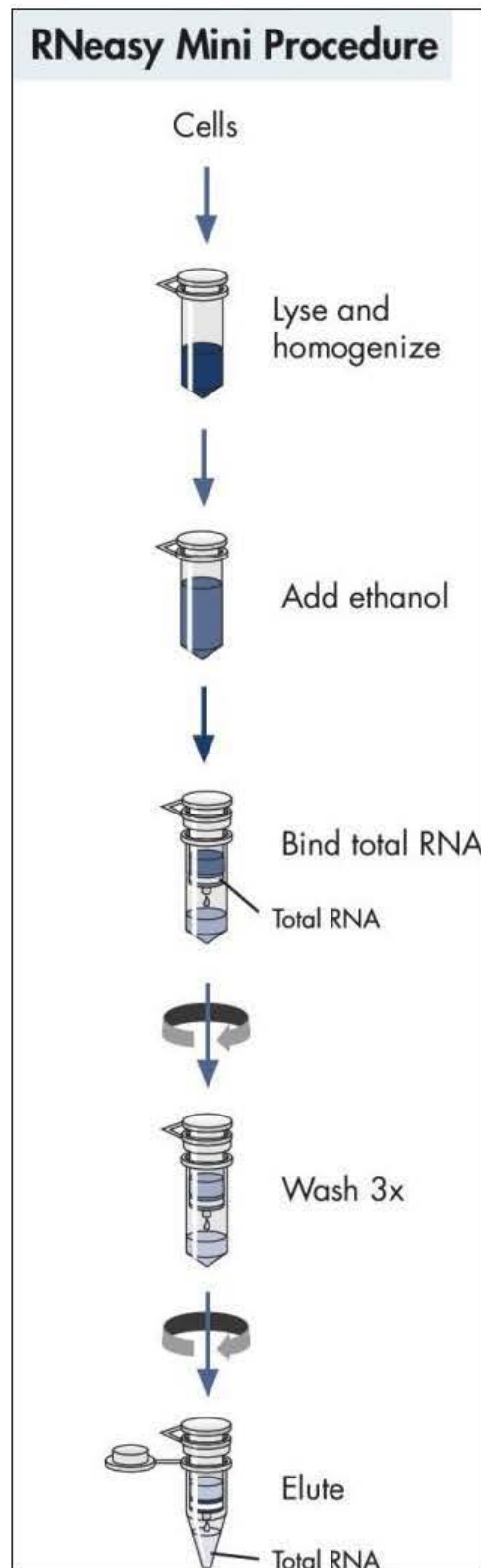
[Extracted from RNeasy Mini Handbook, QIAGEN (2012)]

Appendix 11: The RT-qPCR Two-Step Method Illustration
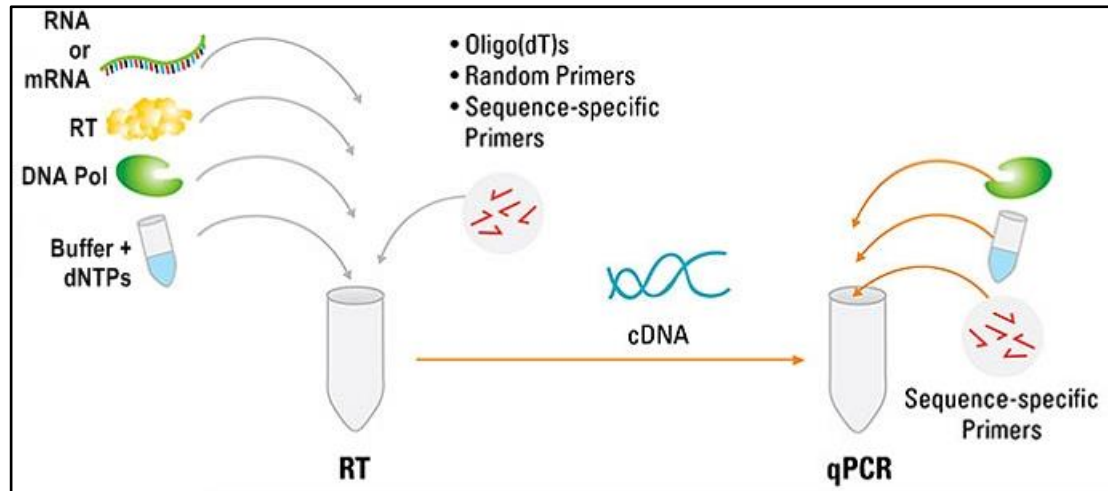
[Extracted from ThermoFisher Scientific website (https://www.thermofisher.com/content/dam/LifeTech/global/brands/Images/1114/One-Step_vs-Two-large.jpg)]

Appendix 12: The QuantiTect Reverse Transcription Procedure

QuantiTect Reverse Transcription Procedure

(Step A) Mix RNA, gDNA Wipeout Buffer, and RNase-free water

Incubate at 42°C for 2 min

(Step B) Add Quantiscript Reverse Transcriptase, Quantiscript RT Buffer, and RT Primer Mix, and mix

Incubate at 42°C for 15 min

Incubate at 95°C for 3 min to inactivate Quantiscript Reverse Transcriptase

Add cDNA to real-time PCR mix and distribute

Quantitative, real-time PCR

[Extracted from QuantiTect® Reverse Transcription Handbook, QIAGEN (2009)]

Appendix 13: RNA to cDNA Calculation

cDNA sample labels	Original concentration (ng/µl)	Calculation (400 ng of total RNA) $(M_1V_1 = M_2V_2)$
A1	90	$M_1V_1 = M_2V_2$ $(90 \text{ ng/µl})(x) = (20 \text{ µl})(20 \text{ ng/µl})$ $x = 4.5 \text{ µl}$
A2	110	$M_1V_1 = M_2V_2$ $(110 \text{ ng/µl})(x) = (20 \text{ µl})(20 \text{ ng/µl})$ $x = 3.6 \text{ µl}$
A3	131	$M_1V_1 = M_2V_2$ $(131 \text{ ng/µl})(x) = (20 \text{ µl})(20 \text{ ng/µl})$ $x = 3.1 \text{ µl}$

Original cDNA sample labels	Original concentration (ng/µl)	Calculation $(M_1V_1 = M_2V_2)$
B1	89	$M_1V_1 = M_2V_2$
		$(89 \text{ ng/µl})(x) = (20 \text{ µl})(20 \text{ ng/µl})$
		$x = 4.5 \text{ µl}$
B2	145	$M_1V_1 = M_2V_2$
		$(145 \text{ ng/µl})(x) = (20 \text{ µl})(20 \text{ ng/µl})$
		$x = 2.8 \text{ µl}$
B3	85	$M_1V_1 = M_2V_2$
		$(85 \text{ ng/µl})(x) = (20 \text{ µl})(20 \text{ ng/µl})$
		$x = 4.7 \text{ µl}$

Appendix 14: RNA Samples Western Blot Bands Intensity ImageJ Analysis

Result

Samples	Band intensity of ribosomal RNA (peak area, pixel)	
	28S	**18S**
A1	2053.497	1853.891
A2	3346.79	2131.598
A3	7155.296	2848.548
B1	6517.054	3629.861
B2	5151.761	3286.447
B3	5972.296	3438.811

Appendix 15: List of Presentations and Conferences

Title of presentation	Presentation	Participation	Seminar/Conference	Venue & Date
1. Establishment of Collection, Storage and Preservation of Human Saliva-Derived Exosome for Biomarker Discovery	Oral Presenter	Participant	International Anatomical and Biomedical Scientific Conference (IABS) 2015	18-20th August 2015 UPM, Selangor Malaysia
2. Effect of Human Saliva-Derived Exosome on The Gene Expression of Human Periodontal Ligament Fibroblast Cell Line	Oral Presenter	(3rd Prize) Best Oral Presenter	International Scientific Conference (iNASCON) 2016	16-17 May 2016 Hotel Perdana, Kota Bharu, Kelantan, Malaysia

OR-018

Establishment of Collection, Storage and Preservation of Human Saliva-Derived Exosome for Biomarker Discovery

Tuan Siti Mastazliha Long Tuan Kechik*, Wan Nazatul Shima Shahidan
School of Dental Sciences, Universiti Sains Malaysia Health Campus, Malaysia.
*Corresponding author:
Tel: +60179154743; Fax: +6(09)7675727
E-mail: mastazliha@gmail.com

Human saliva has many important functions which not only for oral system but also for other body systems. Due to the established functions showed by exosomes derived from saliva and other body fluids, we studied the stability of saliva-derived exosome by establishing the collection, storage, and its preservation methods. Unstimulated saliva samples were collected from healthy subjects. Protease inhibitor were added and stored at difference temperature for difference time period. Exosome was isolated by ultracentrifugation and confirmed by using Western Blot. Exosome morphology was characterized by SEM and protein concentration was determined by using Protein (Bradford) Assay. The exosome particle size distribution and concentration were calculated using Nanoparticle Tracking Analysis (NTA). Protein assay results have showed no significant different on the exosome protein concentration value, regardless the presence of protease inhibitors or different storage temperature and time period condition. Western Blot analysis also showed no different in the present of exosome with all samples were positive for protein CD63. SEM analysis showed the fine shape of exosome which were round, in vesicle form with range of size between 10 nm to 100 nm. NTA determined the concentration and tracked exosome individually within the size range with the mean individual and clumping exosome size of 203 nm. Salivary-derived exosome remain intact in the absent of protease inhibitor and stored under different temperature for longer period. Therefore, limitation factors regarding collection, storage and preservation of human saliva-derived exosome can be excluded for future experimental biomarker discovery.

Keywords: exosome, human saliva, NTA

Appendix 15 (b): Copy of certificate (IABS2105

International Anatomical and Biomedical Scientific Conference (IABS) 2015
"From Cell Towards Translational Medicine"

This certificate is proudly presented to

TUAN SITI MASTAZLIHA BTE LONG TUAN KECHIK

in recognition and appreciation for your involvement as

Presenter

in the

International Anatomical and Biomedical Scientific Conference (IABS) 2015

at Faculty of Medicine and Health Sciences, Universiti Putra Malaysia
Selangor, Malaysia

on 18-20th August 2015

Assoc. Prof. Dr. Mohamad Aris Mohd Moklas
Chairman, IABS 2015

Prof. Dr. Nasaruddin Abdul Aziz
President, Malaysian Anatomical Association (MAA)

Organised by:

UPM
UNIVERSITI PUTRA MALAYSIA
BERILMU BERBAKTI
Faculty of Medicine & Health Sciences
Universiti Putra Malaysia

MALAYSIAN
ANATOMICAL
ASSOCIATION

Appendix 15 (c): Copy of abstract from booklet (iNASCON2016)

O 03

EFFECT OF HUMAN SALIVA DERIVED EXOSOME ON THE GENE EXPRESSION OF HUMAN PERIODONTAL LIGAMENT FIBROBLAST CELL LINE

Tuan Siti Mastazliha Long Tuan Kechik, Zurairah Berahim, Wan Nazatul Shima Shahidan

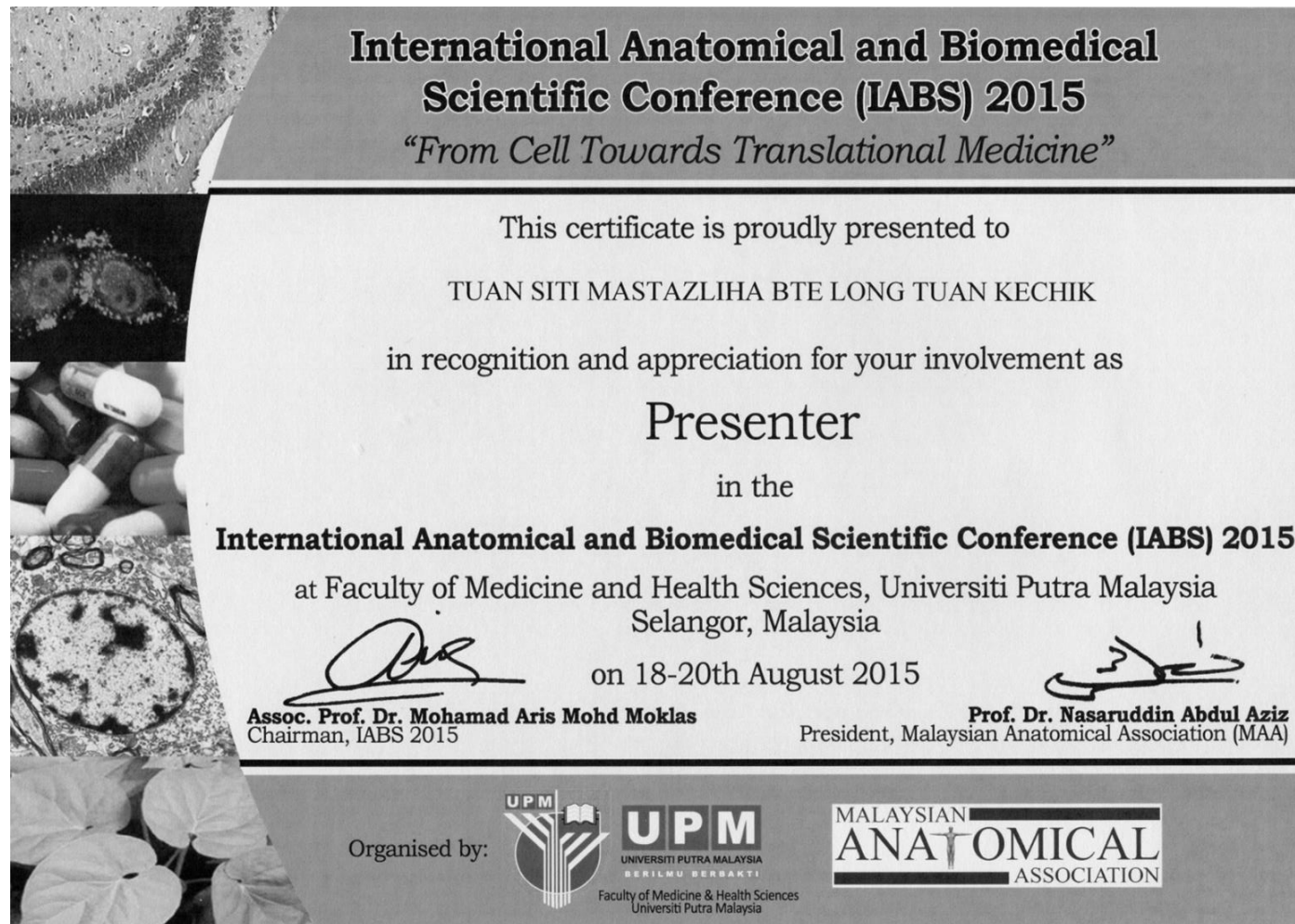School of Dental Sciences, Universiti Sains Malaysia Health Campus, 16150 Kubang Kerian, Kelantan, Malaysia.

Introduction: The increasing incidence of periodontal diseases has lead to the advancement in periodontal theraphy including periodontal tissue regeneration. Exosome was shown to play important functions in various clinical applications. Human salivary exosomes might become a potential element to improve cell-based tissue engineering for periodontal regeneration. **Objectives:** To study the effect of human saliva derived exosome on the gene expression of in basic fibroblast growth factor (bFGF) and collagen type 1(COL1) of HPdLF cell line. **Methodology:** An experimental study was performed on HPdLF cells in the presence and absence of human-saliva derived exosome for 24 hours. The morphology and quantity changes of exosome treated HPdLF cells were viewed under inverted microscope and calculated by using trypan blue respectively. Gene expression level of bFGF and COL1 were determined by quantitative RT- PCR. **Results:** There were no significant difference in the morphology and quantity for both treated and untreated exosome on the HPdLF cells. However, both bFGF and COL1 genes expression levels showed significantly higher in the presence of exosome. **Conclusion:** This study demonstrated that human saliva derived exosome upregulated genes that involved in the cell proliferation. Consequently, human saliva derived exosome may represent a suitable, cheaper and potential alternative biomaterial in tissue engineering for periodontal tissue development.

Appendix 15 (d): Copy of certificate (IABS2105)

Certificate of ACHIEVEMENT

This is to certify that

Tuan Siti Mastazliha Long Tuan kechik

with the abstract entitled

EFFECT OF HUMAN SALIVA DERIVED EXOSOME ON THE GENE EXPRESSION
OF HUMAN PERIODONTAL LIGAMENT FIBROBLAST CELL LINE

has awarded the

(3rd PRIZE) BEST ORAL PRESENTER

in the

International Scientific Conference (iNASCON) 2016

from 16th - 17th May 2016

at

Hotel Perdana Kota Bharu, Kelantan, Malaysia

organised by

Persatuan Pegawai Sains USM (PPSUSM) Malaysia
and supported by

MOHD. NADZRI ABU YAZID
PRESIDENT
PERSATUAN PEGAWAI SAINS USM (PPSUSM) MALAYSIA

RUSIDAH MAT YATIM
CHAIRMAN
INTERNATIONAL SCIENTIFIC CONFERENCE (iNASCON) 2016

Appendix 16: Permission to Use HeLa Cell Image as Reference

M Gmail   **Tuan Siti Mastazliha <mastazliha@gmail.com>**

PERMISSION REQUEST FOR IMAGE USE
4 messages

Tuan Siti Mastazliha <mastazliha@gmail.com>   Sat, Jul 2, 2016 at 2:00 AM
To: dnmason@liverpool.ac.uk

Dear Mr Mason,

I am Tuan Siti, a postgraduate student from Universiti Sains Malaysia (USM), currently doing a research for my masteral thesis, would like to request for your permission on using your image to be included in my thesis.

The image is as follow.

link : http://pcwww.liv.ac.uk/~cci/gallery.html
title: Differential Interference Contrast Imaging
cell: DIC Image of HeLa cell (http://pcwww.liv.ac.uk/~cci/images/gallery/HeLa_DIC.png)

I am sorry that I cant find the core source of the image, or the original article of it, however as stated in the website, the image is courtesy by Dave Mason, so I assume, it is right to ask the permission from you.

If u may tell me the way I can use the image to be included in my thesis, with the correct way to quote you as the references, please do inform me.

Hope to hear reply from you soon.
Thank you.

Miss TUAN SITI MASTAZLIHA BTE LONG TUAN KECHIK
[Supervisor: Dr Wan Nazatul Shima Bt Shahidan (PPSG)]
**MSc Student P-SGM0008/15(R),
Craniofacial Science Laboratory,
School of Dental Science,
Health Campus, Universiti Sains Malaysia
16150, Kubang Kerian,   Kelantan
Off: (+09-7671416) , Hp: (+6017-9154743)**

Mason, David [dnmason] <D.N.Mason@liverpool.ac.uk>   Mon, Jul 4, 2016 at 3:59 PM
To: Tuan Siti Mastazliha <mastazliha@gmail.com>
Cc: CCI <cci@liverpool.ac.uk>

Good Morning and thank you for your email.

Could you please let me know in what context the image will be used? This image has not been published in a peer reviewed paper, but is used as a demonstration of a contrast technique. It has also undergone several manipulations which would be unacceptable for publication.

If you can clarify it's intended use, I'm happy for you to use the image under the CCBY licence whereby acknowledgement is required and should be given as "Image Courtesy of David Mason, Centre for Cell Imaging, Liverpool, UK"

I look forward to hearing back from you,

Best Regards,

Dave Mason

David Mason, PhD
Centre for Cell Imaging, Institute of Integrative Biology,
University of Liverpool, L69 7ZB

Tel: +44 (0)151 795 4454
Web: http://pcwww.liv.ac.uk/~cci
Blog: http://postacquisition.wordpress.com

From: Tuan Siti Mastazliha [mastazliha@gmail.com]
Sent: 01 July 2016 19:00
To: D.N.Mason@liverpool.ac.uk
Subject: PERMISSION REQUEST FOR IMAGE USE

[Quoted text hidden]

Tuan Siti Mastazliha <mastazliha@gmail.com>   Tue, Jul 12, 2016 at 9:24 AM
To: "Mason, David [dnmason]" <D.N.Mason@liverpool.ac.uk>

Dear Mr. Mason,

Thank you for your response and sorry for the late reply.
The image with labels will be the references for my cell morphology characterization especially in labeling.
No further modification will be done on the image.
Therefore, I think the appropriate way of crediting is as you mentioned above.

Thank you.

Miss TUAN SITI MASTAZLIHA BTE LONG TUAN KECHIK
[Supervisor: Dr Wan Nazatul Shima Bt Shahidan (PPSG)]
MSc Student P-SGM0008/15(R),
Craniofacial Science Laboratory,
School of Dental Science,
Health Campus, Universiti Sains Malaysia
16150, Kubang Kerian,   Kelantan
Off: (+09-7671416) , Hp: (+6017-9154743)

[Quoted text hidden]

Mason, David [dnmason] <D.N.Mason@liverpool.ac.uk>   Tue, Jul 12, 2016 at 3:58 PM
To: Tuan Siti Mastazliha <mastazliha@gmail.com>, "Mason, David [dnmason]" <D.N.Mason@liverpool.ac.uk>

Great, I'm perfectly happy for you to use the image in this way.

Best,

Dave

From: Tuan Siti Mastazliha
Sent: 12/07/2016 02:25
To: Mason, David [dnmason]
Subject: Re: PERMISSION REQUEST FOR IMAGE USE

[Quoted text hidden]

Appendix 17: List of Chemicals and Reagents

1. 2-mercapthoethanol (Bio-Rad, United States)

2. Acetic acid (Glacial) 100% (Sigma-Aldrich, United States)

3. Acetone (Sigma-Aldrich, United States)

4. Acrylamide (Bio-Rad, United States)

5. Agarose powder (Bio-Rad, United States)

6. Albumin (Thermo Fisher Scientific, United States)

7. Ammonium persulfate (Bio-Rad, United States)

8. Bis-acrylamide (Bio-Rad, United States)

9. Blue Juice Gel Loading Buffer (Thermo Fisher Scientific, United States)

10. Bovine serum albumin (BSA) (Thermo Fisher Scientific, United States)

11. Buffer RPE (QIAGEN, Germany)

12. Buffer RWT (QIAGEN, Germany)

13. Chloroform (Sigma-Aldrich, United States)

14. Comassie Plus (Bradford) Assay Reagent (Thermo Fisher Scientific, United States)

15. Diethyl pyrocarbonate (DEPC) (Bio-Rad, United States)

16. Dimethyl sulfoxide (DMSO) (Sigma-Aldrich, United States)

17. Ethanol (Sigma-Aldrich, United States)

18. Fetal Bovine Serum (FBS) (LONZA, Switzerland)

19. gDNA Eliminator Solution (QIAGEN, Germany)

20. gDNA Wipeout Buffer (QIAGEN, Germany)

21. Gentamycin Sulfate Amphotericin-B (GA-1000) (LONZA, Switzerland)

22. Glutaraldehyde (Sigma-Aldrich, United States)

23. Glycine (Sigma-Aldrich, United States)

24. HEPES Buffered Saline Solution (HBBS) (LONZA, Switzerland)

25. Hexamethyldisilazane (HMDS) (Sigma-Aldrich, United States)

26. Human fibroblast growth factor-B (rhfgf-B) (LONZA, Switzerland)

27. Insulin (LONZA, Switzerland)

28. Isopropanol (Sigma-Aldrich, United States)

29. LB Buffer (QIAGEN, Germany)

30. Methanol (Sigma-Aldrich, United States)

31. Osmium Tetroxide (Sigma-Aldrich, United States)

32. Phosphate buffer saline (Thermo Fisher Scientific, United States)

33. PowerUp^{TM} SYBR® Green Master Mix (QIAGEN, Germany)

34. Protease inhibitor (Thermo Fisher Scientific, United States)

35. QIAzol® Lysis Reagent (QIAGEN, Germany)

36. Quantiscript RT Buffer (QIAGEN, Germany)

37. Quantiscript® Reverse Transcriptase (QIAGEN, Germany)

38. RNase-Free Water (QIAGEN, Germany)

39. RNaseZap™ RNase Decontamination Solution (Thermo Fisher Scientific, United States)

40. RT Primer Mix (QIAGEN, Germany)

41. Sodium dodecyl sulfate (SDS) (Bio-Rad, United States)

42. SYBR Safe (Bio-Rad, United States)

43. Tetramethylethylenediamine (TEMED) (Bio-Rad, United States)

44. Tris-hydrochloride (Tris HCl) (Bio-Rad, United States)

45. Trisaminomethane (Tris) (Bio-Rad, United States)

46. Trypan Blue Solution (0.4%) (Sigma-Aldrich, United States)

47. Trypsin Neutralizing solution (LONZA, Switzerland)

48. Trypsin/ Ethylenediaminetetraacetic acid (EDTA) (LONZA, Switzerland)

49. Tween® 20 (Bio-Rad, United States)

Appendix 18: List of Instruments

1. Airstream® Gen 3 Laminar Flow Clean Benches, Horizontal (Glass Side Wall) (Esco, Singapore)

2. AllSheng Mini Centrifuge Mini-6K (Hangzhao AllSheng, China)

3. Alpha Innotech Fluorchem FC2 (Alpha Innotech, United States)

4. AND GR-200 Semi-Micro Analytical Balance (A&D, Japan)

5. Axiovert 25 Inverted Microscope (Carl Zeiss, Germany)

6. Beckman Coulter Optima L-90K Ultracentrifuge (Beckman Coulter, United States)

7. Class II Biological Safety Cabinet (NuAire, United States)

8. Hemocytometer Slide Counting Chamber (Optik Labor, United Kingdom)

9. EppendorfTM AG 22331 Hamburg MasterCycler Personal 5332 Thermocycler (Eppendorf, Germany)

10. EppendorfTM BioPhotometer Plus (Eppendorf, Germany)

11. EppendorfTM Microcentrifuge 5415D (Eppendorf, Germany)

12. EppendorfTM MiniSpinTM Microcentrifuge (Eppendorf, Germany)

13. Eppendorf™ Refrigerated Microcentrifuge 5417R (Eppendorf, Germany)

14. Eppendorf™ Mastercycler™ pro PCR System (Eppendorf, Germany)

15. FastPette™ V2 Pipette Controllers (Labnet, United States)

16. FEI Quanta 450 Scanning Electron Microscope (FEI, United States)

17. Gel Doc™ XR+ Gel Documentation System (Bio-Rad, United States)

18. Hettich Universal 32R Centrifuge (Hettich, United States)

19. HICLAVE HVE-25 Autoclave (Hirayama, Japan)

20. IKA® Lab Dancer Test Tube Shaker (IKA, Germany)

21. ilShin -86°C Deep Freezer 484 liter (DF8517) (ilShin, Korea)

22. Micropipette 1-10 µl (Eppendorf, Germany)

23. Micropipette 10-200 µl (Eppendorf, Germany)

24. Micropipette 200-1,000 µl (Eppendorf, Germany)

25. Mini-PROTEAN® Tetra Cell Systems (Bio-Rad, United States)

26. NanoSIGHT NS300 (Malvern, United Kingdom)

27. National Microwave (Panasonic, Japan)

28. NuAire IR Autoflow Automatic CO2 Water Jacketed Incubator (NuAire, United States)

29. PowerPac^{TM} Basic Power Supply (Bio-Rad, United States)

30. ProTech Laboratory Dryers FSD-380 (ProTech, Malaysia)

31. Sanyo Medicool Refrigerator MPR-161D (Sanyo, Japan)

32. StepOnePlus^{TM} Real-Time PCR System (Applied BioSystem, United States)

33. Sunrise^{TM} ELISA Microplate Reader (Tecan, Switzerland)

34. Trans-Blot® SD Semi-Dry Cell (Bio-Rad, United States)

35. TW8 Water Bath (JULABO GmbH, Germany)

Appendix 19: List of Apparatus and Consumables

1. 0.2 ml Flat Cap PCR Tubes-Clear (Biologix, China)

2. 0.5-20 µl Pipette tips (Greiner Bio One, Austria)

3. 1.5 ml Microcentrifuge Tube (Biologix, China)

4. 10-200 µl Pipette tips (Greiner Bio One, Austria)

5. 1,000 µl Pipette tips (Greiner Bio One, Austria)

6. 15 ml Flat-top Centrifuge Tubes (Biologix, China)

7. 50 ml Flat-top Centrifuge Tubes (Biologix, China)

8. CryoKING Cryogenic Vials 2.0 ml (Biologix, China)

9. KIMTECH SCIENCE* KIMWIPES* Delicate Task Wipers (Kimberly-Clark, United States)

10. MicroAmp^{TM} Fast 8-Tube Strips (Thermo Fisher Scientific, United States)

11. MicroAmp^{TM} Optical 8-Cap Strips (Thermo Fisher Scientific, United States)

12. Nunc™ Cell Culture Treated 6 Well Plate (Thermo Fisher Scientific, United States)

13. Nunc™ Cell Culture Treated 96 Well Plate (Thermo Fisher Scientific, United States)

14. Nunc™ Cell Culture Treated EasYFlasks™ T25 (Thermo Fisher Scientific, United States)

15. Nunc™ Cell Culture Treated EasYFlasks™ T75 (Thermo Fisher Scientific, United States)

16. Parafilm M® All-Purpose Laboratory Film (Bemis, United States)

17. PS Sterile 10 ml Pipette (LP Italiana, Italy)

18. PS Sterile 25 ml Pipette (LP Italiana, Italy)

19. PS Sterile 5 ml Pipette (LP Italiana, Italy)